System for Assessment of the Vehicle Motion Environment (SAVME)

A tool for quantifying
natural driving behavior
in statistically powerful datasets

Agreement No. DTNH22-H-07003
Report No. UMTRI-2000-21-1

Final Report Volume I
August 1, 2000

For:
National Highway Traffic Safety Administration

U.S. Department of Transportation
400 7th Street, S.W.
Washington, D. C.20590

By:

University of Michigan
Transportation Research Institute **(UMTRI)**
Veridian Environment Research Institute
of Michigan International **(V ERIM)**
Nonlinear Dynamics Inc. **(NDI)**

Technical Report Documentation Page

1. Report No.	2. Government Accession No.	3. Recipient's Catalog No.

4. Title and Subtitle	5. Report Date
System for Assessment of the Vehicle Motion Environment (SAVME) Volume I	August 1, 2000
	6. Performing Organization Code: UMTRI-2000-21-1
7. Author(s): R. Ervin, C. MacAdam, J. Walker, S. Bogard, M. Hagan A. Vayda, E. Anderson	8. Performing Organization Report No.
9. Performing Organization Name and Address: The University of Michigan Transportation Research Institute 2901 Baxter Road, Ann Arbor, MI 48109-2150	10. Work Unit No. (TRAIS)
	11. Contract or Grant No.: DTNH22-H-07003
12. Sponsoring Agency Name and Address: U.S. Department of Transportation National Highway Traffic Safety Administration 400 7th Street, S.W. Washington, D.C. 20590	13. Type of Report and Period Covered: Final 1/19/99 - 3/31/00
	14. Sponsoring Agency Code

15. Supplementary Notes

16. Abstract

A method has been developed and applied for processing special video images of motor vehicle traffic taken from roadside towers so as to create permanent trackfiles that quantify the vehicle trajectories and intervehicular relationships that prevail in normal driving. The SAVME method collects video data from multiple cameras, processes and merges the image data to produce one track file for each vehicle that passes through the road site, and compiles a permanent database to enable analysis of the natural driving process and a host of what if questions involving driver assistance functions in the normal driving environment. A first production run of empirical data has been accomplished based upon roadside measurement of some 30,500 vehicles. The resulting database has been analyzed to illustrate the broad utility that can be gained from data of this kind. Track file data were validated against measurements from instrumented vehicles conducting maneuvers through the same test site. The validated database was queried in driving scenarios that included the flying pass, left turn across oncoming traffic, emerging from a sign intersection, queue formation and dispersal, and braking propagation along a vehicle string. Presented results include X-Y trajectories and motion time histories for individual vehicles and vehicle clusters. Range, range-rate, and azimuth angle histories are also presented, matching the same fundamental measures that are obtained by modern automotive radar packages. Queries of the database were run to find and display summary data for all cases of vehicles in defined scenarios, presented by means of case counts, histograms, and computed-measure distributions.

17. Key Words	18. Distribution Statement
vehicle motions, crash avoidance, kinematics, traffic modeling, validation, safety	Unrestricted

19. Security Classif. (of this report)	20. Security Classif. (of this page)	21. No. of Pages	22. Price
None	None	110	

Executive Summary

This project has developed an empirical measurement method for documenting how vehicles move and position themselves in proximity to others during normal driving. Constituting a "System for Assessment of the Vehicle Motion Environment" (SAVME), this technique obtains an archival record of the control behavior of drivers on public roads by capturing and processing data from specialized roadside cameras. Thus, SAVME data serve to quantify how all nearby vehicles relate to one another and to the road constraints—in time and in space. In this sense, SAVME results provide an authoritative form of "truth data" documenting the conventional driving process, even with its near-misses, and enabling one to explore the potential impact of new "driver-assistance" technologies. Such study is made convenient by the use of modern database tools, interacting with SAVME data as a permanent archive using common client-and-server computing equipment.

In this project, the SAVME technique was refined and applied in a full-scale deployment through the collaboration of the University of Michigan Transportation Research Institute (UMTRI), Veridian ERIM International, and Nonlinear Dynamics, Inc. The work brings the SAVME concept to fruition after approximately eight years of development.

The SAVME technique collects dense digital video images from several roadside towers at a 10 Hz sampling rate. Once recovered as magnetic tapes, the images are processed to produce one track file, or 10-Hz trajectory, for each vehicle that passes through the selected road site. A time base for each track file is established by a master clock, while each vehicle operates over the surveyed piece of roadway. Thus, the time-stamped motions of each vehicle are expanded through later processing to determine the so-called "inter-vehicular" variables of range, range-rate, and azimuth angles that situate it relative to all other vehicles that coexisted on the road at the same moment in time. Expanded further through Kalman filtering, the dataset is then augmented with additional variables that could not be derived directly from the video images. These variables include longitudinal acceleration, yaw rate, front wheel angle, lateral velocity, and heading angle. The track files are then compiled as a permanent record within a relational database that is made very friendly to analysis by virtue of being embedded within commercially available database software. Thus, any competent database analyst should be able to transact analyses of the SAVME database, once an investigator knows what to look for.

A first production run of the entire SAVME technique was accomplished, conducting roadside measurement of some 30,500 vehicles operating on a 5-lane arterial street in Ann Arbor, Michigan. The resulting database has been analyzed to illustrate the broad utility that can be gained from data of this kind. Track file data were validated by comparison with simultaneous measurements obtained from two instrumented vehicles conducting maneuvers through the same test site. Validation results show that spatial accuracies are within 2 ft (0.6m) and the accuracy of velocity components is typically within 2 ft/sec (0.6m/s).

The collected database was exercised to explore various common driving scenarios including flying passes, left turn across oncoming traffic, emerging from a signed

intersection, queue formation and dispersal, and braking propagation along a vehicle string. Results include X-Y trajectories and motion time histories for individual vehicles and vehicle clusters. Range, Range-rate, and azimuth angle histories are also presented, showing the same fundamental intervehicular measures as are obtained with modern automotive radar packages. Because lane locations are explicitly defined in the database, one obtains crisp indications of lane position as an overlay on all tracking of vehicle motions and their relationships with other vehicles.

Queries of the database were run to find and display all cases of vehicles engaged in defined maneuver scenarios. The queries discovered on the order of fifty to a few hundred cases of vehicles engaged in the maneuver types mentioned above. Results of each query are presented in the report by case-counts, histograms and computed-measure distributions including headway times, times-to-collision, driver reaction delays, queue startup delays, and the like.

Moreover, the project showed that the SAVME method is both viable and powerful. The quality of the data is high, such that even the modest initial database that was collected here renders useful indicators of safety-related performance in normal driving. The kind of measures resident in a SAVME database is noted to be unprecedented. No prior technique has produced a general-purpose tool of this kind for studying the kinematics of pre-crash safety. The project has yielded both equipment and software which constitute the basic tools for future collections of SAVME data. Noting the power and significance of SAVME data, it is recommended that a field data collection program be undertaken, with the goal of creating a national SAVME archive of normal driving data.

1.0 Introduction

This constitutes the final report on cooperative agreement no. DTNH22-99-H-07003, *System for Assessment of the Vehicle Motion Environment (SAVME).* This most recent phase of research on this subject follows from that which was begun in 1992 under the simpler title Vehicle Motion Environment.

The overall project has developed and proven a method for imaging motor vehicles in normal traffic from roadside towers so as to create permanent trackfiles that quantitatively capture the vehicle trajectories and intervehicular clearances that prevail in normal driving. The University of Michigan Transportation Research Institute (UMTRI) has served as the prime contractor on this project from the beginning, developing the SAVME concept and seeking to validate its usefulness. The Environmental Research Institute of Michigan (now a unit of the Veridian Corporation and known as Veridian ERIM International) has served as the subcontractor concerned with collecting imagery data from the roadside. A second subcontractor, Nonlinear Dynamics, Inc. (NDI), has served as the party processing the image data to produce output trackfiles for each vehicle that was observed in the field of regard. UMTRI's role has been that of SAVME concept development and program direction, with a focused effort on creating the tools and procedures for converting raw trackfiles into a permanent database and for analyzing such data to produce findings on the natural driving process. In this recent phase of the SAVME program, a first production run of empirical data has been accomplished based upon roadside measurements and the resulting database has been analyzed to illustrate the broad utility that can be gained from data of this kind.

Data previously collected using the SAVME system at an arterial street site in Ann Arbor, Michigan, had confirmed earlier hopes that such data would vastly increase our understanding of the everyday crash avoidance behavior of motorists. Even the small quantities of track file data that had been processed through 1997 suggested that SAVME would, indeed, become a principal tool for studying normal driving behavior, estimating the likely benefits of crash avoidance technologies, and guiding the design and development of road and vehicle technologies that might impact upon the driving control process. At the outset of the recent phase of work, the system was producing useful data, although the overall procedure was rather inefficient. A one-hour sample of track file data had been generated in 1996 using previously developed algorithms, showing the detailed driving activity of some 1,400 vehicles. Although these data revealed many of the attractive attributes for which the SAVME program was originally undertaken, the long-term requirement (to document driving behavior over perhaps a hundred or more hours at each selected road site) required that a large improvement in the productivity of the method be obtained.

Accordingly, this recent extension phase was to address a list of improvements in processing algorithms and associated details of the imaging method so that known problems would be fixed. The problems in question existed almost exclusively at the level of the image data, themselves, due to issues of contrast between adjacent vehicles,

changes in roadway illumination, small motions of the camera-support towers, shadows, entry/exit of vehicles at the edge of the scene, retaining a useful background image of the pavement beneath a vehicle that had stopped, and other effects. The rate of occurrence and the seriousness of each problem had already been defined. Thus, each of the needed improvements was understood in clinical terms and solution approaches had been developed as the basis for proceeding ahead.

Additionally, there was a desire to validate samples of the final track file data by comparison with data collected from instrumented vehicles at the same test site. Thus a validation step was undertaken, once software improvements had been made to establish an improved level of system performance, overall. The resulting trackfiles from an approximate 18-hour period of traffic observation, including the validation segment, were produced, archived within the database, and analyzed during this study. The trajectories and associated response variables for approximately 30,500 individual vehicles are now represented within the dataset.

The report is assembled as follows. Section 2.0 provides an overview of the SAVME system, describing the concept in terms of the data types that are being sought, the rationale for their collection, and the general method used for obtaining such data using three primary subsystems. Section 3.0 presents the subsystems one at a time. Each description refers to the corresponding Appendix A, B, or C, within which a complete users manual for each subsystem is presented. The three subsystems function in series with one another, by a process that goes from data collection to data processing to data archiving and analysis. Of course, since the SAVME concept is that of compiling an authoritative data archive, the matter of analysis, per se, implies an open-ended capability that supports study of a limitless variety of questions. Nevertheless, certain common analysis procedures have been identified and provided for in the analysis tools that have been developed.

Section 4.0 presents a selection of results drawn from the 18 hours of finished data. This section of the report includes commentary on the quality of collected data and the issues addressed in data collection and processing. A lengthy set of example analyses is presented in order to illustrate the contents of a SAVME database and to tease out the kind of inquiry toward which SAVME data are peculiarly suited.

2.0 Overview of SAVME

Taken in the large, SAVME is simply a means of creating a permanent record of how all vehicles move within a defined segment of roadway, as captured against a common time base such that all of the intervehicular relationships that developed in time and space are explicitly defined. This SAVME concept is discussed below, firstly in terms of how such data might be applied, given the generic nature of the information, and secondly in terms of the implementation scheme that has been realized during this work.

2.1 SAVME Application Concept

A modern argument for directly measuring the detailed motions of vehicles in normal driving arises from the need for an engineering effort to create and evaluate crash avoidance technologies for future vehicles. In particular, the eventual commercialization of so-called driver assistance systems (DAS) calls for automotive products that are very well tuned to the dynamic elements of the actual crash-hazard environment through which all vehicles travel. Real drivers tend to anticipate these dynamics from experience, and they respond to the exigencies as they develop around them. But the detailed observations we make as drivers are locked away with all of the other so-called right-brain skills and adaptations which are vision dominant and which cannot be meaningfully expressed as a knowledge base for engineering usage. Accordingly, DAS advancements within industry and government attempts to stimulate/evaluate/regulate DAS product will proceed significantly in the dark until this microtraffic context we call the vehicle motion environment becomes usefully measured and analyzed.

As conceived here, this need is addressable by means of an instrumentation system that would capture the motions of individual vehicles within a permanent data record. In any of the various applications to be discussed below, it is clear that a rather faithful recording of each vehicle's trajectory, or motion history, is needed at a sampling rate in the vicinity of 10 Hz, in order to span the natural modes of cornering and braking response that lie near 1 Hz. Such sampled motion records are referred to as trackfiles. At a given road site, one track file would be recorded for each vehicle passing through the scene that is under the immediate observation of the SAVME system. In addition to trajectory information, the system would also describe the size of the body envelope of each vehicle by estimating a nominal length and width, thereby also fixing the approximate size and weight class of vehicles in the scene. A fully portable measurement system of this type would be installed for a modest time period at each of a sample of road sites around the country, compiling an archival data set that would eventually serve to document the kinematic realm of driving behavior in the United States.

Since the measured trackfiles would all have a common time base, later processing of these data can determine the intervehicular relationships which prevailed during the measurement. Such enriched-variable files can each support new statistical analysis if inquired simply as another layer of data. Alternatively, a set of direct track file data plus an ancillary file of derived variables could be operated upon to support the simulation of a

DAS concept system as an overlay on the kinematic truth environment comprised in SAVME data.

A characterization of the vehicle motion environment that is suitable to support new product development and kinematic-domain evaluation will require that measurements be made at selected sites for a period of time that may span several weeks. A national program of such measurements would presumably cover a representative sample of sites covering geographic, climatic, road design, illumination, driver and traffic factors that are each seen as influential in determining the driving behavior of people. At a given road site, each motion and space variable must be quantified from one instant in time to the next so that, eventually, data are collected providing statistical distributions of these variables representing the vehicular behaviors and interrelationships which eventually determine normal operations. Altogether, such an archive would constitute a massive data resource and would require a sustained commitment for its acquisition and maintenance.

Without SAVME data, it can be argued that the process of refining collision warning and intervention systems will be a cut & try process and is thus quite handicapped as an engineering endeavor. The brute empiricism of this process will derive from the simple fact that the precrash environment remains utterly unquantified, in the dynamic temporal/spatial terms by which vehicle motions and clearances are determined, from moment to moment. Thus, the only way one can tell if a given sensor/processor package is any good, under the current state of affairs, is to take it out on the road and try it. But wherever one tries it, the intervehicular variables at the time of testing will be unknown and unrepeatable in any controlled sense—thus making it difficult to relate the package's performance to the condition variables. Since intervehicular relationships vary stochastically and since true crash-bound trajectories appear only with great rarity, it is virtually impossible to take any system prototype and try it in a meaningful way against an authoritative distribution of kinematic exposure variables. Also, attempts to simulate the application environment will always lack validation until some robust form of "truth data" is brought forward through a direct-measurement characterization.

The basic problem is that we have essentially no information that is both quantitatively and statistically representative of the headways, lateral clearances, angles of approach, time spacing between vehicles, or the correspondence between these intervehicular variables and the steering and braking accelerations which are driver induced in response to this motion environment. Thus, we are without definitive data on an exceedingly complex application environment toward which a large industry around the world is now targeting a vast array of new technology that may hold promise as crash avoidance countermeasures.

The extent of the need for SAVME data can be seen upon consideration of the challenge in DAS system development. The central observation, confirmed now by some industry engineers who have begun to work on active safety packages, is that the detection of full-blown, fast-closing collision threats is not too difficult if the system waits long enough to make a decision. But then, the time-to-respond may be intolerably short. Many sensing technologies, even with crude processing algorithms, can tell a bonafide crash-in-the-making when it is well developed and more or less inevitable. The hard part is to create

sensor/processor systems that can discern the probably-harmless intervehicular actions from the very-likely-harmful events early in the time sequence. Clearly, since candidates for crash-interaction develop around each motor vehicle hour after hour, day in and day out, the opportunities for false alarm are many, indeed. Any acceptable active safety product must accomplish the remarkably complex task of appraising and dismissing the many thousands of episodes which are, indeed, benign without ending up in such a processing stupor that the bonafide collision threat is missed or its detection is delayed beyond the minimal time window needed for safe intervention.

On the expectation that frequent false alarms and, worse yet, false control interventions, will simply make such systems unacceptable, the achievement of high levels of active safety intelligence seems a requirement. But the engineering of such intelligence into these products appears, in turn, to require an accurate targeting of the technology to the complex motion environment which actually prevails. Such a task, in turn, requires that the targeted environment be representatively quantified.

However industry may use such quantitative data for product planning and development, government may be disposed to employ SAVME data for such purposes as identifying opportunities for crash avoidance countermeasures, projecting DAS benefits at a preliminary level, and evaluating specific system designs by subjecting them to SAVME sequences that have been selected from the archive for use in repeatable and statistically meaningful examinations of product performance. A "standard" evaluation sequence might emerge by which industrial developers of technology can communicate with government regulators, and vice versa, perhaps eventually even using a SAVME data sequence to develop product standards covering certain macro aspects of safety performance.

In this context, a national archive of SAVME data has been viewed as analogous to the archive of accident data, itself. That is, just as we have used the police-reported accident record to document our national crash experience and, in turn, to support the thirty-five years of developments in passive safety technology, so the SAVME data record would document our national everyday-driving experience in terms that would help develop, evaluate, and perhaps regulate active safety technologies. SAVME data would be so fundamental in their characterization of the driving kinematics that they are also likely to be useful in highway and traffic engineering, many of whose design and operational standards have been developed without the aid of the definitive analyses that SAVME can readily support.

2.2 SAVME System Overview

When the SAVME program first began in 1992, it was felt that the state of commercially available video technology was insufficiently developed to support the quality of imaging that would be needed for capturing vehicular images from tall towers at the roadside. Thus, the original technological approach for SAVME involved the development of laser range imagery. A 10-Hz scan rate covering broad sections of roadway was effected with a high-power, noneye-safe, scanning laser, whose controlling laser diode was rated at 1 watt of output. In the end, this approach was found to be unacceptably ahead of the state of production in commercial lasers and was later abandoned.

By 1994, digital video cameras began to provide good resolution and very short (1 msec) frame exposure times at reasonable purchase prices, thereby opening up a much more conventional, passive-imaging path for the SAVME application. On the basis of success in other applications of digital video technology to automotive imaging problems, a SAVME approach based upon digital video products was undertaken in 1996. The current project represents the second of two phases in the application of this technology to SAVME.

The system implementation concept involves three serial steps in the creation of an archival file of SAVME data, as shown in Figure 2.2-1 below. A data collection subsystem is installed at the roadside, collecting image data from a number of individual cameras, each of whose output is recorded on a separate magnetic tape. These tapes are then processed to capture individual vehicle images and track their motions as they move across the entire multi-camera scene, yielding binary trackfiles for each vehicle. The raw track file data are then converted into a relational database for study using a variety of specialized tools. Because the data are always produced through a sustained period of measurement at individual sites, each batch of data in the SAVME archive represents both the driving behavior of tens to hundreds of thousands of individuals plus the particular driving context afforded by the site. Thus, although certain aspects of driving behavior may be more or less generic at any site (e.g., braking reaction delays), other aspects may be highly determined by the traffic signature of the site (e.g., the car/truck mix, or say, the distribution of lane-change conflicts as occasioned by flow into a nearby exit or intersection.)

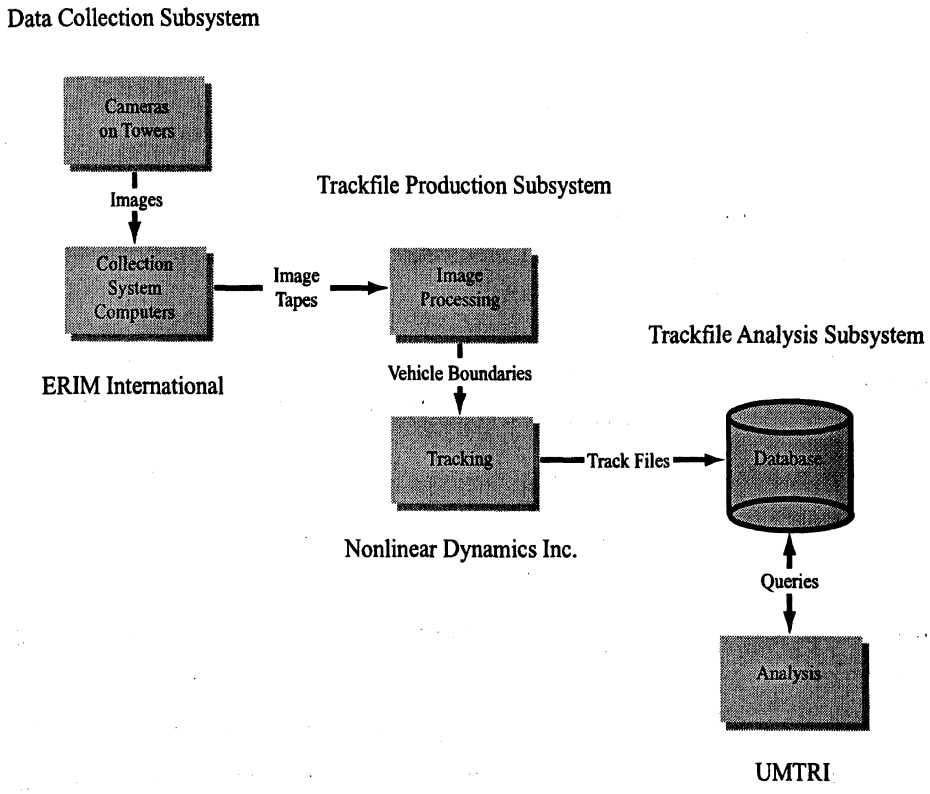

Figure 2.2.1. Block Diagram of Data Collection, Processing, and Analysis

3.0 Presentation of SAVME Subsystems

In this section, each of the SAVME subsystems is briefly introduced. More complete presentations of the subsystem tools appear in Appendices A, B, and C.

3.1 Data Collection Subsystem

The SAVME data collection subsystem was developed for this project by Veridian ERIM International. This subsystem constitutes the entire complement of equipment that would go to the road site and would effect the collection of digital videotape from each roadside camera. Each camera is mounted on a telescoping tower that is 100 feet in height when fully extended from the utility trailer on which it is stored. Once the tower has been erected, the trailer and tower structures are fixed firmly in place by means of guy wires and stout anchors. The camera is mounted to the top of each tower on a pan/tilt control unit that allows precise pointing of each camera toward the road segment in question. Overlapping views are obtained by adjacent cameras so that the processed tracks for any given vehicle can be spliced together across the boundaries of adjacent video scenes. Other practical questions of site installation deal with the granting of approval by local jurisdictions for erecting the towers on a temporary basis and with ensuring the security of the equipment, including prevention of access by children who might climb on the towers and ensuring that the towers, themselves, do not constitute a roadside hazard to motorists.

Shown in Figure 3.1–1 is a sketch of the data-flow and camera control features involved in SAVME data collection. We see, in this two-camera example, that individual frame-grabber cards are triggered by a common square-wave generator to capture video frames from each camera by way of video serial links. The collected frames are then temporarily written to hard disk memory, for later compression and permanent recording on tape. This process, and the software used in controlling the video collection procedure, is further described in Appendix A.

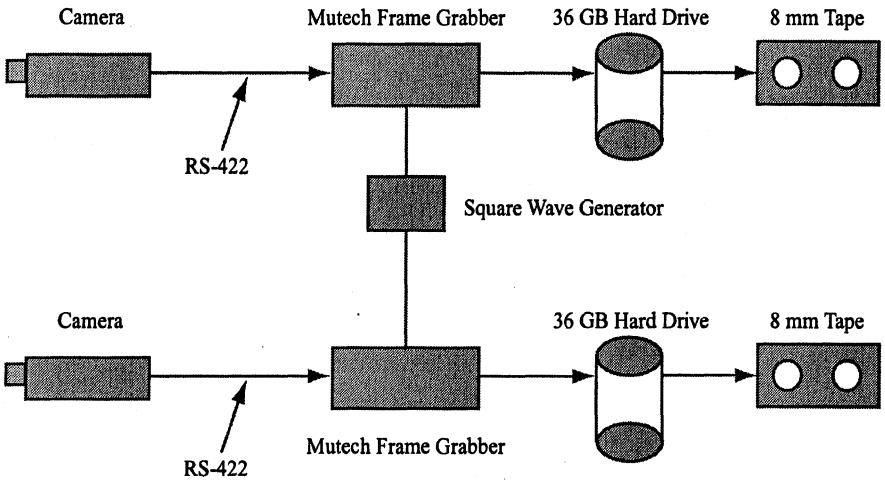

Figure 3.1-1. Block Diagram Showing Data Flow of SAVME Digital Video

3.2 Trackfile Production Subsystem

The SAVME trackfile production subsystem consists of five main modules as shown in Figure 3.2-1. The primary inputs to the subsystem are sequences of digital *images* from two cameras. A secondary input to the subsystem is a *site survey* which is required for the *calibration* process that makes it possible to locate points on the road that correspond to points in the images. The output from the subsystem is a *trackfile* which describes the travel paths of all of the vehicles in the image sequence. The automatic processing takes place in two stages. First the *detection* module identifies potential vehicles in the images. Then, the *tracking* module links up the detections through multiple images to track the vehicles as they move down the road. A *quality control* step includes manual review and correction of the automatic processing results to ensure that the output of the subsystem is of the highest possible quality. The *production management* module consists of tools used to manage the trackfile production process.

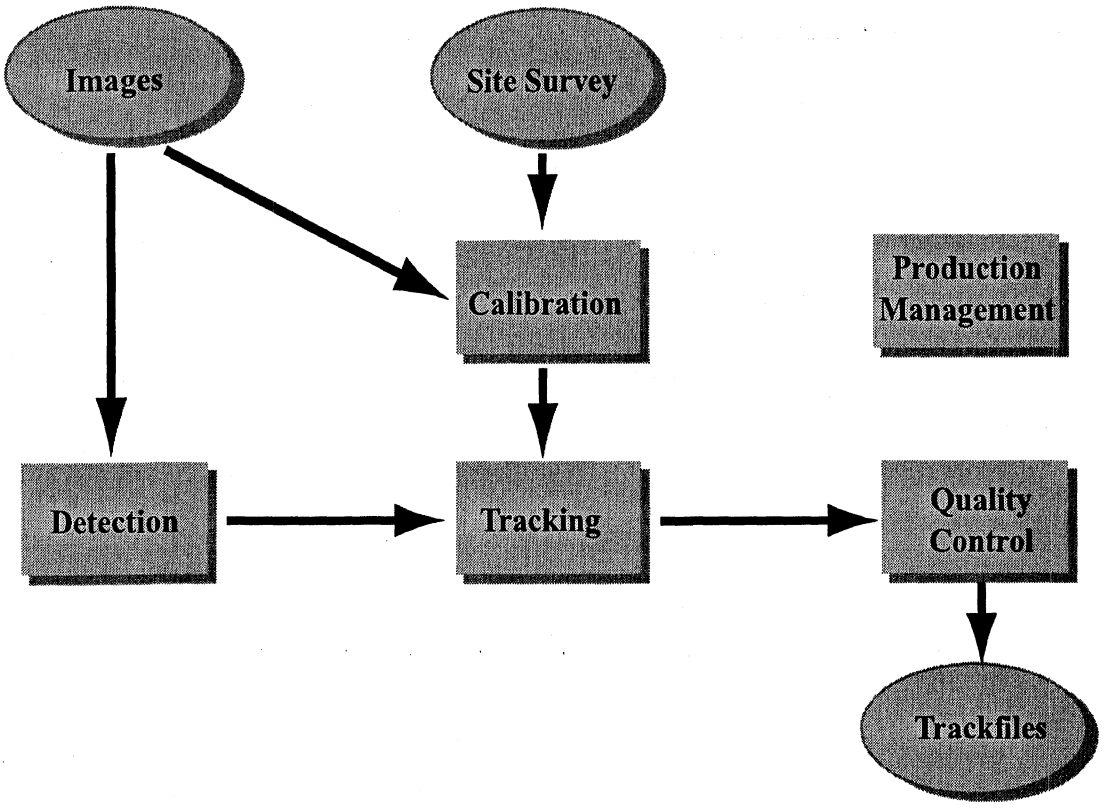

Figure 3.2-1. Trackfile Production Subsystem

Camera *calibration* is required to derive the mathematical transformation necessary to determine the location of points on the road that correspond to points in the image. The input to the camera calibration process is a set of road points and image points in correspondence. These calibration points must have known positions on or around the road and must be readily discernable in the images. A topographic site survey must be performed to determine the absolute positions of road markings and other features used as calibration points. The positions of the calibration points in the images are determined manually. These calibration points are used as input to the camera calibration software which determines the appropriate parameter values for a parameterized camera model. The calibration parameters are then used in conjunction with the camera model to locate road points when given image points or to locate image points when given road points.

The *detection* module uses image-processing operations to detect areas within the images that appear to be vehicles. These detections are characterized by bounding polygons which are the primary inputs to the tracking module. The basic approach used is to maintain a background image which represents an approximation of what the scene would look like at the current time without any vehicles. The background image must be updated every frame because the illumination of the road changes constantly. The background image is then subtracted from the current image and the regions that differ are further processed to determine if they represent vehicles. This processing includes merging small adjacent regions into larger regions and splitting large regions into parts at likely split points. A bounding polygon is then fit to each of the resulting regions and saved as the output for the module.

The *tracking* module uses the polygons representing possible vehicles in each image as it steps through all of the images, building up tracks representing the paths that the vehicles are travelling. The basic approach is to predict vehicle positions for the next image based on the recent history of current tracks. The predicted positions are compared with the polygons in the next image and, when matches are found, the track positions for that image are updated. New tracks are started when polygons are found that do not extend any current track. Tracks are ended when they leave the field of view. Various constraints are applied throughout the tracking process to minimize the effects of detection errors. When each track is complete, the vehicle size is estimated using data from all of the images containing the vehicle. Tracking is carried out independently for each camera. After tracking is complete for all cameras, tracks from multiple cameras are merged by examining the overlap region to find matches and then blending the matching tracks from the two cameras.

Quality control is the last step. All tracks are reviewed manually to detect and correct problems. A custom software tool with an interactive graphical user interface streamlines the process. It allows the analyst to step through the data in frame order or to skip through the data by tracks. It facilitates the deletion, modification, and creation of tracks. The final output of the quality control step is a trackfile.

The *production management* module integrates all of the other modules into a production process. It standardizes and automates directory structures, file names, program options, and process steps.

3.3 Subsystem for Trackfile Archiving and Analysis

The SAVME software package used to process trackfiles involves several basic steps. The first step is to import and format the trackfiles into a form suitable for subsequent processing. (The trackfiles received at this stage are simply the x and y time histories of each vehicle's centroid location moving through the field of regard.)

The next steps involve processing the trackfiles through the Kalman filtering stage and then through the intervehicle variable calculation stage.

Kalman Filtering

Kalman filtering involves the application of a model filter to extract additional vehicle response information from the x and y trackfile time histories. Since the Kalman filter utilizes a simple vehicle dynamics model (scaled to the size of each vehicle based upon the vehicle's indicated length in its trackfile header record), the Kalman filter output yields estimates of additional vehicle response variables available from the applied model:

- improved estimate of x location
- improved estimate of y location
- estimate of vehicle heading (yaw) angle
- estimate of vehicle forward speed
- estimate of vehicle lateral speed
- estimate of vehicle yaw rate
- estimate of driver steering angle input (at the road wheel)
- estimate of vehicle longitudinal acceleration (primarily reflecting driver throttle and brake applications)

These additional eight vehicle response variables, plus the raw x and y time histories, are then stored in an MS Access table known as the trackfile data table within the total SAVME database. An example trackfile data table appears in Appendix C.

Intervehicle Variables Calculation

Following the completion of the Kalman filtering calculations, the data are then processed to obtain the so-called intervehicle variables, consisting of range (R), range-rate (R-dot), and angle-of-attack (a), that define the relative locations and motions of each vehicle in the field of regard with respect to any other vehicle. Figure 3.3-1 further describes this set of relationships. The range and range-rate variables are defined relative to each vehicle's centroid. Range is always positive. Range-rate is positive if range is increasing over time; it is negative if range is decreasing.

The angle of attack is defined as the angle between each host vehicle's longitudinal x-axis and the vector connecting the host and target vehicle centroids. The angle-of-attack is defined as positive clockwise when viewed from above. (A target vehicle ahead and to the right of a host vehicle would have a positive angle-of-attack relative to the host, with a value between 0 and 180 degrees. The angle-of attack, a1, seen in Figure 3.3-1 is therefore negative using this sign convention.) An example Intervehicle variable table appears in Appendix C.

The final step is to archive the Kalman filter and intervehicle variables as Microsoft Access tables within the SAVME database. These are then available for subsequent querying and/or further processing that might include animation of various portions of the data, plotting of certain variables, or exporting of SAVME data to other programs such as Microsoft Excel or various statistical analysis programs.

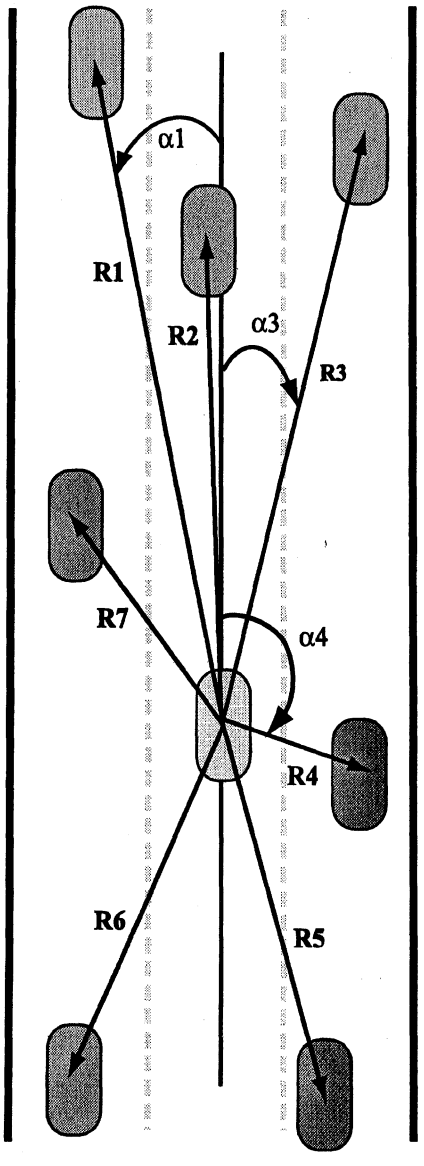

Figure 3.3-1. Range and Angle-of-Attack Variables Calculated as Intervehicle Variables

Appendix C, entitled "User's Manual for SAVME Trackfile Archiving and Analysis," provides a more complete description of the mechanics needed to operate the Microsoft Windows software and to process trackfiles. Figure 3.3-2 provides a simple overview of the various interactions between a program user and the trackfile processing software.

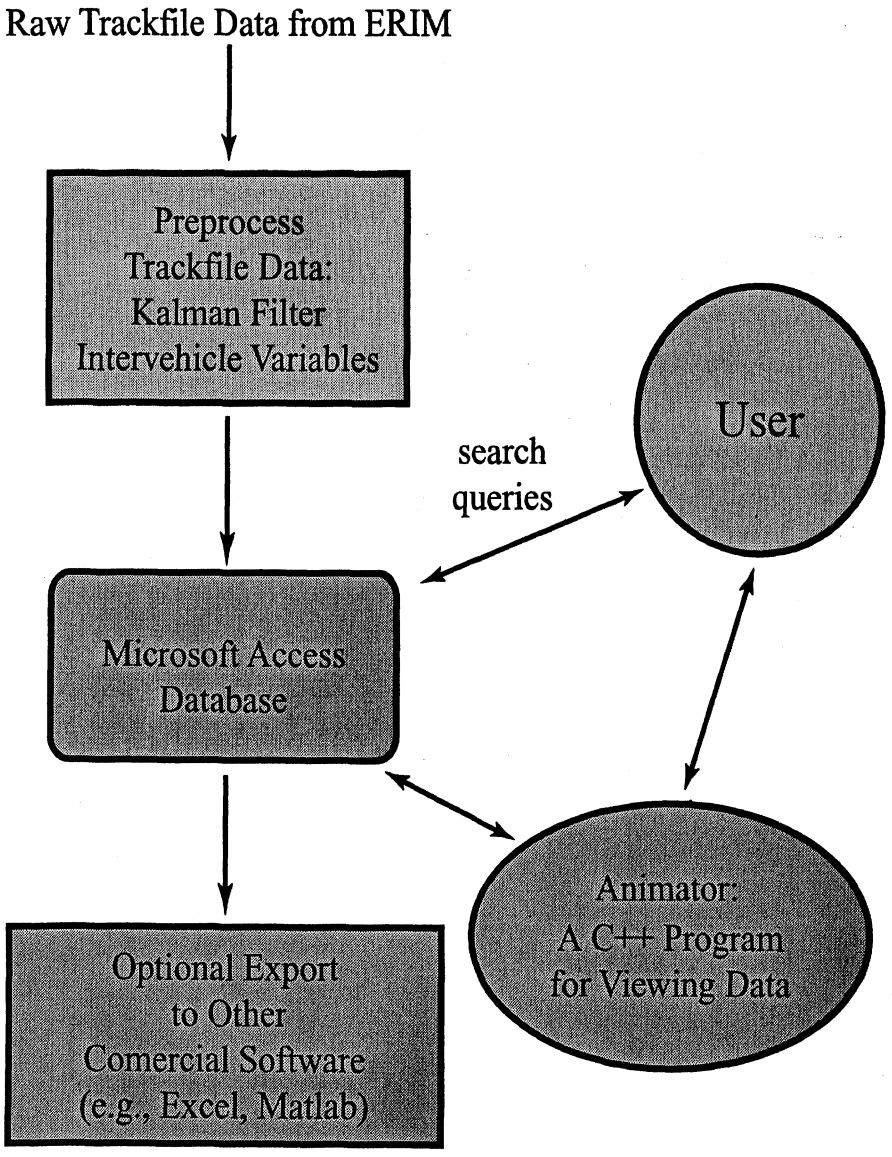

Figure 3.3-2. Block Diagram Depicting the Basic SAVME Trackfile Processing Software Elements

4.0 Presentation of SAVME Results

This section presents and discusses results associated with the data collected at the original SAVME test site in Ann Arbor, Michigan. In section 4.1, samples of data obtained from the two basic levels of production are considered. These stages involve firstly, video imagery and secondly, trackfiles produced for each individual vehicle. Section 4.1.1 presents a discussion of images, from the viewpoint of certain repeating artifacts that tend to complicate the image-processing task. Section 4.1.2 presents samples of trajectory tracks, as overlaid on scene video, together with a discussion of certain artifacts from image processing that manifest themselves as anomalies in the finally produced raw trackfile for an individual vehicle.

The second major section, 4.2, addresses itself to trackfile results, only. In section 4.2.1, results of the validation exercise are presented and discussed. This presentation expands upon the notation of trajectory artifacts in section 4.1.2, but introduces reference data obtained by driving two instrumented vehicles before the SAVME cameras so as to later compare instrument recordings with raw trackfile results. In section 4.2.2, an extensive sampling of SAVME results are presented, as a means of illustrating the application of trackfile analysis tools and the process of querying the relational database to find and display results having certain common attributes matching the query. The results also serve to illustrate the broad utility of SAVME data for addressing a host of questions regarding the driving process.

4.1 The Nature and Quality of Video and Trackfile Samples

4.1.1 Discussion of Video Data Quality

The performance of the trackfile production subsystem is affected by the quality of the images provided by the data collection subsystem. Factors which affect the quality of the digital images obtained from the data collection subsystem fall into three categories: geometric, environmental, and system-related.

The geometry of camera tower configuration has a direct impact on the quality of the data. The tower height and distance from the road constrain the aim of the camera which affects the ground area imaged and the potential for occlusion of one vehicle by another. The spacing between two towers affects the overlap area which is required for merging tracks from the two cameras. The lens focal length affects the magnification of the image and may in some cases add fish-eye distortion to the images. The resolution of the camera and the frame grabber impact the resolution of the data to be processed. If the system only records a part of each image in order to reduce the data storage requirements, the area covered by the images is correspondingly reduced.

For both SAVME data collections, the towers were 100 feet tall. For the 1996 data collection, the cameras were 93 feet from the center of the road and 200 feet from each other. In order to increase overlap across the full width of the road, towers for the 1999 collection were placed 100 feet from the center of the road and 182 feet from each other. The five-lane road is 60 feet wide. The lenses added some fish-eye distortion to the images. Because the road was oriented horizontally in the view of the cameras, only the middle 200 rows of the 480 image rows were recorded but all 768 columns were recorded. At the top of the image, the horizontal field of view is 400 feet, and at the bottom of the image, it is 200 feet. At the middle of the image the vertical field of view is 100 feet. The overlap in the camera fields of view is 200 feet at the far curb and 100 feet at the near curb. At the top of the image, a pixel covers about 0.52 feet, and at the bottom of the image, a pixel covers about 0.26 feet. At the corners of the image, the resolution is lower. The drop in resolution from the center of the images towards the edges resulted in the accuracy of the tracks being dependent on the position of the vehicles within the images. The problem was most noticeable when tracks from two cameras were merged and the low resolution of the overlap areas at the edges made it difficult to smoothly blend the two tracks.

Figure 4.1.1-2 shows the areas of the road imaged by the two cameras. The shapes of the imaged areas highlights the fish-eye distortion, resolution differences between the top and bottom of the images, and the shape of the overlap region.

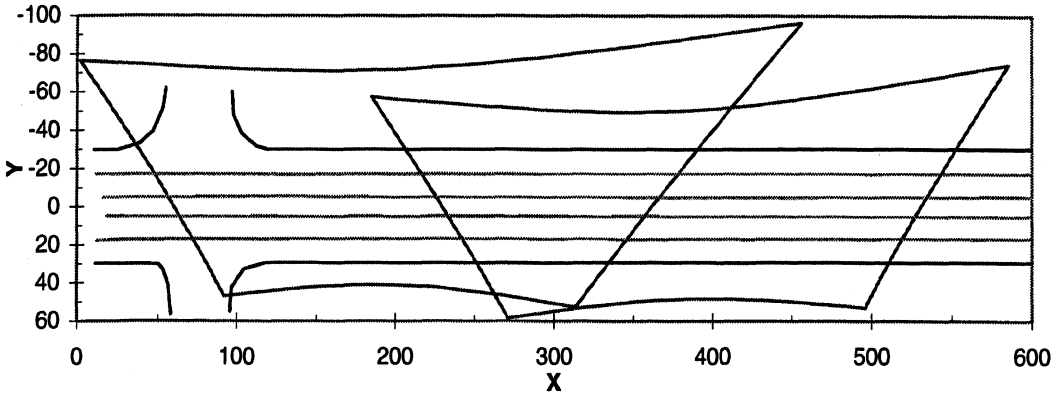

Figure 4.1.1-2. Camera Views of the Road

Figure 4.1.1-3 shows three images of the same car. The top image shows the car entering at the right. The middle image shows the car near the middle of the image where the resolution is the highest. The bottom image shows the car leaving at the left. Notice that when the car is in the middle of the image, the view is directly at the side of the car, but when the car is at the edge of the image, the view includes the front or back of the car. The combined front and side views of vehicles near the edges of the images results in reduced accuracy in determining vehicle locations on the road. Notice also that the car is larger when it is in the middle of the image than when it is at the sides. This is a result of fish- eye distortion which results in reduced accuracy near the edges of the images.

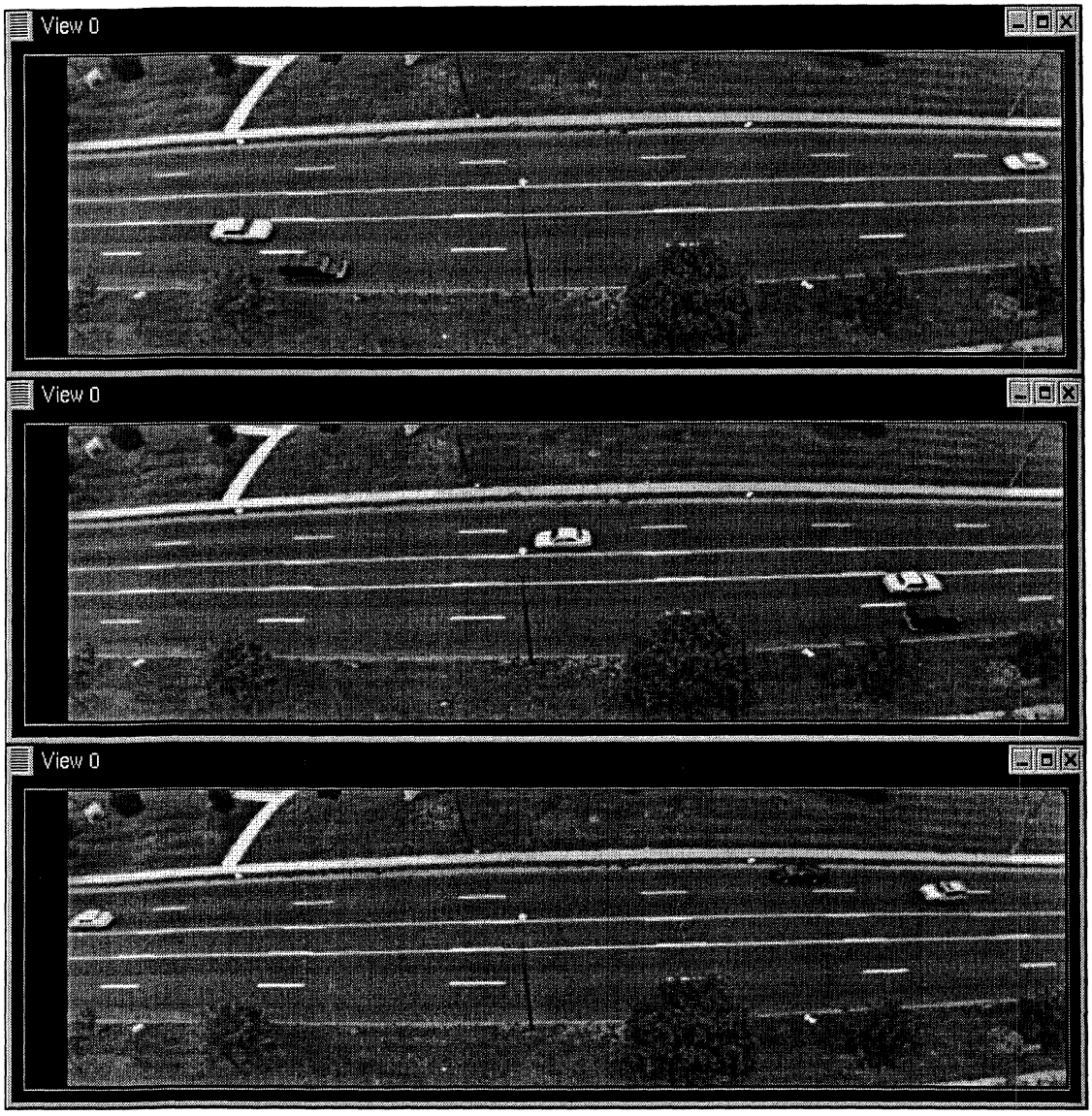

Figure 4.1.1-3. Effects Related to Vehicle Position within the Image

The viewing angle results in vehicles in adjacent lanes sometimes partially occluding one another. The occlusion problem is worse for larger foreground vehicles. In the worst case, a large truck in the foreground can completely occlude a car. Placing the camera towers closer to the road would reduce the occlusion problems. The trackfile production subsystem was usually able to track vehicles that were partially occluded by other vehicles. Figure 4.1.1-4 shows three images where cars are occluded by trucks. In the top image, only the top of the car is visible. In the middle image, only about a quarter of the car is occluded. In the bottom image, the same car is almost entirely occluded.

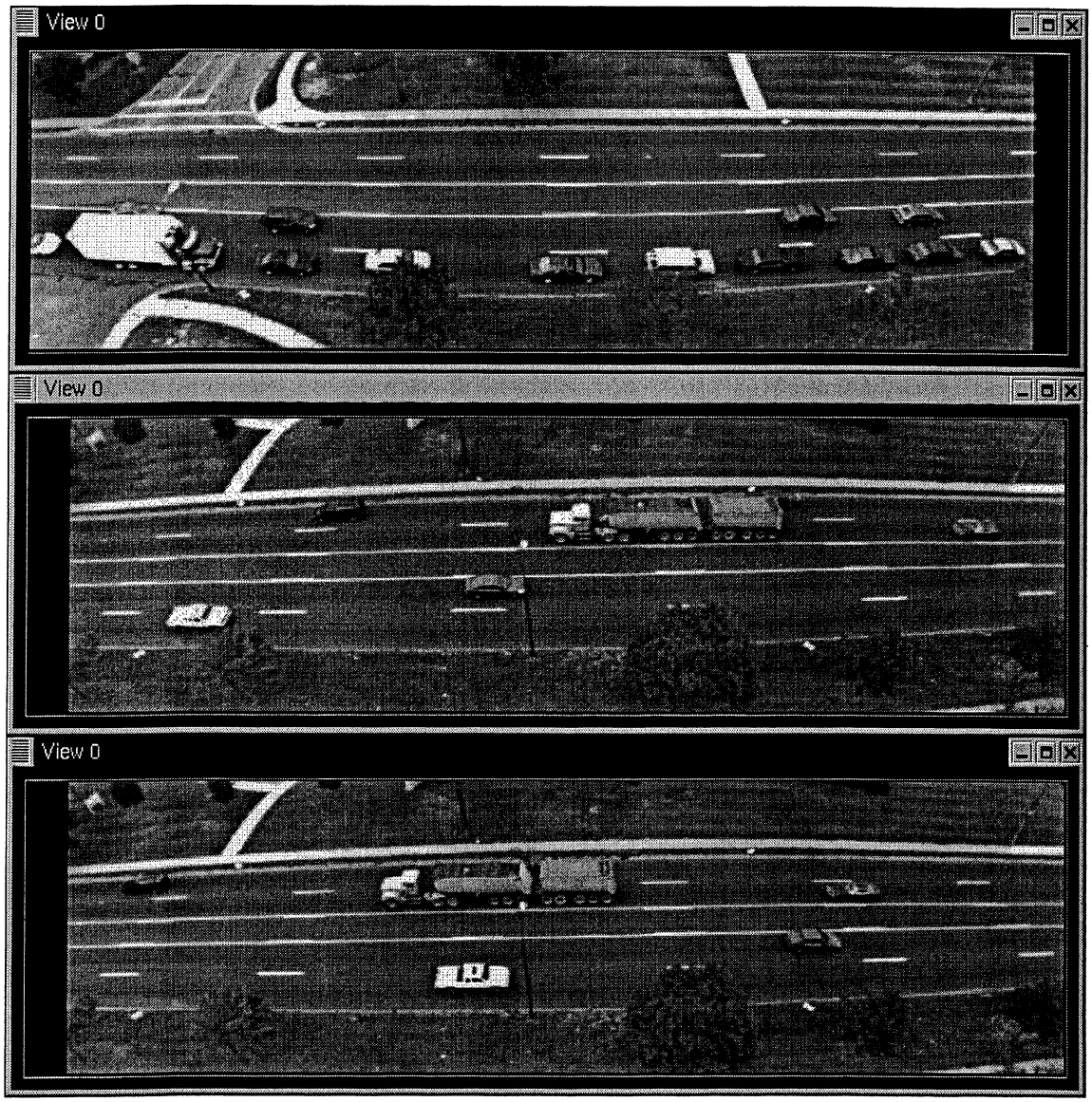

Figure 4.1.1-4. Occlusion by a Vehicle

Environmental factors include permanent factors and temporary factors. A permanent factor affects all data collected from a given configuration, while temporary factors only affect certain data. An example of a permanent factor is a tree, which occludes the road. For the 1996 data collection, there were a few trees which partially occluded the road. However, because the collection was conducted in the late fall after the leaves had fallen off of the trees, the occlusion problem was manageable. For the 1999 data collection, the trees had grown significantly and the leaves were still on the trees. As a result, one of the trees fully occluded a portion of the near lane. The Trackfile Production Subsystem is usually able to track vehicles that were occluded by trees during part of their travel. Figure 4.1.1-5 shows three examples of occlusion by a tree. In the top image, a white car is occluded by the tree but is slightly visible. In the middle image, the white car is starting to emerge from occlusion. In the bottom image, the dark Sport Utility Vehicle two cars back from the white car is completely occluded by the tree.

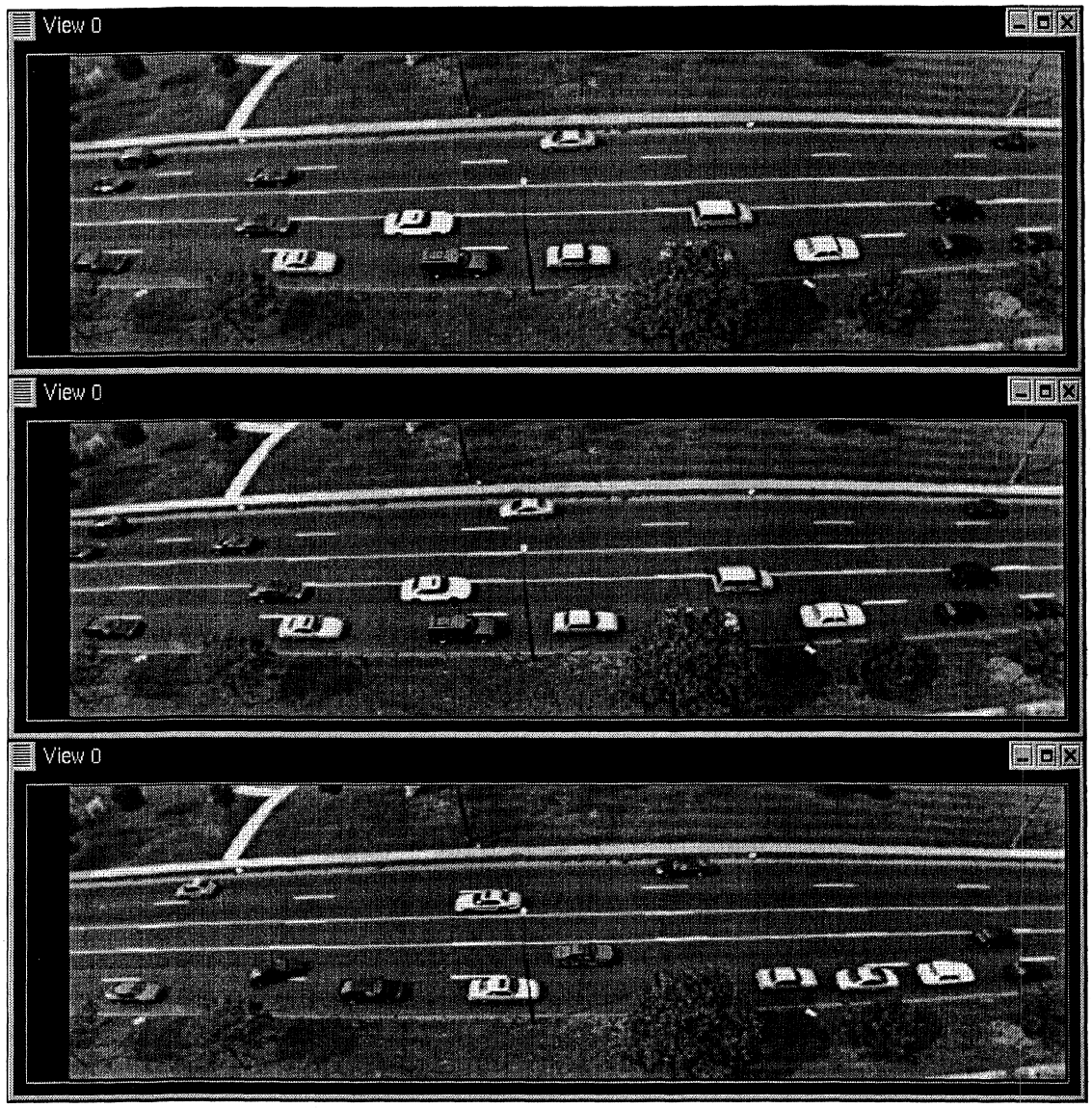

Figure 4.1.1-5. Occlusion by a Tree

Other environmental factors include weather and lighting. In rainy conditions, rain drops land on the camera lenses producing distorted images. In windy conditions, the towers sway, which results in points on the road moving within the image over time. In snowy conditions, the cameras compensate for the overall brightness by reducing the contrast to the point that the images are difficult to process. Night presents special problems because the overall illumination is low but the vehicle headlights illuminate the road and each other. There was no attempt to collect or process data under any of these conditions, therefore the Trackfile Production Subsystem has not been tested under these adverse conditions.

The primary environmental factor affecting both data collections was the scene illumination. For image processing purposes, the best conditions are consistent, diffuse sunlight with no shadows. Bright sunlight results in strong shadows which are difficult to distinguish from vehicles and cause vehicles to appear to be touching because the shadow

of one vehicle touches another vehicle. Additionally, trees and light poles can cast shadows on the road, further complicating the image interpretation process. The Trackfile Production Subsystem operates on images with shadows but the performance is degraded. Figure 4.1.1-6 shows an example of an image with strong shadows. In this case, the shadows appear to extend the lengths of the vehicles. When the sun is from the side, the shadows will appear to extend the width of the vehicles.

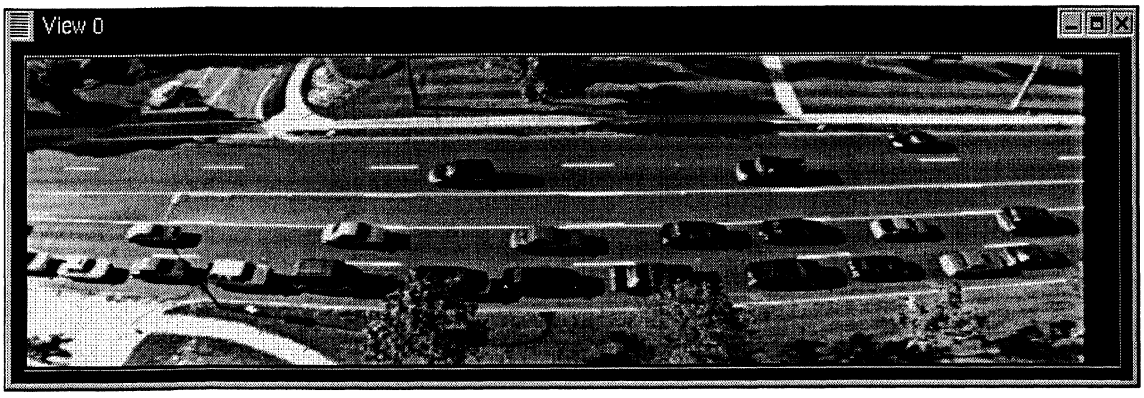

Figure 4.1.1-6. Strong Shadows

Another illumination problem occurs on partially cloudy days. As clouds move across the sun, parts of the road are brightly illuminated and other parts are in the shadow of the clouds. The variation over time can cause problems with the process for maintaining the background image. Within any one image, the inconsistent illumination makes the segmentation process more difficult. Data with extreme illumination problems were not selected for processing by the Trackfile Production Subsystem. Figure 4.1.1-7 shows an image with partial cloud cover. The right half of the image is much brighter than the left half.

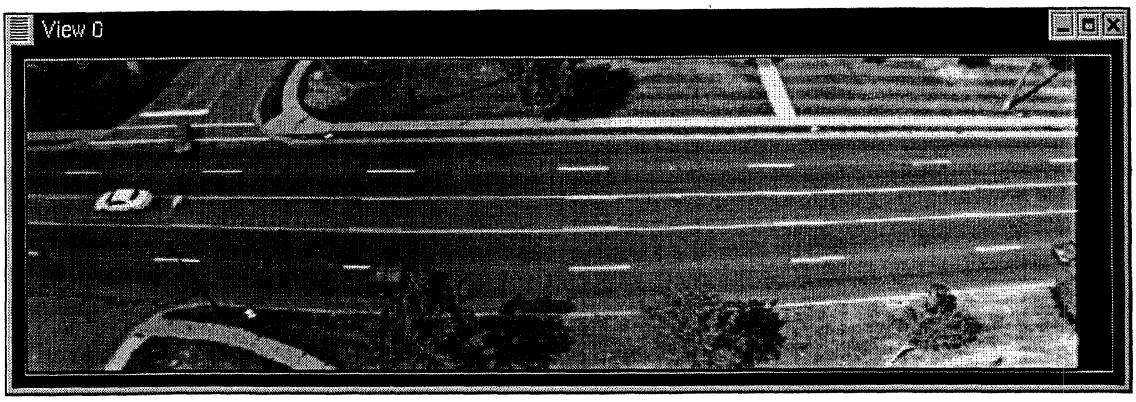

Figure 4.1.1-7. Partial Cloud Cover

System-related factors derive from a variety of sources including auto-iris instability, image synchronization problems, image noise, and tower motion. Auto-iris problems in the cameras can result in slow or rapid anomalous variations in overall image intensity. These variations are a challenge to the detection algorithm which uses a background subtraction approach to detect vehicles. Data from the 1996 collection did not have auto-iris problems but nearly all of the data from the 1999 collection suffers from anomalous intensity variations of some degree. In the 1999 data collection, rapid variations typically result in problems with three to five consecutive images. The Trackfile Production Subsystem was usually able to identify images where the intensity variation made it impossible to detect vehicles. For these cases, no vehicles were identified but the prediction process made it possible to continue tracking the vehicles until the image intensity returned to normal. Figure 4.1.1-8 shows a sequence of seven frames (covering 0.7 seconds) which contains an intensity variation incident. Maximum brightness levels appear in the first and seventh frames compared with minimum of the fifth frame.

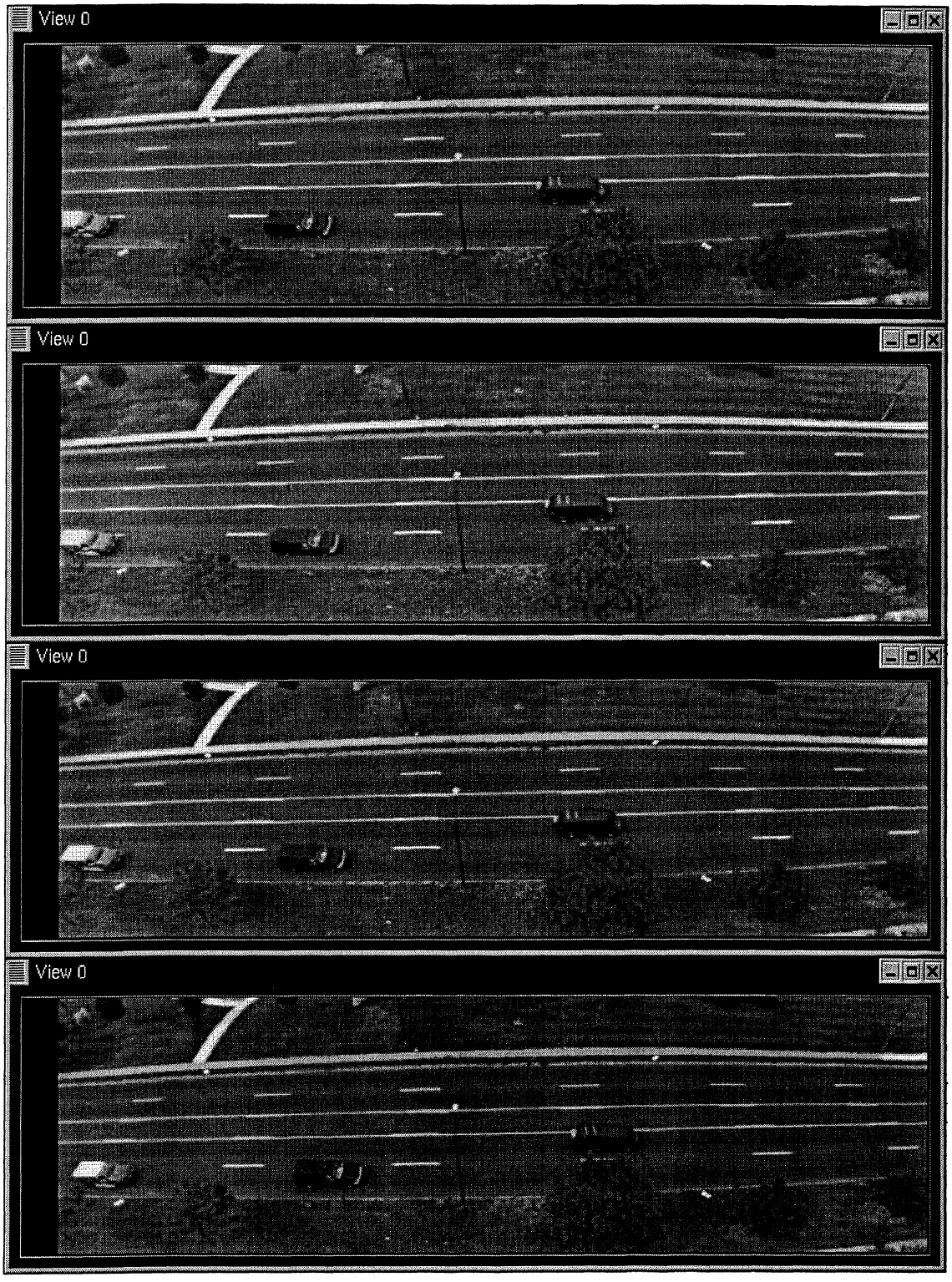
View 0
View 0
View 0
View 0

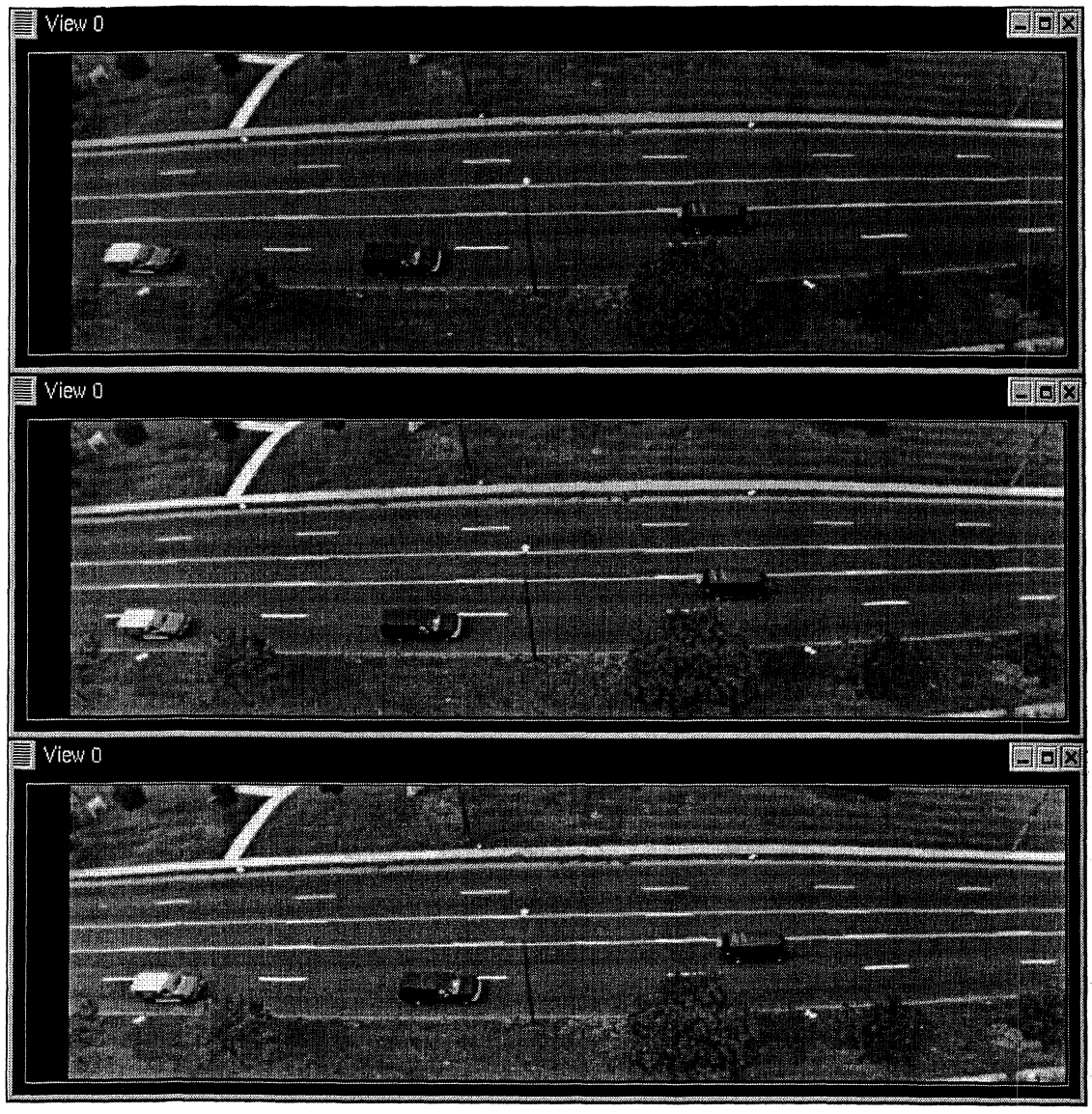

Figure 4.1.1-8. Rapid Intensity Variation

Cable noise problems can cause the collection system to trigger between normal image collection times resulting in an additional frame being inserted into the sequence for one of the cameras. We have also observed cases where one to five images were not saved. There is a correlation wherein dropped frames usually occur after a corrupted frame. These corrupted frames typically are divided horizontally with either the top or the bottom part being normal and the other part containing data from the full camera image either above or below the 200 middle rows normally recorded. Figure 4.1.1-9 shows a corrupted image. The bottom third of the image is correct but the top two thirds contain data that is from the bottom of the full camera image that should never be seen because it is below the 200 middle rows that are normally recorded.

Figure 4.1.1-9. Corrupted Image

If the missing or extra frame problems are not corrected, the vehicles in the images will appear to slow down or speed up due to the extra or missing frames respectively and all following images will be out of synchronization. The synchronization problems cause problems with the merging of tracks from the two cameras because a vehicle will not be at the same location in both views if the frames are out of synchronization. Data from the 1996 collection did not have synchronization problems but all of the data from the 1999 collection does suffer from synchronization problems. Deleting extra frames or adding blank frames to fill gaps corrected synchronization problems. The Trackfile Production Subsystem was able to track vehicles normally after synchronization correction. The short runs of blank frames used to fill gaps did not present a problem to the tracking algorithm.

An image noise problem seen during the 1999 data collection was the horizontal bar problem. It appeared to be related to cable noise. The problem was that at a large number of points throughout an image, a pixel value was repeated for a small number of pixels to the right of the point. The effect was most visible when it happened near a contrast boundary in the image. This problem affected only a few days of data from the 1999 collection. Data with the horizontal bar problem were not selected for processing by the Trackfile Production Subsystem. Figure 4.1.1-10 shows an example of an image with the horizontal bar problem.

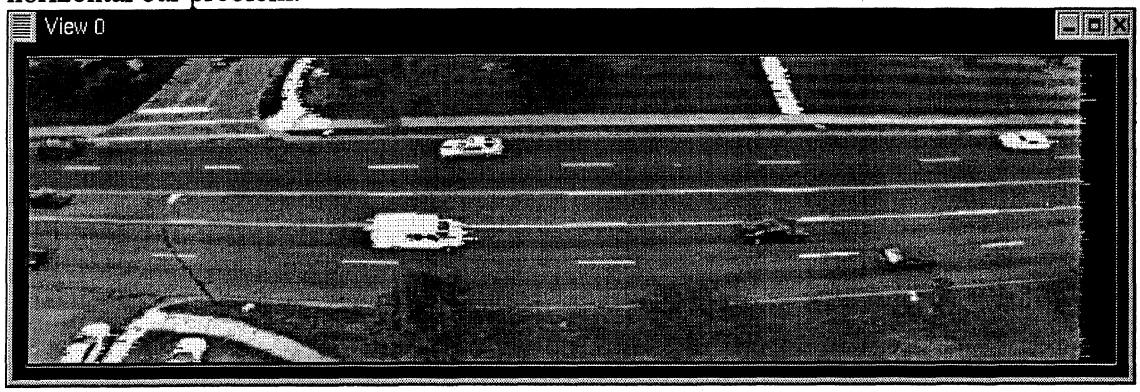

Figure 4.1.1-10. Horizontal Bar Problem

Under windy conditions, the towers sometimes sway resulting in a small shift in the area imaged by the camera. Although the shift was typically only a pixel or two, it sometimes

resulted in vehicle detection problems due to the background subtraction approach used to detect vehicles. This problem was present in many of the datasets from the 1996 collection but only a few of the datasets from the 1999 collection. The Trackfile Production Subsystem contains algorithms which detect and compensate for tower motion by shifting the image. This process corrects the most problematic case, when the towers are moving sideways. It does not compensate for forward or backward motion. The Trackfile Production Subsystem was usually able to track vehicles under moderate tower motion conditions. Data with the most extreme tower motion problems were not selected for processing by the Trackfile Production Subsystem.

4.1.2 Samples of Trackfile Overlays on Scene Video and Associated Artifacts

Figures 4.1.2-1 through 4.1.2-5 show representative trackfile overlays corresponding to particular vehicle maneuvers. The indicated trajectory in each figure corresponds to the centroid location of a particular vehicle — determined by image processing — as it moves through the scene. These path trajectories represent the x-y trackfile data output of the image processing system (following transformation into the ground-plane road coordinates.) and constitute the raw data input to the final data processing and analysis stage outlined in section 3.3 and Appendix C.

If these raw x and y trackfile time histories are examined in more detail, two basic types of artifacts tend to be seen to varying degree on a fairly regular basis. The first artifact relates to irregularities in vehicle trajectory as a vehicle enters or exits a scene along the outside camera boundaries. These edge effects are primarily attributable to certain fish-eye camera distortions along the boundary areas as well as greater problems associated with accurately locating a vehicle's centroid position when it is only partially visible in the scene (e.g., half in, half out) during entry/exit. Consequently, the raw x and y trackfile data are generally less accurate and more irregular in these boundary zones. Figures 4.1.2-6 and 4.1.2-7 show an example of the raw x longitudinal position (left-right direction in the scene) time history. Figure 4.1.2-6 shows the entire time history across the scene (moving from east to west) and indicates a fairly linear relationship (more or less constant speed movement). However, Figure 4.1.2-7 is an enlargement showing the first 1.5 seconds of the same data as the vehicle enters the scene and, on this scale, certain nonlinear irregularities in the data are now observed in the entry region corresponding to the first one second, or so, of time. (The straight reference line also appearing in this figure is a simple extrapolation of the interior scene data out to the edge.)

The other type of data artifact occurs when imagery from one camera is handed off to the next camera within the image processing stage. These camera handoff artifacts can occasionally cause significant lateral path disturbances to occur that lead to later complications in the data processing activities described in Section 3.3. Examples of this type of camera handoff artifact are seen in Figures 4.1.2.8 and 4.1.2.9 where sizeable artificial jumps occur in mid-scene for the lateral y-position data (vertical direction in the scene). (These particular data correspond to two of the validation runs performed with test cars. Onboard vehicle measurements indicate more or less straight-line movement across the scene.) The primary effect of these lateral path artifacts is to cause subsequent data processing calculations to assume that a small lane-change or path disturbance has occurred and to then process the data accordingly to reflect such path motions.

Since these types of path irregularities are known to be artificial, one way of ameliorating their effects is to smooth the raw data with a moving average window prior to passing it along to the final stage of data processing. The smoothing process can best attenuate short-term, temporary disturbances that occur in the data. Those disturbances that are more stepwise in nature, causing a more constant-like lateral shift in position from one camera to the next, are only partially helped by the smoothing operation.

Too much smoothing of course can cause legitimate high frequency lane-change or similar maneuvers to be distorted, causing attenuation of certain high frequency motion content in subsequent data processing stages. The typical frequency content of the vast majority of vehicles seen in this first set of SAVME data does not fall into a category described as rapid maneuvering. Consequently, a moving average smoothing window of 2.0 seconds was applied to all SAVME data to help minimize the effects of the described raw data artifacts.

A small subset of these data, the validation maneuvers conducted with two test cars under the view of the SAVME cameras as described in Section 4.2.1, did include several rapid lane-change and double lane-change maneuvers. These particular validation data were then also processed using a 0.6 second moving average window to illustrate and compare the effects of the level of raw data smoothing on subsequent data processing results for maneuvers containing higher frequency motion content. These results are seen in the validation data of Section 4.2.1.

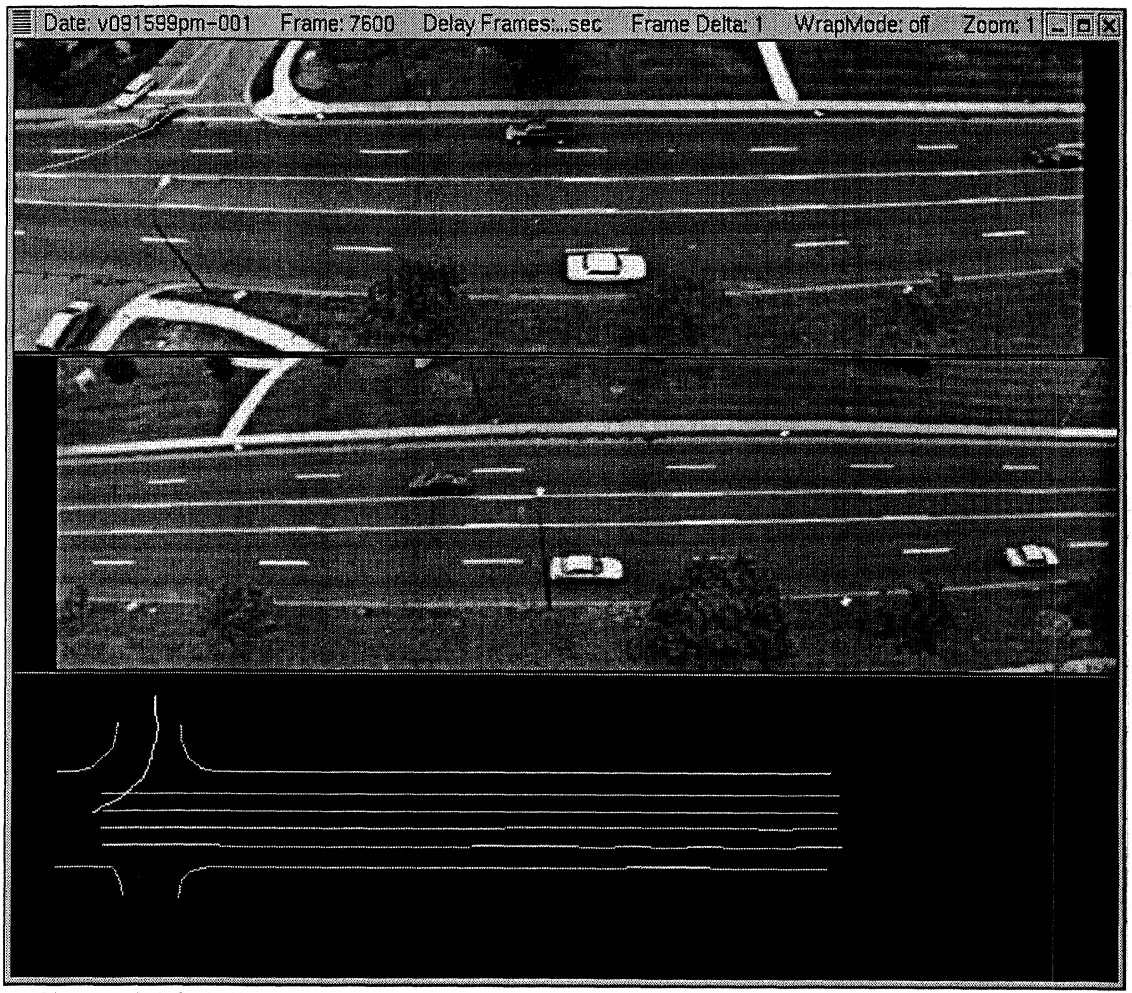

Figure 4.1.2-1. Example Images from the West (top) and East (bottom) Cameras Car Turning into Driveway Across Westbound Traffic (top left scene)

Figure 4.1.2-2. Example Images from the West (top) and East (bottom) Cameras SUV Conducting a Left Lane-Change Passing Maneuver (East camera mid-scene)

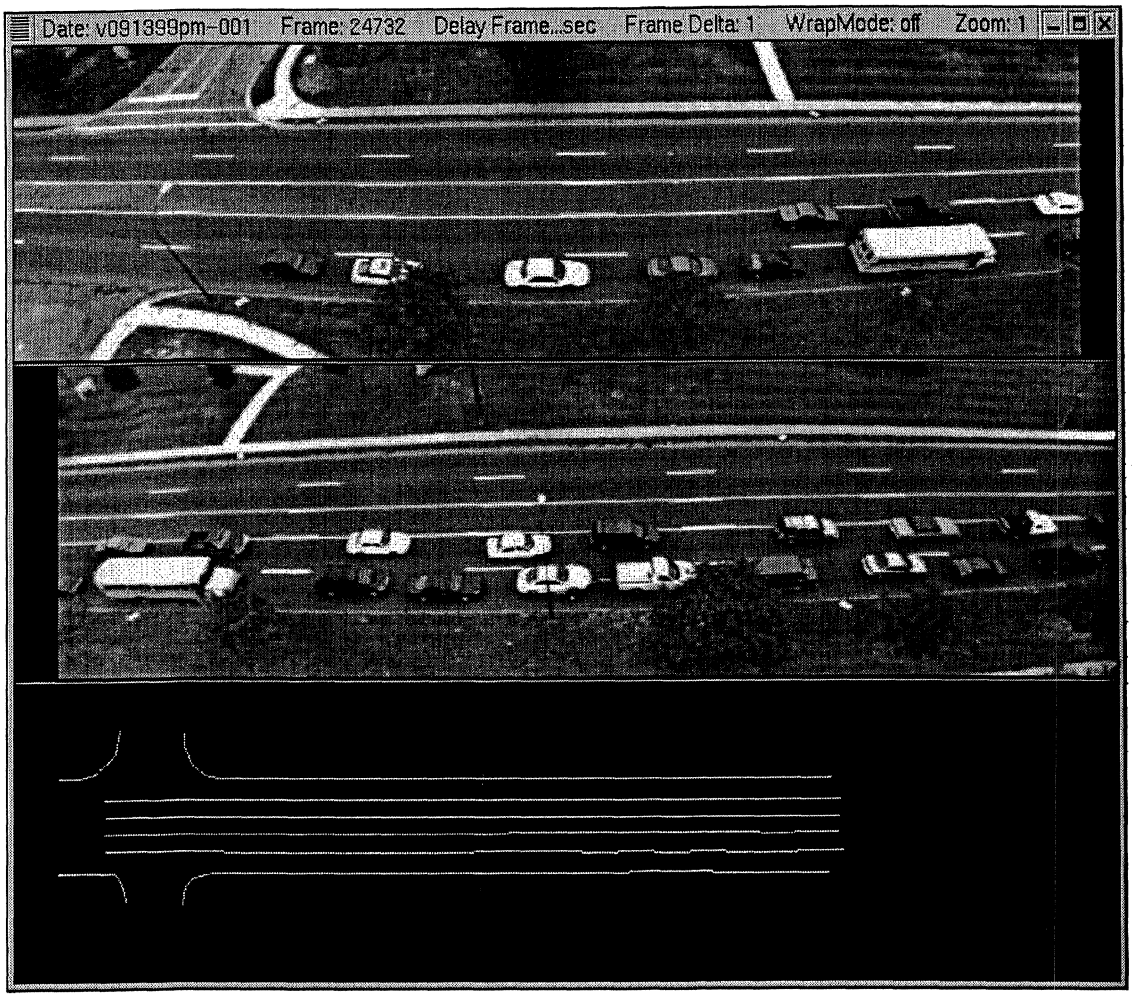

Figure 4.1.2-3 Example Images from the West (top) and East (bottom) Cameras. Traffic Queue Developing in Eastbound Lanes.

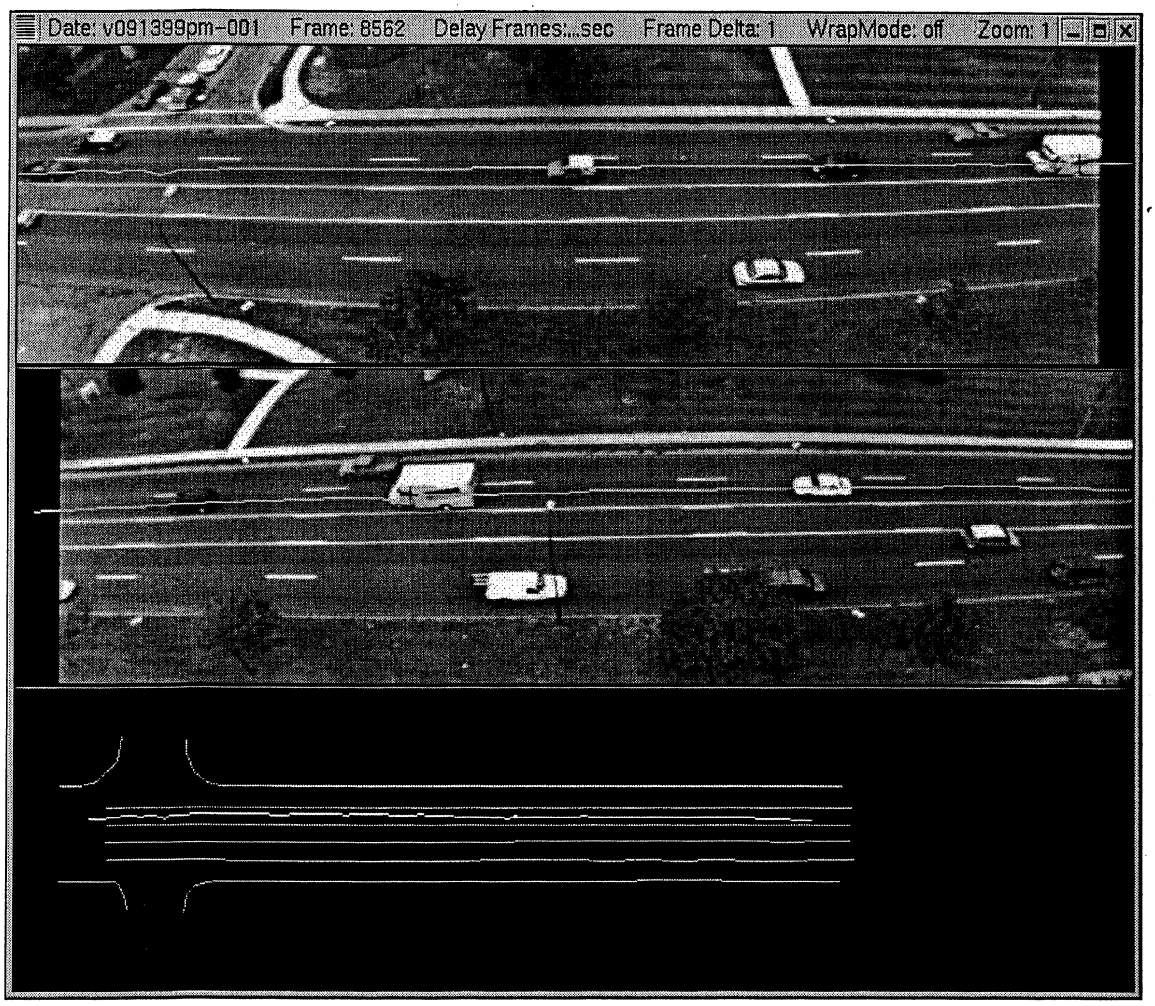

Figure 4.1.2-4. Example Images from the West (top) and East (bottom) Cameras Vehicle Being Passed on Right (Pick-Up Truck Passing White Van)

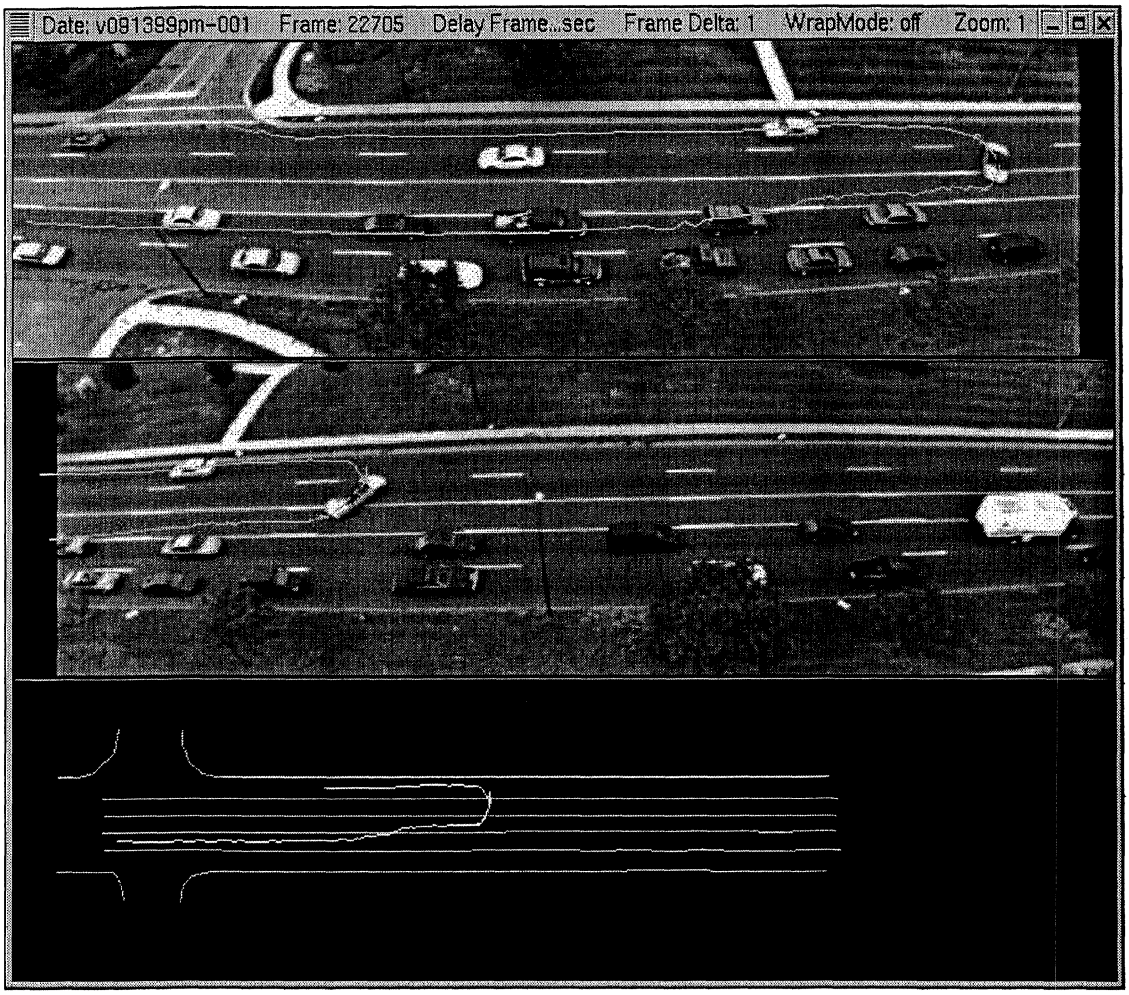

Figure 4.1.2-5. Example Images from the West (top) and East (bottom) Cameras. U-turn in Heavy Traffic.

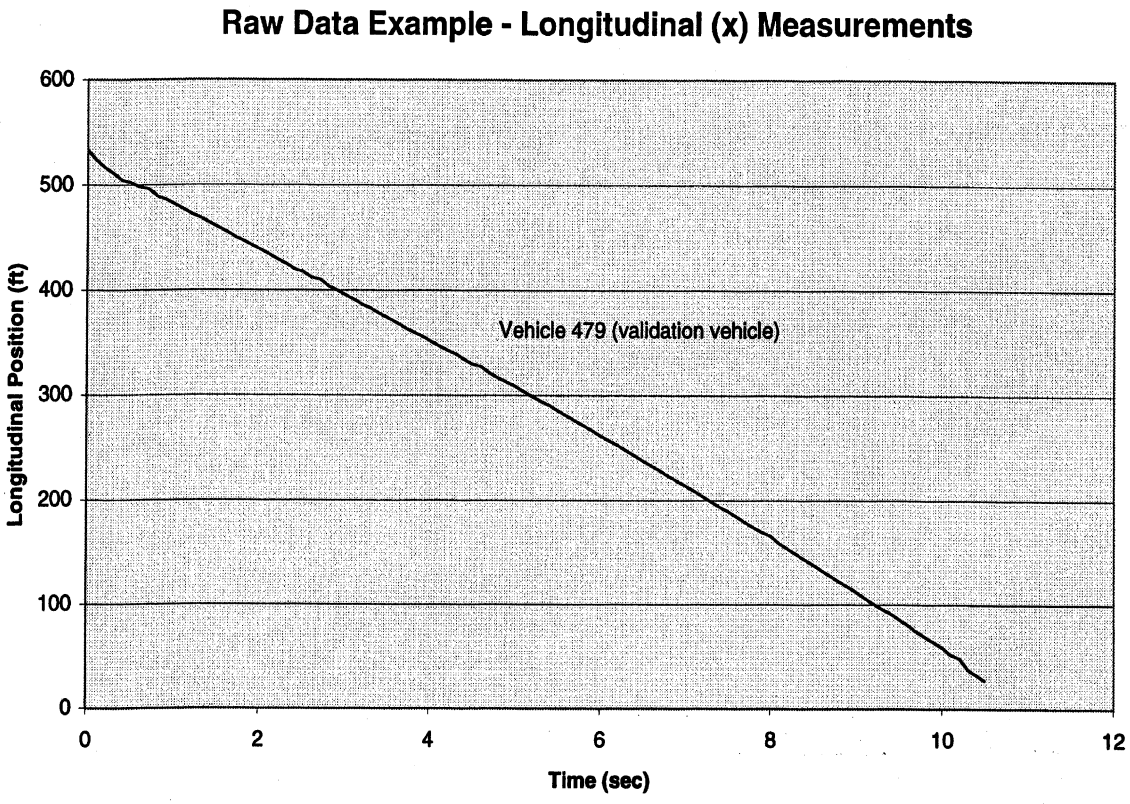

Figure 4.1.2-6. Example Raw Data - Longitudinal Position vs. Time

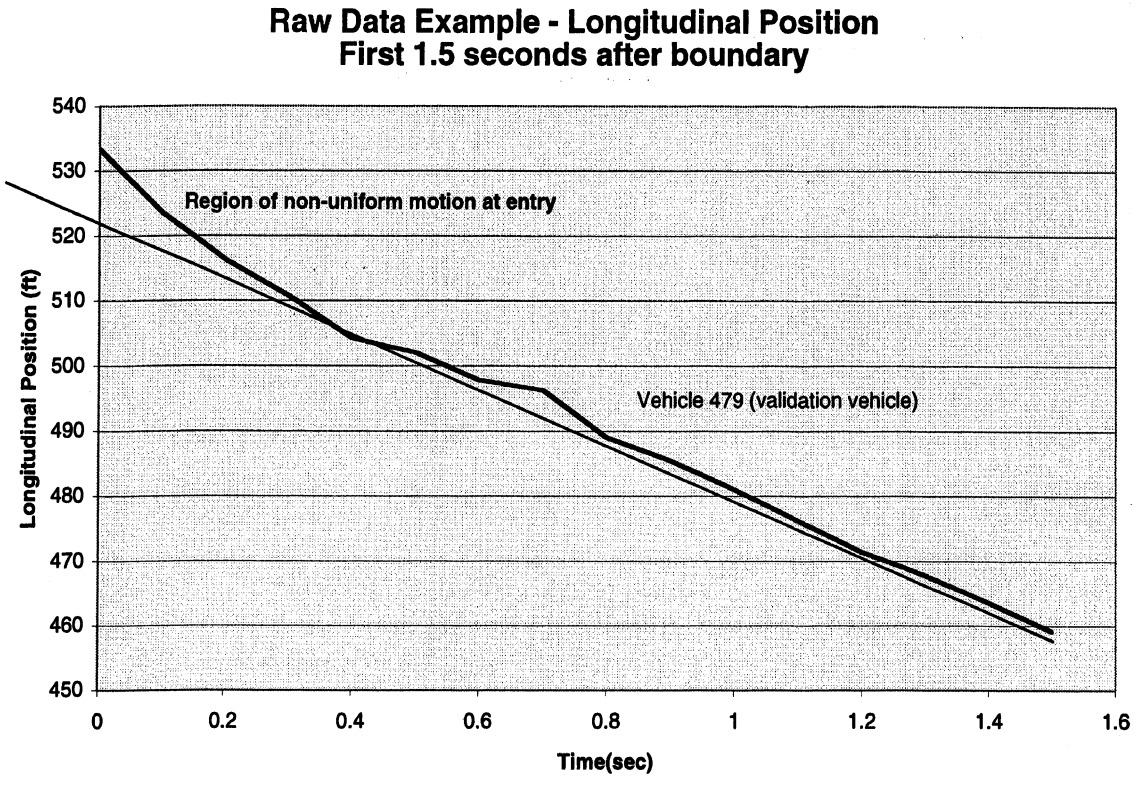

Figure 4.1.2-7. Enlarged Scale - Raw Data Irregularities near Endpoints

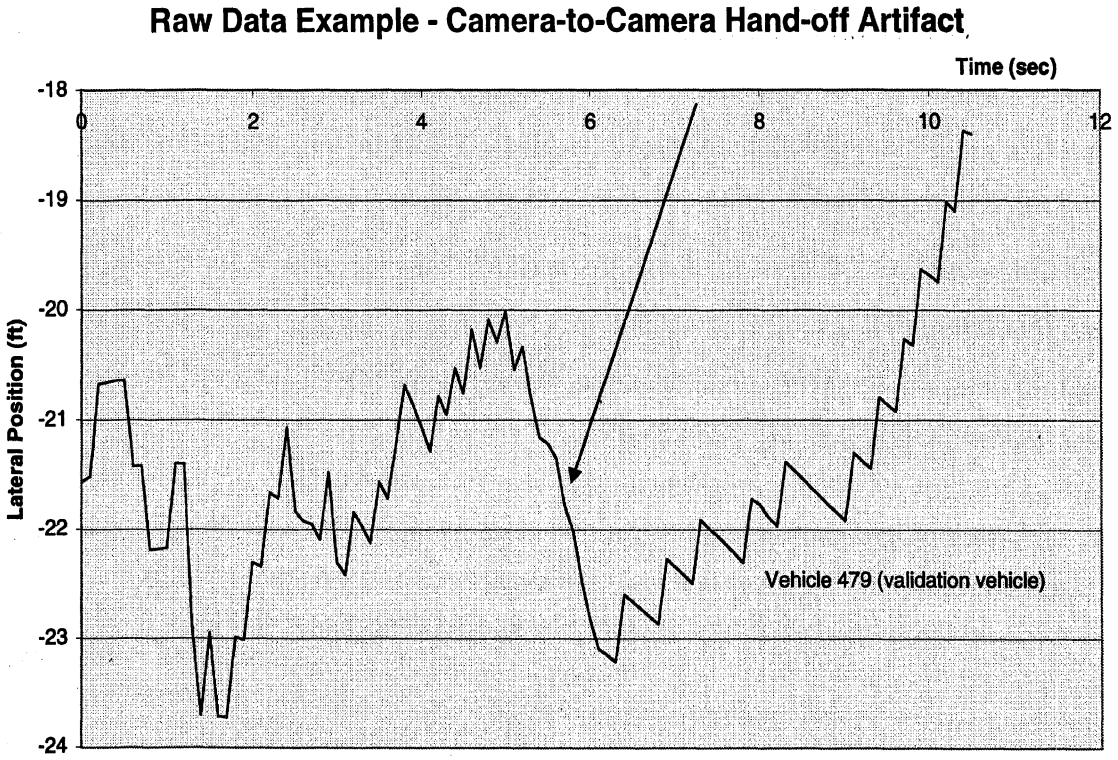

Figure 4.1.2-8. Raw Data Artifacts. Camera-to-Camera Hand-off

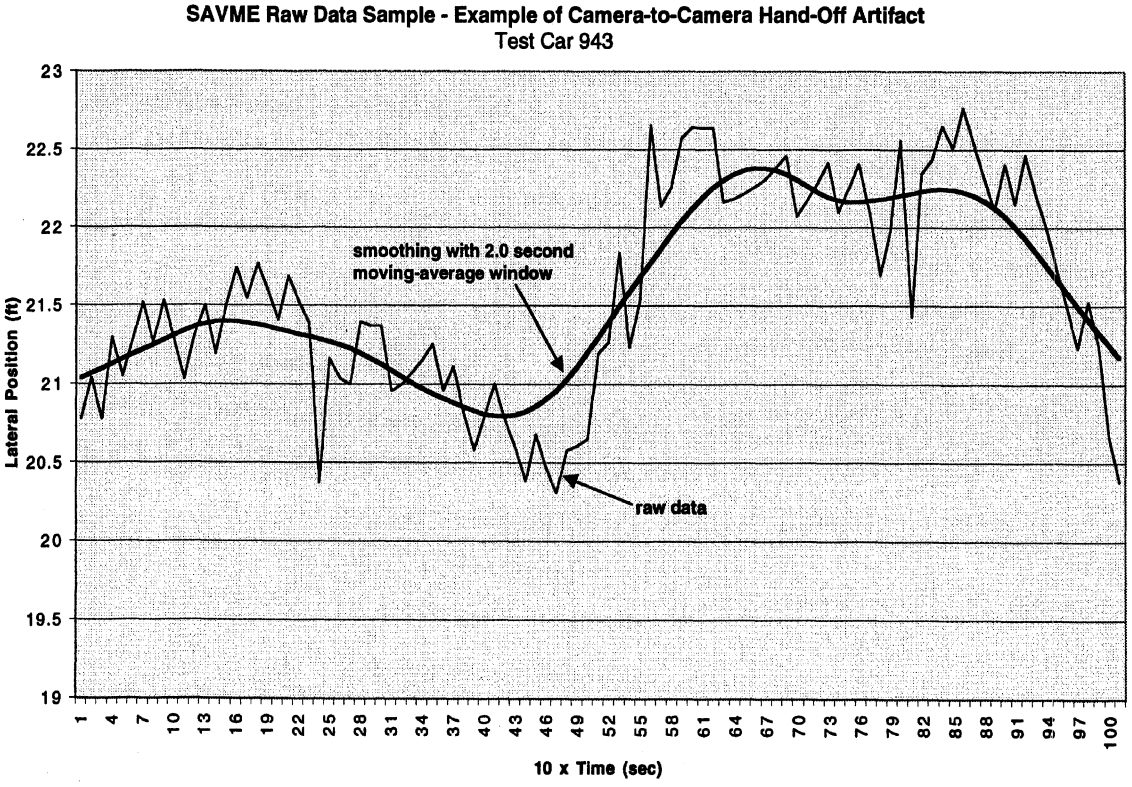

Figure 4.1.2-9. Raw Data Artifacts and Effect of Smoothing

4.2 Results from Final, Archival Trackfiles

4.2.1 Validation of the Trackfile Data

A special series of test maneuvers were conducted with two identical instrumented vehicles under the surveillance of the SAVME cameras. The test measurements collected by the onboard data collection system of each car were then compared directly against the same measurements provided by the SAVME camera and data processing system.

Test Vehicles and Instrumentation

The two test cars were identical 1996 Chrysler Concordes equipped with a Leica range sensor. The Leica range sensor package provided measurements of range-rate and vehicle yaw rate. (Both test vehicles participated in the previous National Highway Traffic Safety Administration (NHTSA) field operation test program on intelligent cruise control.)

Other vehicle measurements also included vehicle speed provided by the Chrysler engine controller and a Global Polishing Satellite (GPS) package providing latitude and longitude (x-y location) of each vehicle. (Initially, the GPS system was expected to provide a differential GPS signal that would be accurate enough to compare with the SAVME data, but a suitably performing differential GPS capability could not be implemented.)

The accuracy of the five measurements rank from highest to lowest as:

- range
- range-rate (after accounting for a known time delay of about 0.5 seconds)
- yaw rate
- forward speed (as an engine controller signal)
- GPS (x,y)

Test Maneuvers Conducted at the SAVME Site

Five different test maneuvers were conducted by the two test vehicles at the SAVME site. The maneuvers included:

- Steady Following — Test vehicle A and test vehicle B enter the scene in single-file at about the same constant speed and progress across the field of regard at an approximately constant range.
- Lead Vehicle Braking — Test vehicle A and test vehicle B enter the scene in single-file at about the same constant speed. Lead vehicle A then performs a braking maneuver to low speed and accelerates out of the scene. Following vehicle B brakes accordingly in response to the lead vehicle braking. It also slows to a low speed and accelerates likewise out of the scene.
- Passing and Cut-In Maneuver by the Following Vehicle — Test vehicle A enters the scene first in the right-hand lane and drives across the scene at constant speed. Test vehicle B enters the scene behind and to the left of vehicle A in the passing lane. Vehicle B is travelling at a faster speed and proceeds to pass Vehicle A on the left and then briskly cuts in front of vehicle A. Both vehicles leave the scene in single file with vehicle B now ahead of vehicle A.
- Double Lane Change by the Following Vehicle — Vehicles A and B enter the scene at about the same speed in single file formation in the right lane. Following vehicle B then conducts a brisk double lane-change maneuver behind vehicle A, moving from the right lane to the left lane and then back into the right lane.
- Left Lane Change and Braking by the Lead Vehicle — Both vehicles enter the scene in single file in the passing lane at about the same speed. Lead vehicle A performs a lane-change maneuver into the left-hand center turn lane and brakes to a stop. Following vehicle B proceeds ahead at the same speed in the same lane.

In each of these maneuvers, the range sensor from one of the two test cars is sensing the other vehicle during portions of each maneuver during which one test vehicle is ahead of the other vehicle (i.e., in sight of that car's range sensor). For example, during the double lane-change maneuver by the following vehicle, the range signal on the following vehicle initially acquires the lead vehicle in the same lane ahead. As the following vehicle then proceeds to conduct the double lane-change maneuver behind the lead vehicle, the range signal will be temporarily lost but then reacquired as the following vehicle re-enters the initial travel lane behind the lead vehicle. At all times during each vehicle's traversal across the field of regard, the vehicle speed and yaw rate signals from each vehicle are being measured.

The following set of graphs and accompanying discussion provide direct comparisons of the data produced by the SAVME processing system with representative test data from the two test vehicles collected for three of the most interesting and challenging maneuvers (lead vehicle braking, passing and cut in maneuver by the following vehicle, and the double lane change by the following vehicle.)

Lead Vehicle Braking Maneuver Comparison (SAVME vs. Test Cars)

Figure 4.2.1-1 shows a direct comparison between the SAVME system estimate of vehicle speeds and those measured onboard the test vehicles. The labels "351" and "353" refer to the SAVME vehicle ID tags used to identify the two vehicles in the SAVME database. As seen, the speed estimates from the SAVME system are in general agreement with the test car data except at the very end and beginning of SAVME data coverage (commonly caused by entry and exit irregularities in the raw data as noted previously). Also in the very center scene area, there is another small region of discrepancy also possibly related to the camera handoff artifact in the raw trackfile data (likewise discussed previously). Speed measurements provided by the engine controller will occasionally go into an unexplained hold state, an example of which anomaly appears in Figure 4.2.1-1 for car 353 at about the 6-second mark.

The lower portion of the same figure shows a comparison of range-rate measurements provided by the SAVME system and the onboard Leica sensor (from the following vehicle). Again, very good agreement is seen in these data except for a small region around the 4-second mark where the Leica sensor appears to be reading abnormally low (assuming the forward speed measurements are reasonably accurate and that their difference is the range-rate measurement).

Figure 4.2.1.2 shows the corresponding range measurement comparison for the same test maneuver. As noted above for the vehicle speed measurements, the range signal comparison is very good, particularly in the mid-scene region of each camera. Mild discrepancies are noted at the endpoints and in the center area — and are likely attributable to the entry/exit and camera handoff artifacts in the raw data.

Figure 4.2.1-3 provides the same data plotted on the conventional range vs. range-rate diagram commonly used in headway control analyses.

Lastly, Figure 4.2.1-4 illustrates an advantage of SAVME data in conducting certain types of analyses — this one related to headway control and warning. Seen in the figure are plots of lead vehicle and following vehicle acceleration signals computed directly by the SAVME (Kalman filter) system and stored in the SAVME database. Range acceleration, a common response variable used in certain headway control formulations, is simply the difference between the lead and following vehicle accelerations and is likewise plotted on the same graph. Lastly, the NHTSA[1] warning algorithm, which is easily calculated if lead vehicle and following vehicle accelerations are available, is also plotted on the graph (using an Rmin value of 7 feet in this example). As indicated, the NHTSA warning in this case would have been issued for about 1.5 seconds during the braking maneuver — assuming an implementation design that does not cancel the warning following a brake application by the following vehicle driver. (In this case, the following vehicle driver is braking, but not aggressively enough to prevent a collision prior to a complete stop, if all

[1] Burgett, A.L.; Carter, A; Miller, R.J.; Najim, W.G.; and Smith, D.L., "A Collision Warning Algorithm for Rear-End Collisions," *16th International Technical Conference on Enhanced Safety of Vehicles Abstracts*, 98-S2-P-3 1, Washington, D. C., May 1998.

prevailing braking conditions were held constant for the remainder of the stop a la the NHTSA algorithm.)

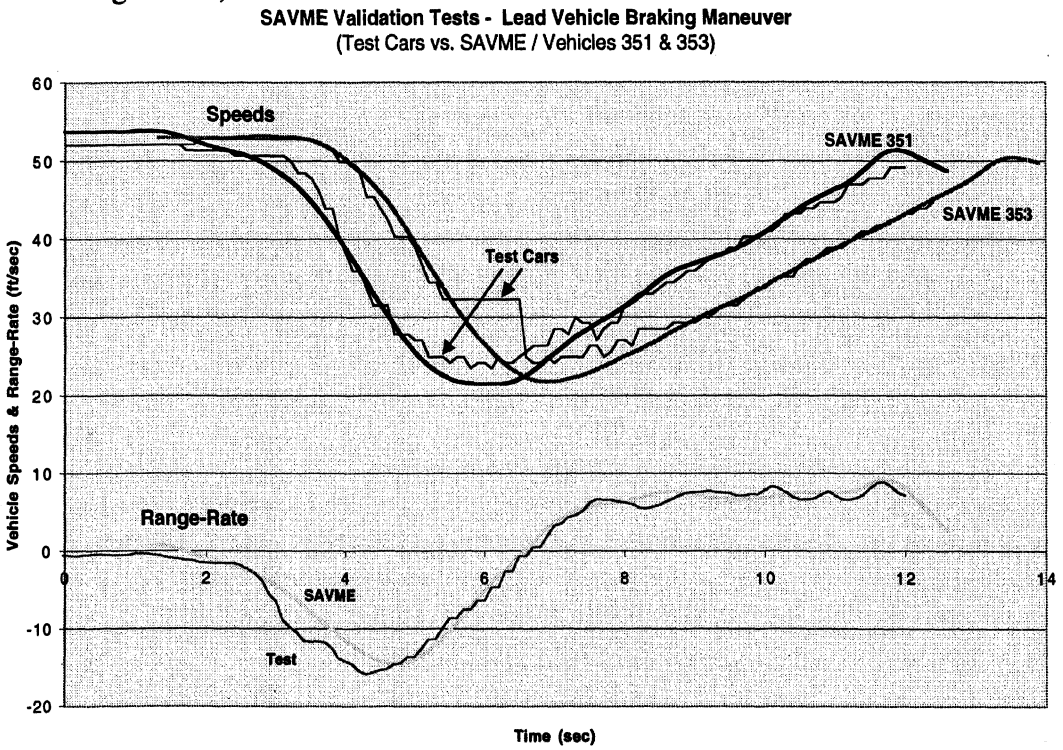

Figure 4.2.1-1. Lead Vehicle Braking Maneuver – Validation

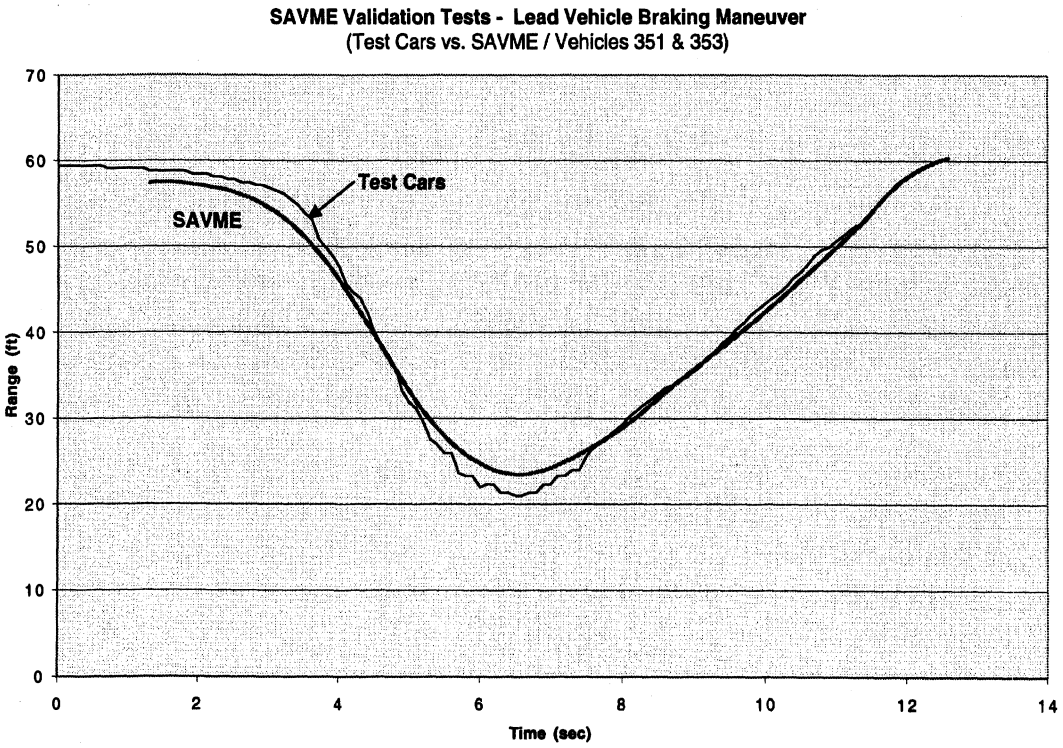

Figure 4.2.1-2. Lead Vehicle Braking Maneuver – Validation

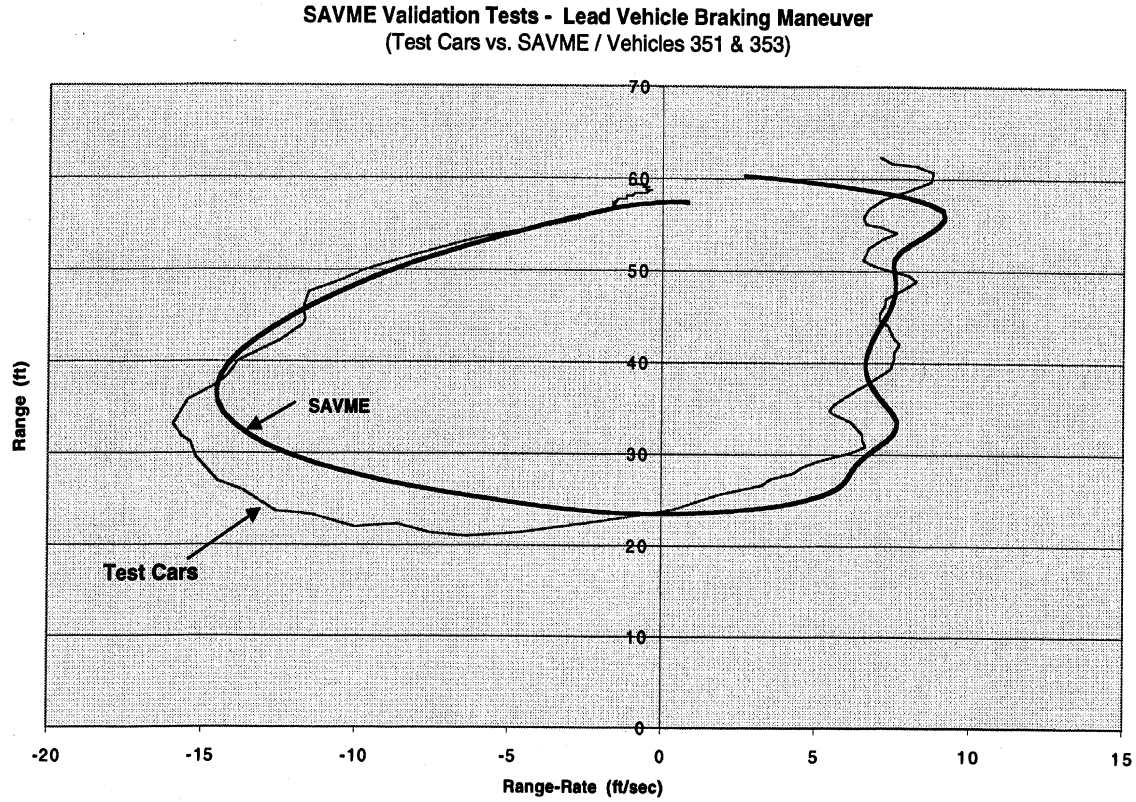

Figure 4.2.1-3. Lead Vehicle Braking Maneuver – Validation

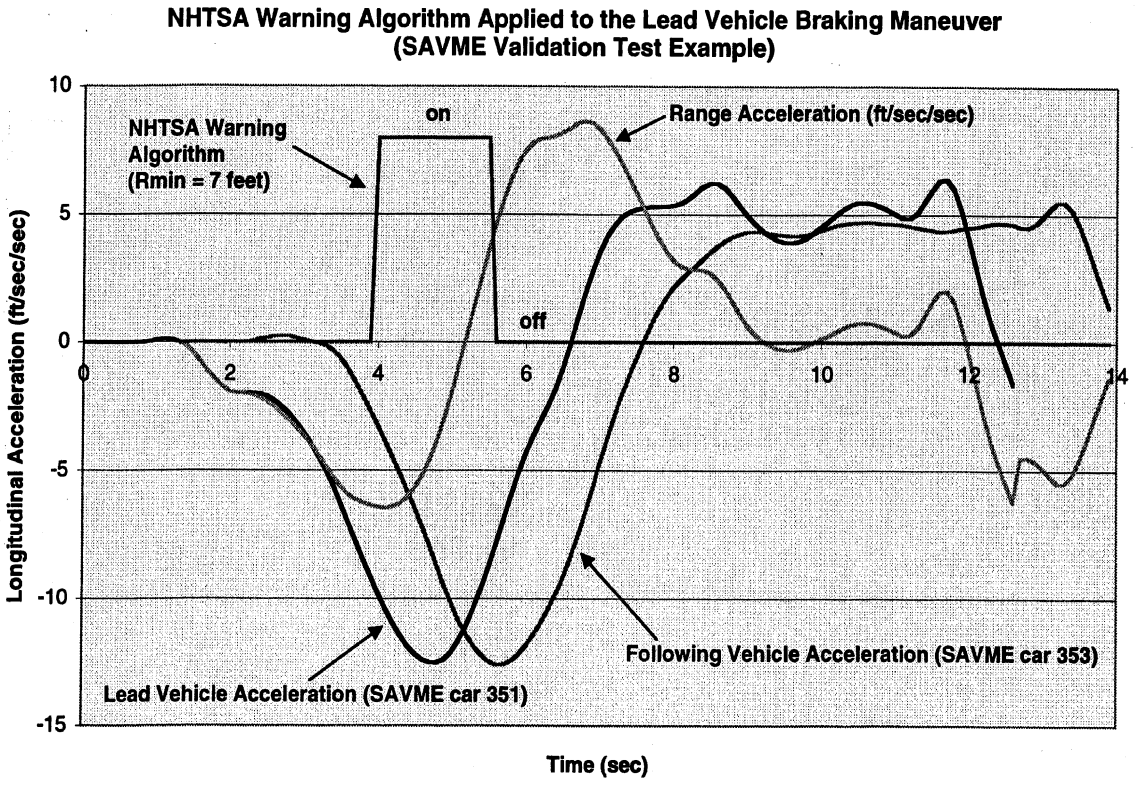

Figure 4.2.1-4. Lead Vehicle Braking Maneuver – Validation

Double Lane Change by the Following Vehicle (SAVME vs. Test Cars)

Figure 4.2.1-5 shows the range and range-rate comparisons for the SAVME and test car measurements. Recalling that the test cars initially enter the scene in single file prior to the double lane-change maneuver by the following vehicle, a range and range-rate measurement from the Leica sensor is initially present. During the double lane-change maneuver these signals are temporarily lost but then reacquired as the following vehicle regains the initial travel lane behind the lead vehicle. As seen, the range and range rate comparisons are quite favorable, aside from the one-second or so endpoint regions where the raw data are generally less reliable.

Figure 4.2.1-6 shows the forward speed comparisons, again indicating basic agreement except for the endpoint portions.

Figures 4.2.1-7 and 8 show the yaw rate measurement comparisons between the SAVME system and the following vehicle test data during the rapid double lane-change maneuver. The first graph illustrates the influence that a 2.0 second smoothing window for the (x,y) raw trackfile data can have on attenuating certain higher frequency information, such as yaw rate seen in this example. The same data are plotted again in Figure 4.2.1-8, but now for a 0.6 second smoothing of the raw trackfile data. The level of agreement is improved considerably here and underscores the point that a tradeoff exists between the amount of beneficial smoothing useful for helping tame the endpoint and camera handoff artifacts present in this raw data, and the degree of accuracy obtainable when estimating higher frequency responses of a vehicle.

Since the most aggressive and rapid maneuvering data present in this entire SAVME data set are represented by these particular validation runs conducted with the test cars, the vast majority of data do benefit from the 2.0 second smoothing treatment. However, a more ideal data processing scenario would include raw data with fewer and smaller camera handoff artifacts, so that a shorter smoothing window could be applied to all of the data, regardless of the frequency content present in the raw motion variables.

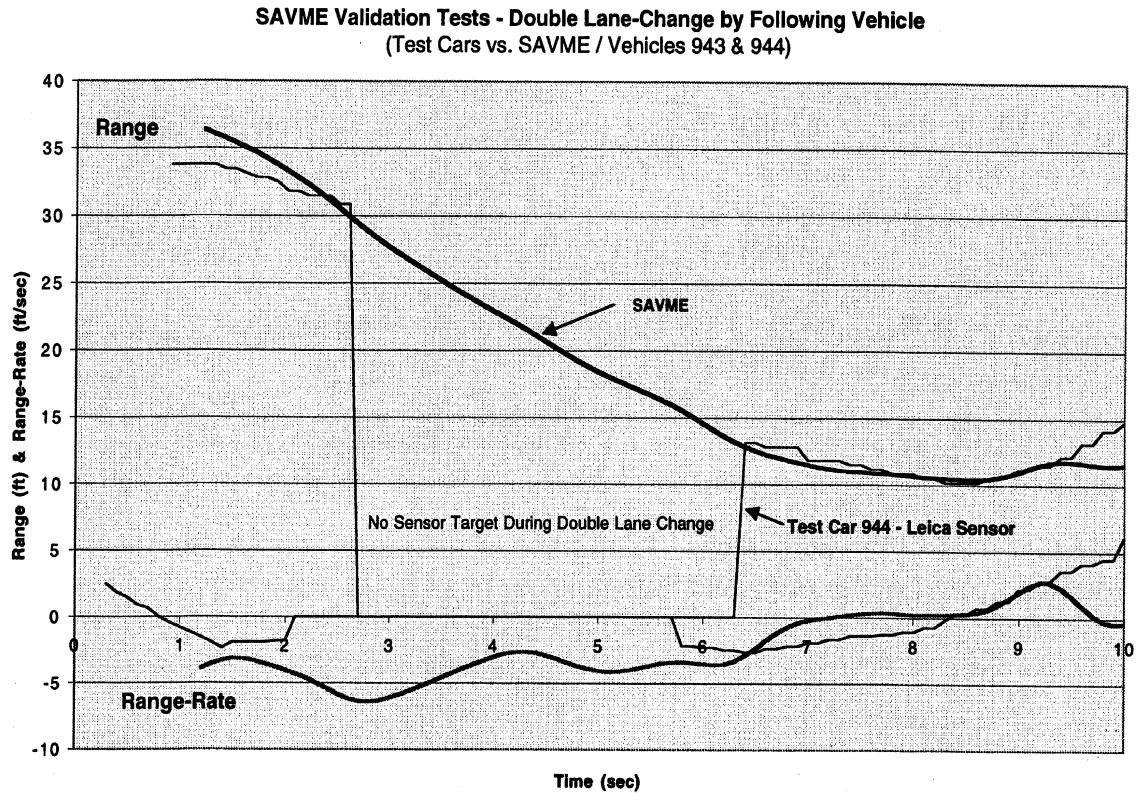

Figure 4.2.1-5. Double Lane Change Maneuver – Validation

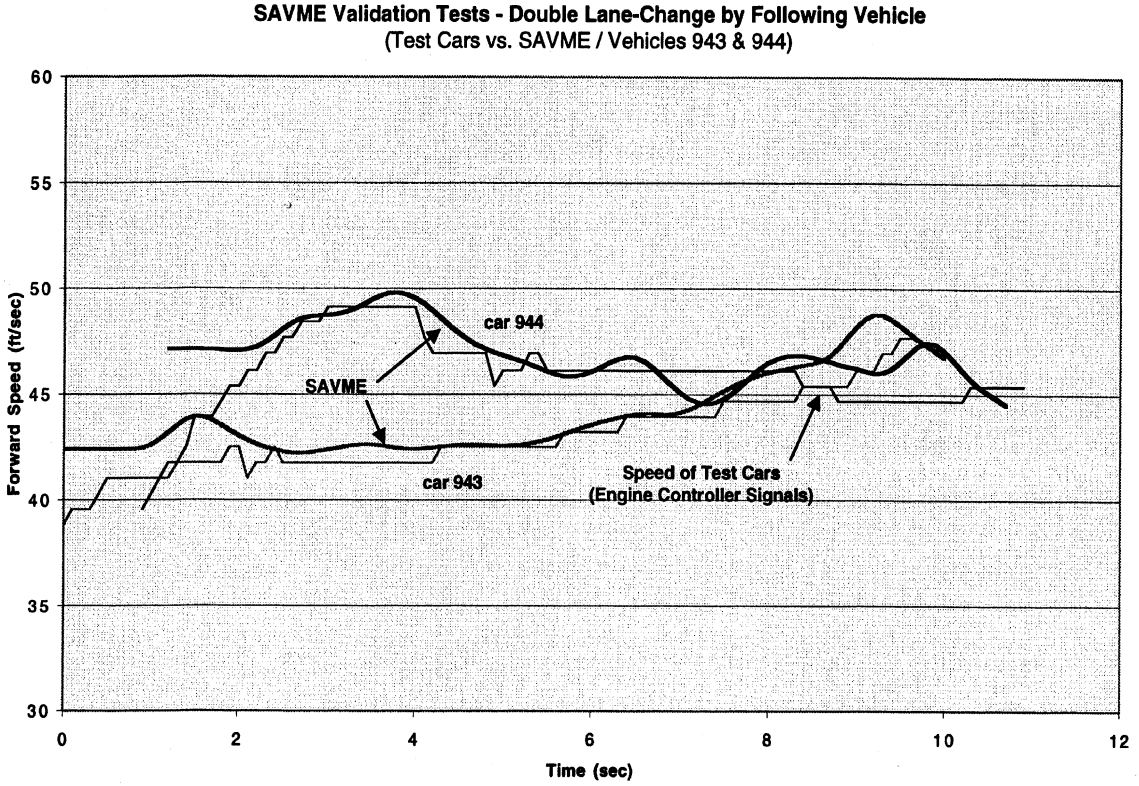

Figure 4.2.1-6. Double Lane Change Maneuver – Validation

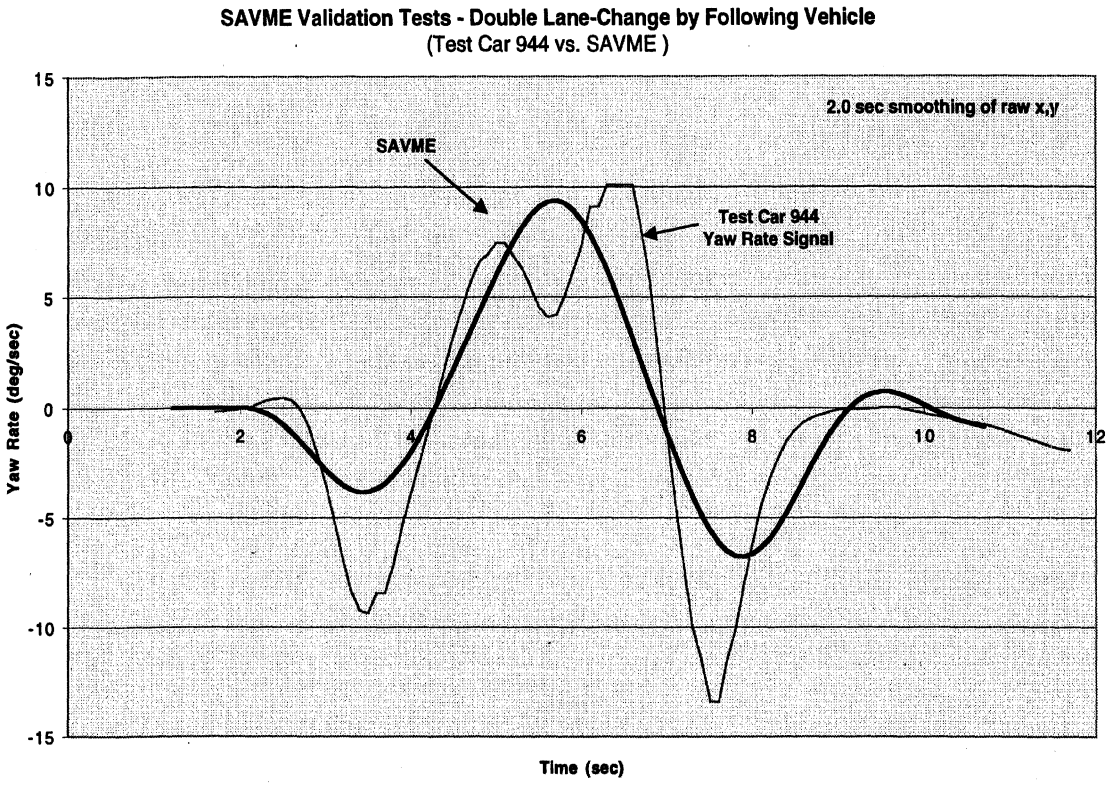

Figure 4.2.1-7. Double Lane Change Maneuver – Validation

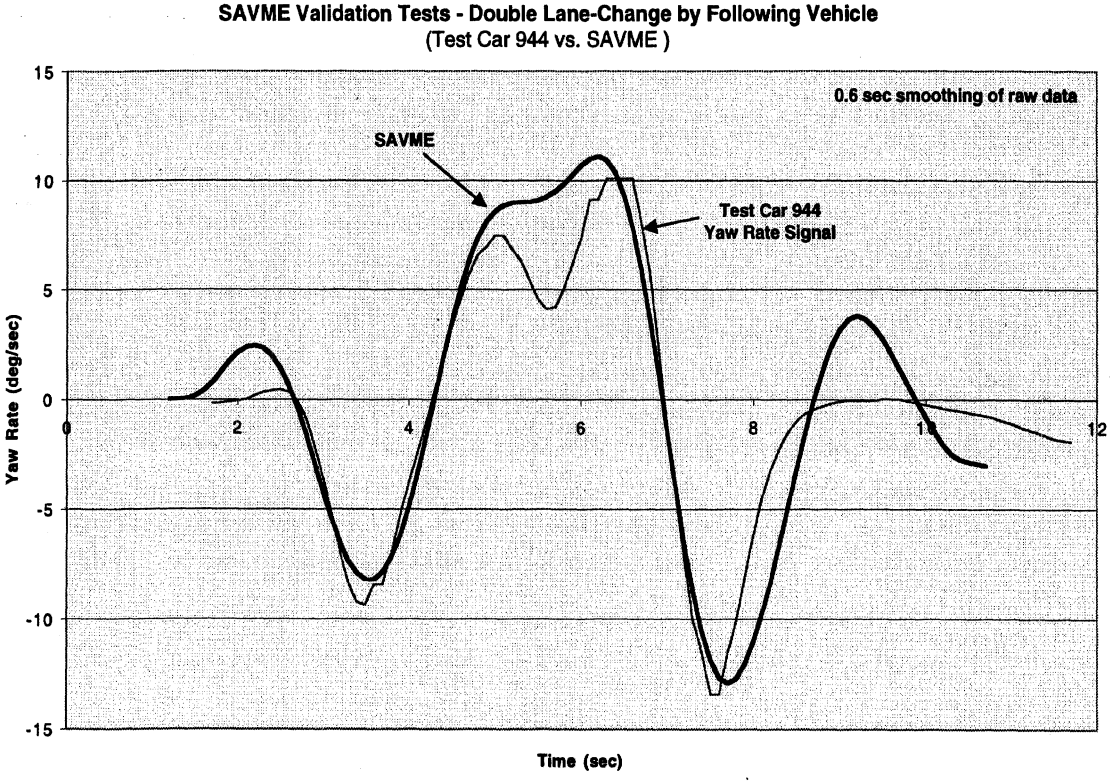

Figure 4.2.1-8. Double Lane Change Maneuver – Validation

Passing and Cut-In Maneuver by the Following Vehicle (SAVME vs. Test Cars)

Figure 4.2.1-9 shows the range measurements provided by the SAVME system and the instrumented test cars in the passing and cut in maneuver (range is defined on this graph as centroid-to-centroid distance, and the Leica range measurement has been increased by one car length to coincide with the SAVME convention during forward-looking encounters). During the initial portion of this maneuver, the passing car is behind and out of range of the sensor on the vehicle being passed. Following the cut-in (lane change) by the passing vehicle, the range signal is acquired by the vehicle behind and appears on the plot at a time of about 3.5-4.0 seconds. The agreement between the SAVME system estimate of range and that measured by the Leica sensor on the following vehicle is again quite good following the target acquisition, up to about the last one second of SAVME data (endpoint).

The SAVME range data is of course present at all times prior to the cut-in maneuver and, as noted above for this comparison, represents the centroid-to-centroid distance between the two vehicles. Thus, the closure of the passing vehicle from behind and to the left is represented on the range graph by an initial decrease in range from about 17 feet or so to a minimum value of 10 feet, where the two vehicles are side by side. The SAVME range signal then increases as the passing maneuver continues.

Figure 4.2.1-10 shows the corresponding range-rate signals from the SAVME system and the Leica sensor onboard the following vehicle. Similar agreement is seen between the SAVME data and the Leica sensor's output of range-rate.

Figure 4.2.1-11 compares the SAVME estimates of forward speeds of both vehicles with that measured onboard by the engine controller signals. Again, except for the very endpoints, the agreement is quite good.

Lastly, Figure 4.2.1-12 again illustrates the effect that raw data smoothing can have on attenuating certain higher derivative information such as yaw rate. The graph compares the onboard measurement of yaw rate corresponding to the passing vehicle during its cut-in maneuver. As seen, the higher frequency lane-change maneuver and its corresponding yaw rate signal is attenuated by about half when the raw data are smoothed with a 2.0 second moving average window. The same data provide a more accurate estimate of yaw rate when the raw data is smoothed with a shorter 0.6-second window.

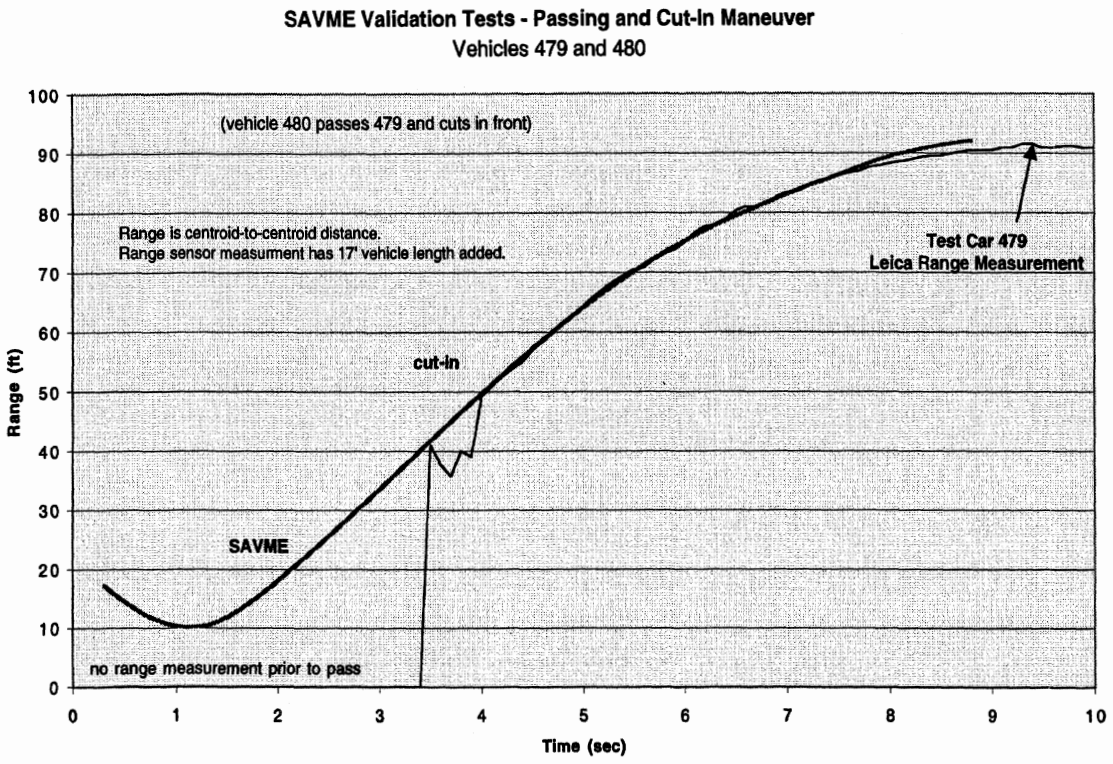

Figure 4.2.1-9. Passing and Cut-In Maneuver – Validation

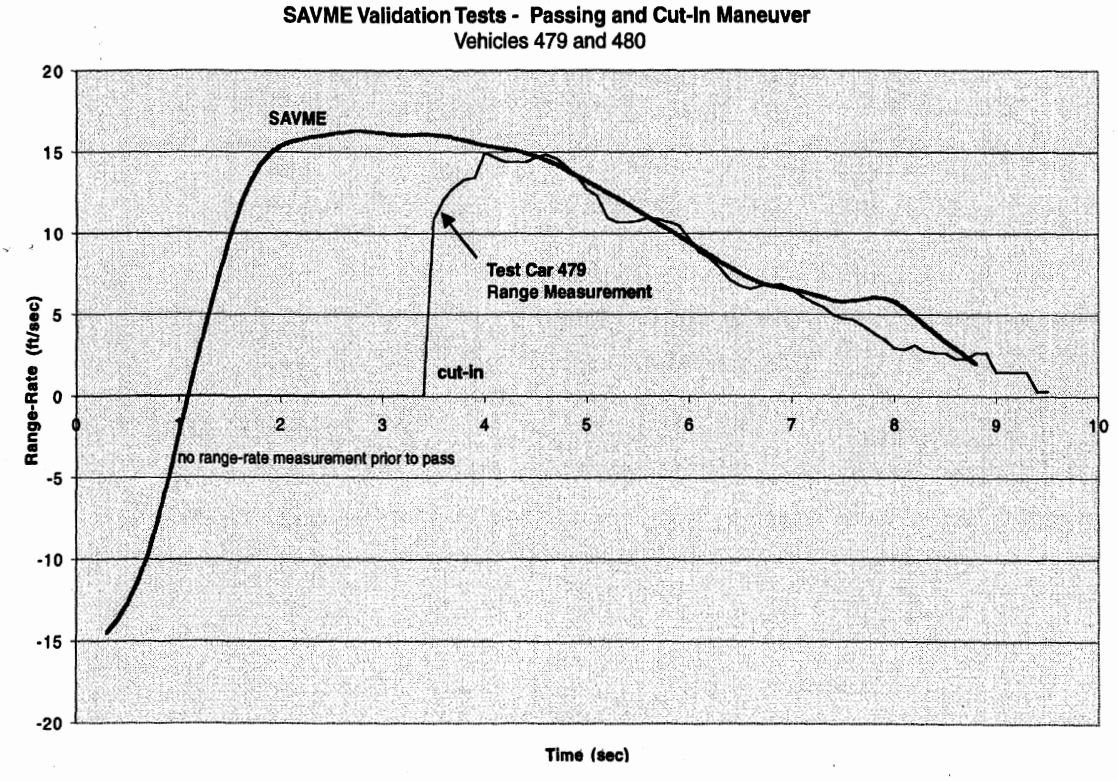

Figure 4.2.1-10. Passing and Cut-In Maneuver – Validation

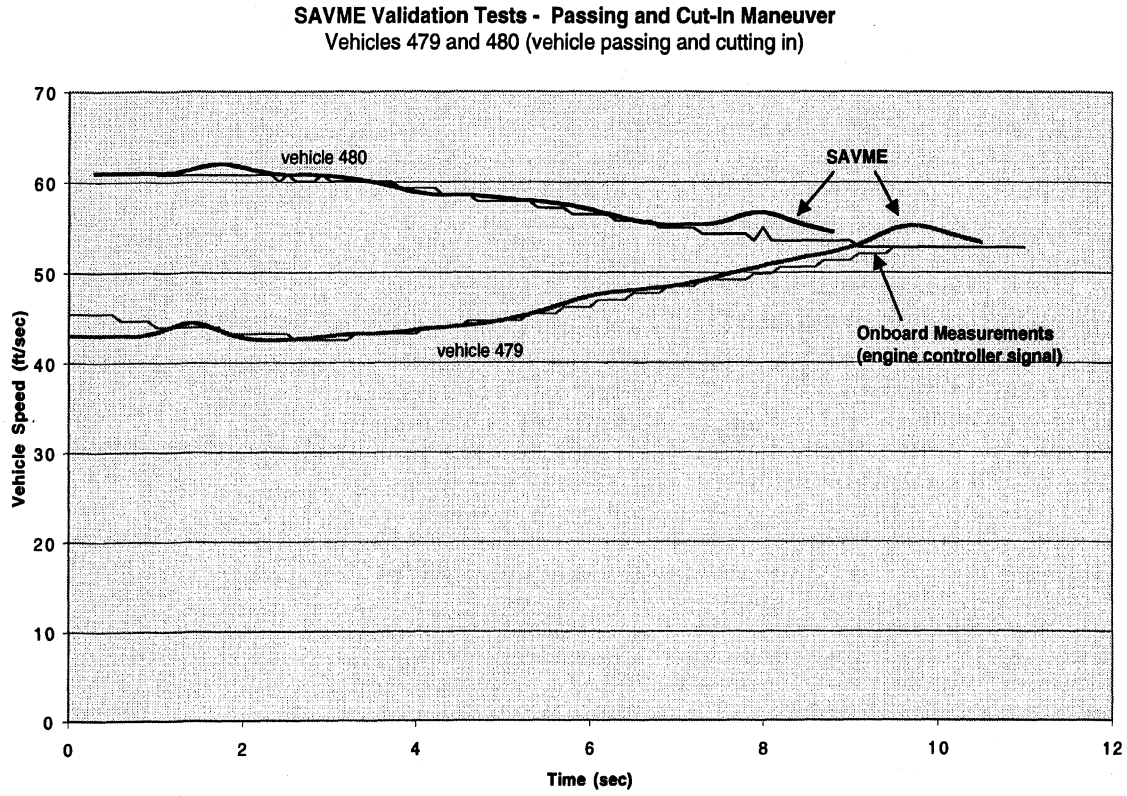

Figure 4.2.1-11. Passing and Cut-In Maneuver – Validation

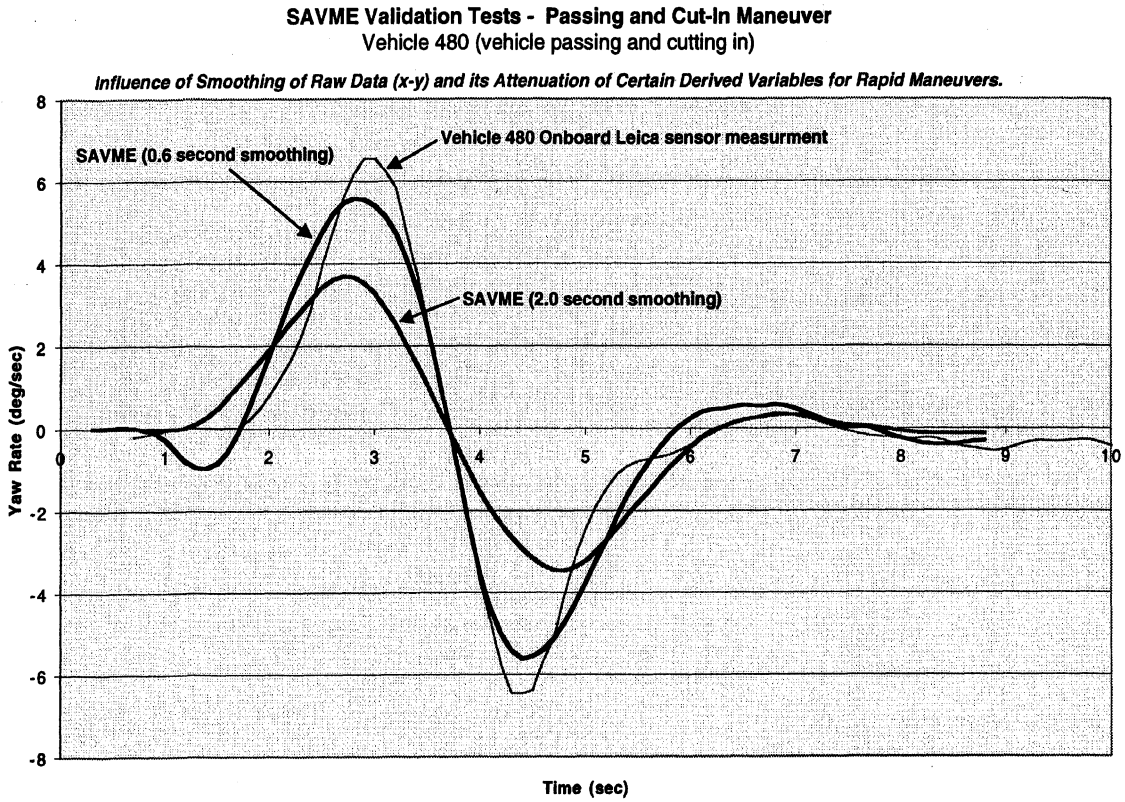

Figure 4.2.1-12. Passing and Cut-In Maneuver – Validation

4.2.2 Illustrative Samples from the Archival File

The approximate 18-hour database of SAVME trackfiles represents a total of 30,561 vehicles that traversed a portion of arterial street in Ann Arbor, Michigan, during daylight hours. Figure 4.2.2-1 shows the counts of vehicular traffic appearing by pairs of entry and exit lanes. For example, at the bottom right-hand corner of the figure, a total 7,156 vehicles both entered and exited the scene in Lane L2. Looking at the upper left, a total of 615 vehicles entered the scene on the intersecting roadway, L-3, and made a right turn to exit in Lane L-2. The figure provides a convenient summary, highlighting the fact that SAVME data always contain an explicit knowledge of the lane locations of all vehicles at all moments in time, including the identification of entry and exit lanes. Note, however, that identification of the entry/exit lane pairs does not necessarily reveal the lane that any vehicle might have been in at the time any specific maneuver was conducted. For example, at the upper left we see that 291 vehicles were counted as having entered in Lane L-1, and having exited at the intersecting roadway, L-3, even though scrutiny of the individual trackfiles would reveal that the majority of these vehicles had already switched from L-1 to the curb lane, L-2, before making their right turn into L-3. In any case, Figure 4.2.2-1 serves to illustrate the mix of basic movement patterns that are present within the existing SAVME database.

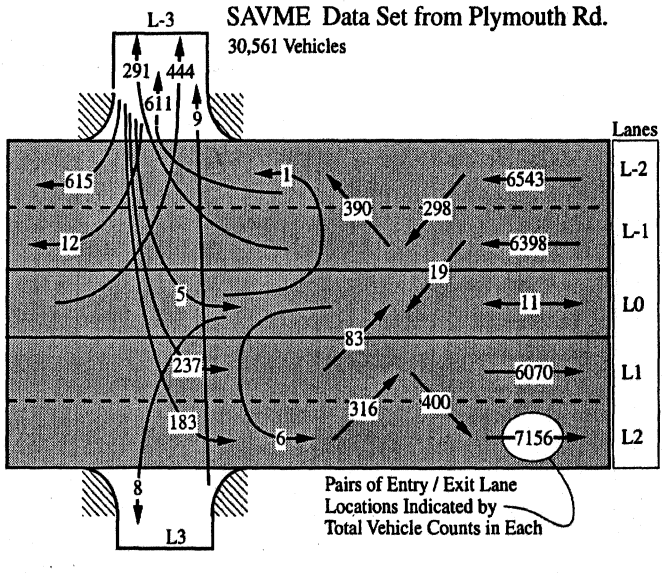

Figure 4.2.2-1. Entry Points and Exit Points for SAVME Data Set

The material that follows in this extensive section of the report covers a set of nine individual maneuver scenarios that serve to illustrate the nature and versatility of a SAVME database. The scenarios will be given descriptive names from common driving experience and will each be illustrated by the camera's view of the scene as well as by time history reproductions of selected vehicle motions and by aggregated results obtained from running queries on the relational database to find and characterize distributions representing all maneuvers of the illustrated type.

Flying Pass

Shown in Figure 4.2.2-2 is the road scene depicting the path of a vehicle that has just executed a flying pass maneuver. The vehicle in question is the dark sedan seen in the center of the bottom image in lane L1. This car entered the scene from intersecting roadway, L3, and accelerated to catch up with and then pass a preceding vehicle within lane L2 proceeding through the lane change with a relatively high value of negative range rate at the time of clearing from lane L2 into lane L1.

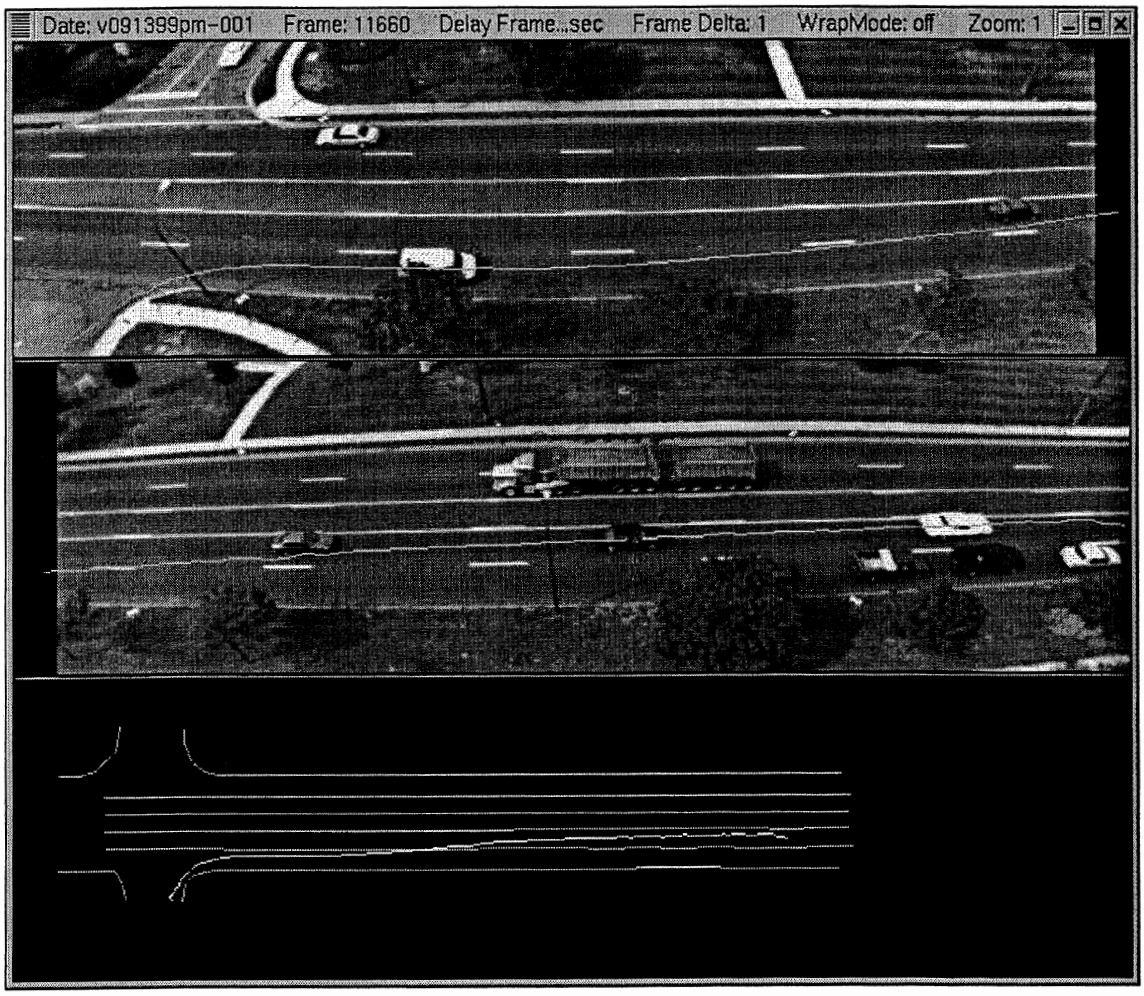

Figure 4.2.2-2. Vehicle in a Flying Pass Maneuver

Figure 4.2.2-3 shows the x-y trajectory of the subject vehicle engaged in the flying pass maneuver, using a compressed longitudinal scale so as to illustrate the lane placements clearly. When vehicle 768 cleared lane L2 and entered lane L1 it lost the first target and acquired another one, as designated in figure 4.2.2- 4 using the parlance Lane 2 target and Lane 1 target. Such designations will be used in several examples to follow in this section. Because the lane location of vehicular centroids are known explicitly in SAVME data, the definitions of target vehicle relationships can be stated with precision, given whatever geometric constraints (such as lane location) as may be useful.

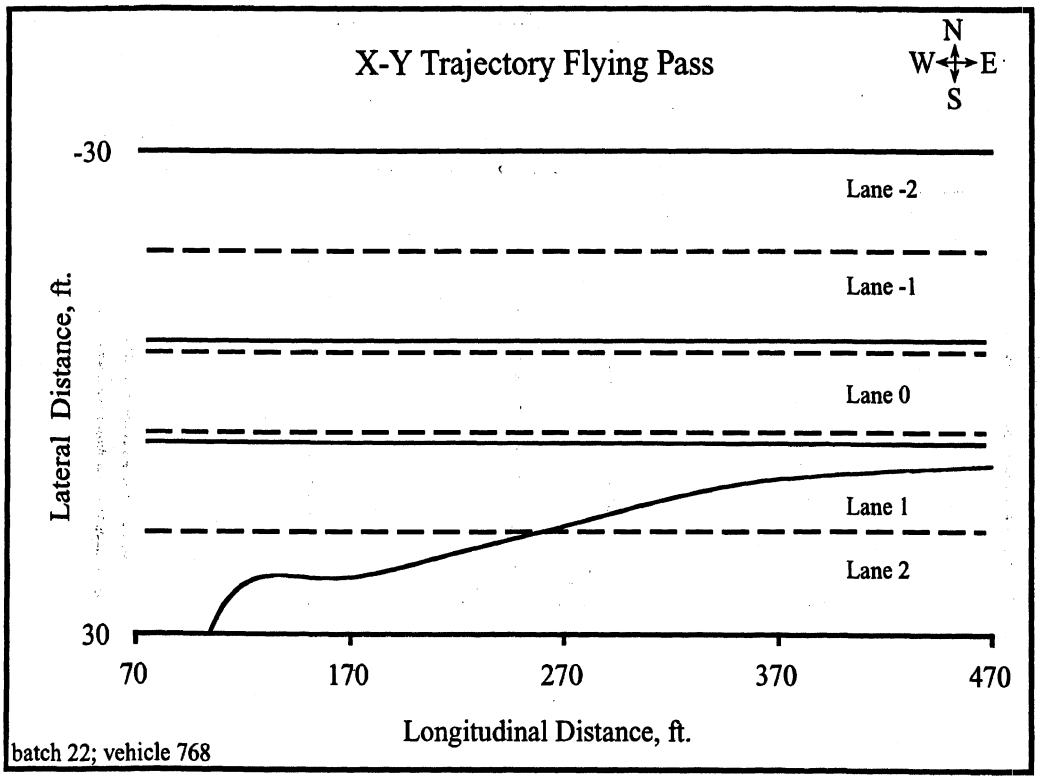

Figure 4.2.2-3. Trajectory of Flying Pass Vehicle 768

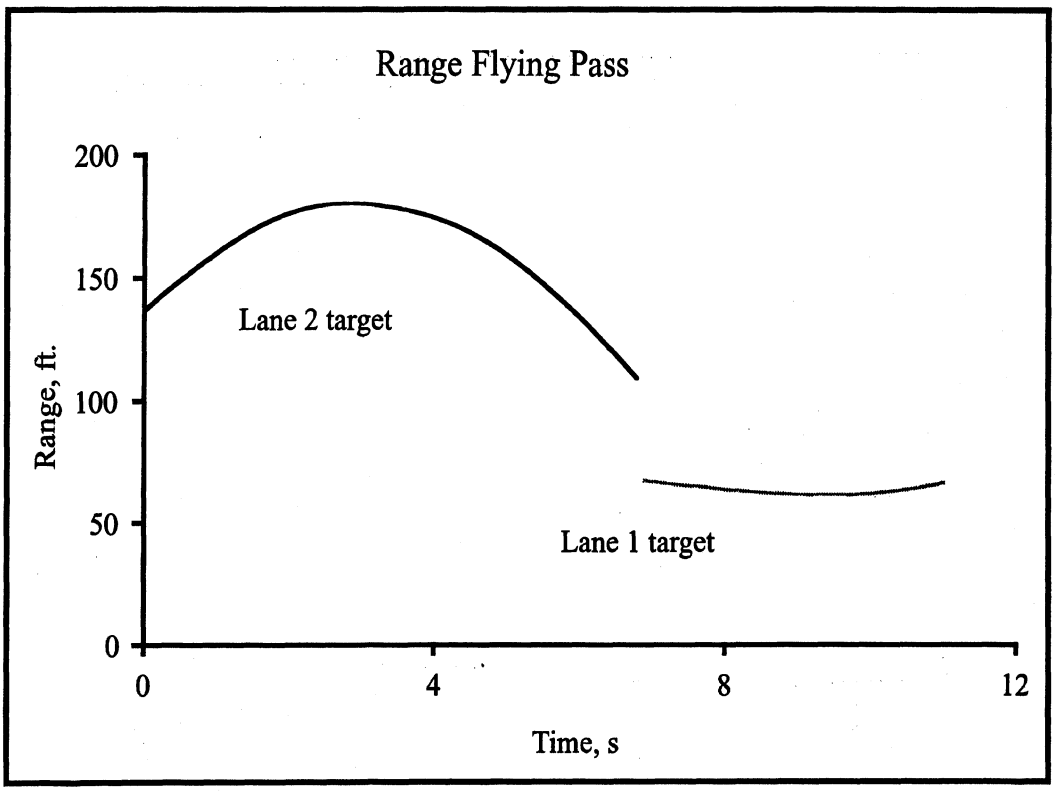

Figure 4.2.2-4. Range History Showing Lane 2 And Lane 1 Targets By Their Ranges Ahead Of Vehicle 768

Shown in Figures 4.2.2-5 and 4.2.2-6 are the range-rate and time-to-collision time histories for vehicle 768. We see that this vehicle first entered the scene with a positive range-rate to its first in-lane target since it began at a slow speed and then accelerated. After about 3 seconds, the range-rate value became negative, following which vehicle 768 began to overtake the preceding vehicle, finally consummating the flying pass at approximately 7 seconds into the maneuver. At this point, vehicle 768 had taken a position close behind a vehicle in lane L1 at almost zero range-rate.

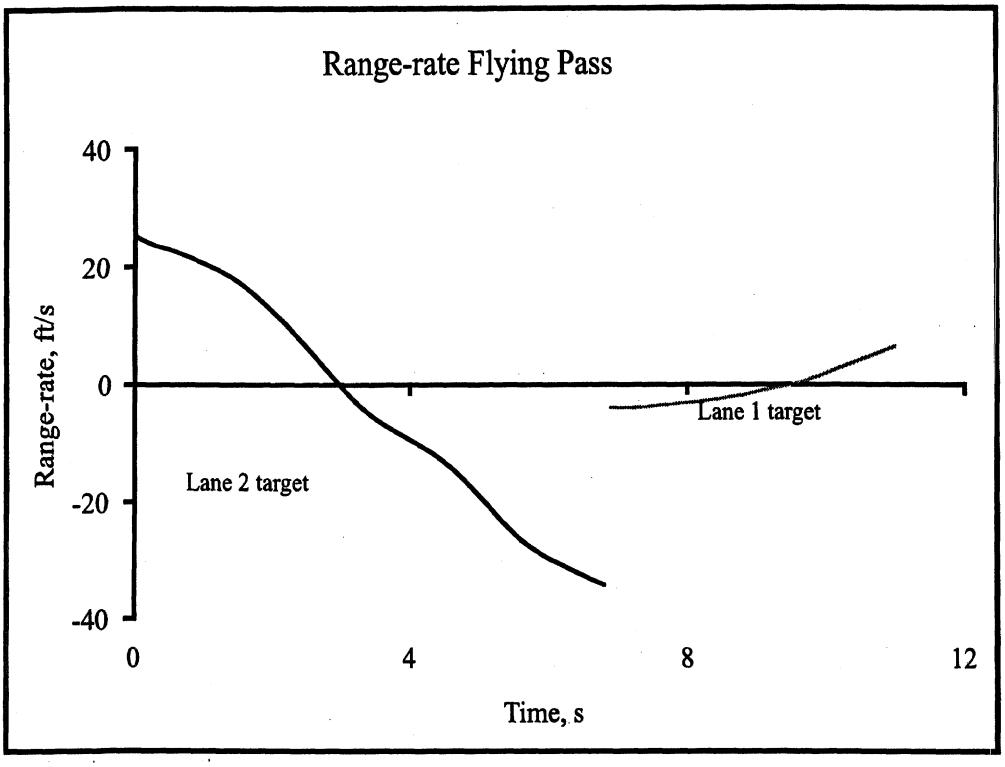

Figure 4.2.2-5. Range Rate History As Seen From Vehicle 768

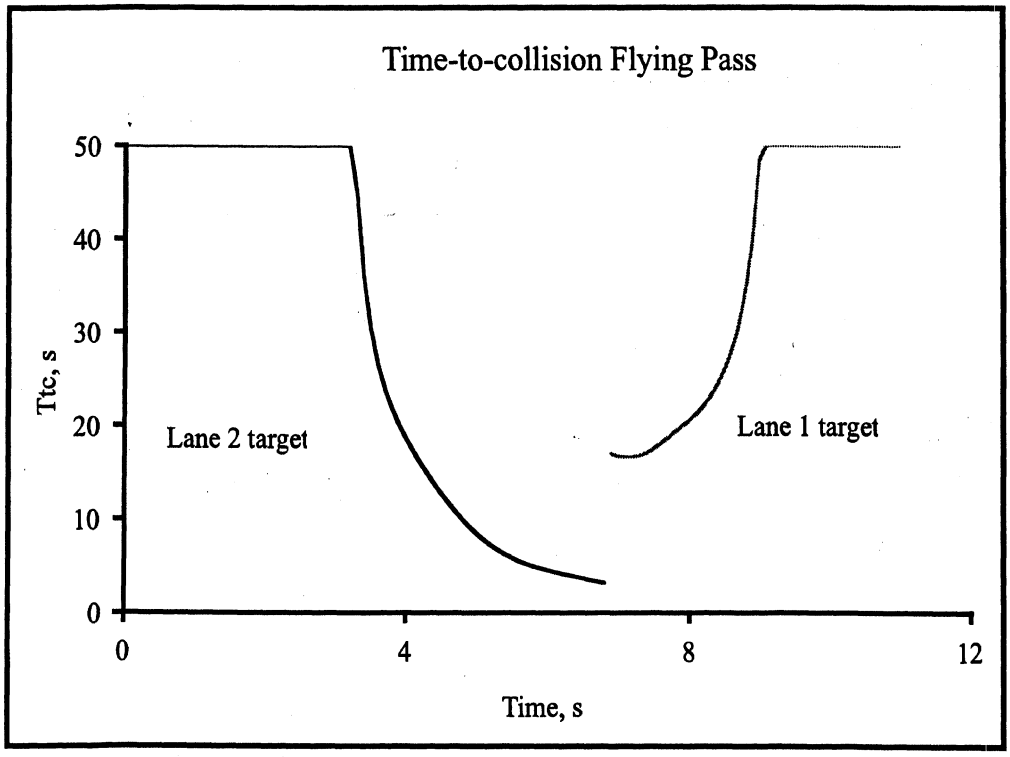

Figure 4.2.2-6. Time-To-Collision History As Seen From Vehicle 768

A query was then posed to find all cases of this type in the database. For the sake of simplicity, the query searched for vehicles that entered the scene in the curb lanes L2 and L-2 and yet exited the scene in the respective interior, through lanes, L1 or L-1. The query also required that the host vehicle have located a target vehicle in its entry lane at the time of transitioning from the curb to the interior lane and that (a) the host speed be above 30 ft/sec, (b) the range rate value at time of the lane change transition be more negative than –10 ft/sec, and (c) that the headway time value at the lane change transition be within 2 seconds.

A total of 150 cases were found, in response to this query, as summarized in the headway-time and time-to-collision histograms in Figures 4.2.2-7 and 4.2.2-8. The two figures show alternative ways of expressing the degree of conflict that existed between the host vehicle conducting the flying pass maneuver and the preceding vehicle that was being approached in the curb lane—right at the moment that the host vehicle's centroid crossed into the interior lane. We see that headway time margins below 1 second tend to predominate, including a substantial incidence of headway times below 0.5 seconds. Similarly, values of time-to-collision tend toward the very short end of the scale (noting that times-to-collision in most normal driving rarely go below 5 seconds or so. Thus, even this very limited sample of SAVME data has value for showing the extent of conflict embedded in a particular type of the flying pass maneuver.

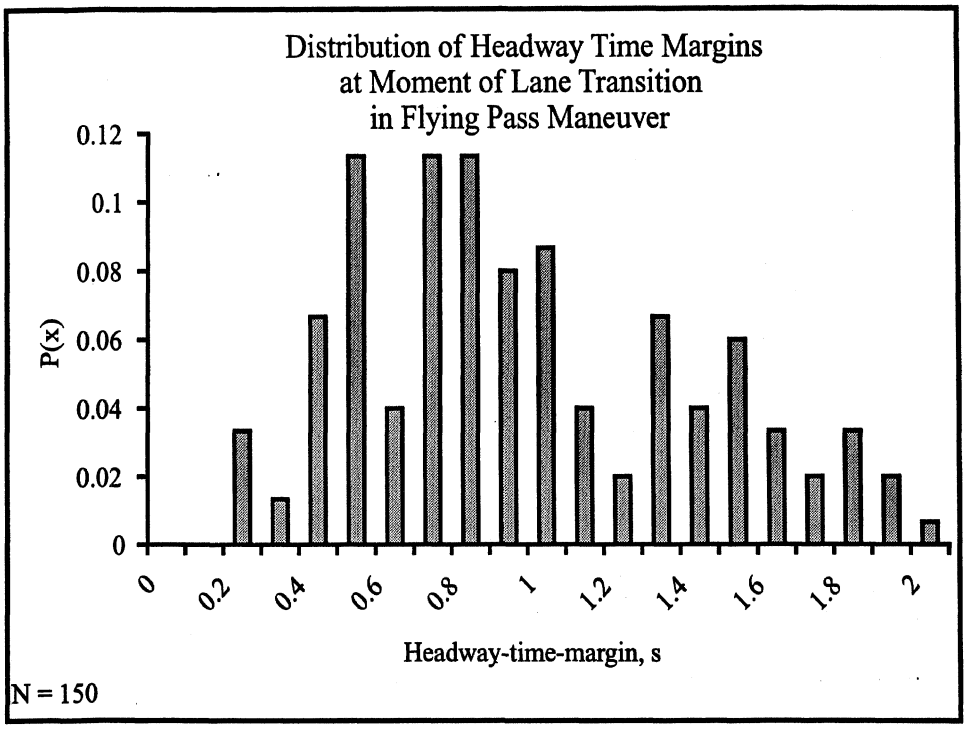

Figure 4.2.2-7. 150 Vehicles Conducting the Queried Type of Flying Pass Maneuver

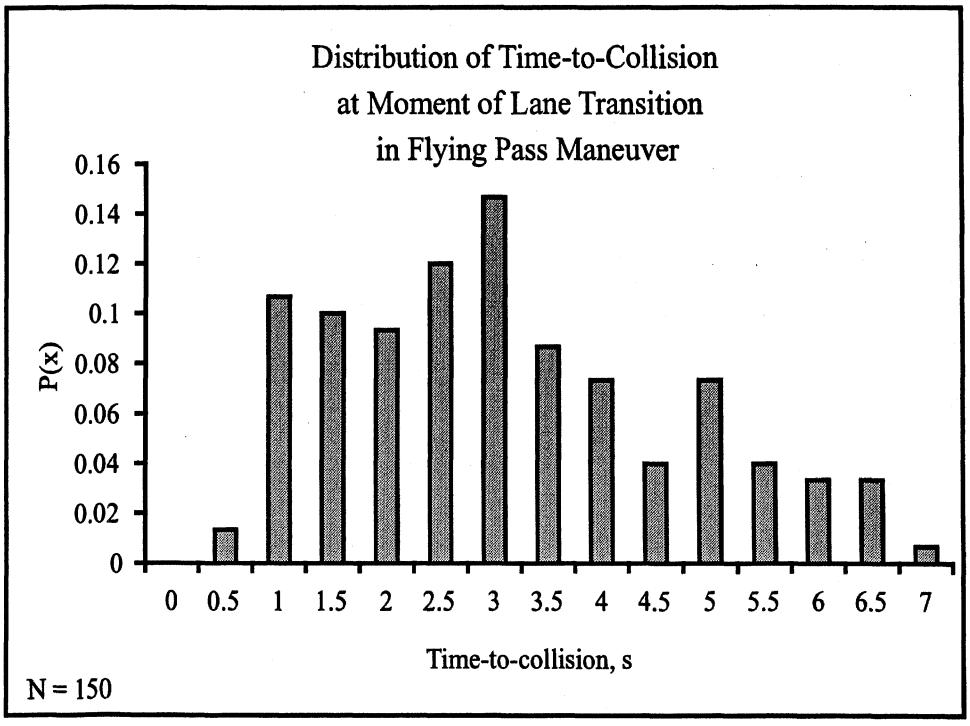

Figure 4.2.2-8. 150 Vehicles In The Queried Type of Flying Pass Maneuver

Passing on the Right

Shown in Figure 4.2.2-9 is the road scene depiction of a camper-van, vehicle 571, being passed on the right by a pickup truck. The pickup truck entered the scene in Lane L–2 proceeded to pass the van moving more slowly in Lane L-1. In some states, passing on the right is an illegal maneuver, one that can be readily captured in SAVME data.

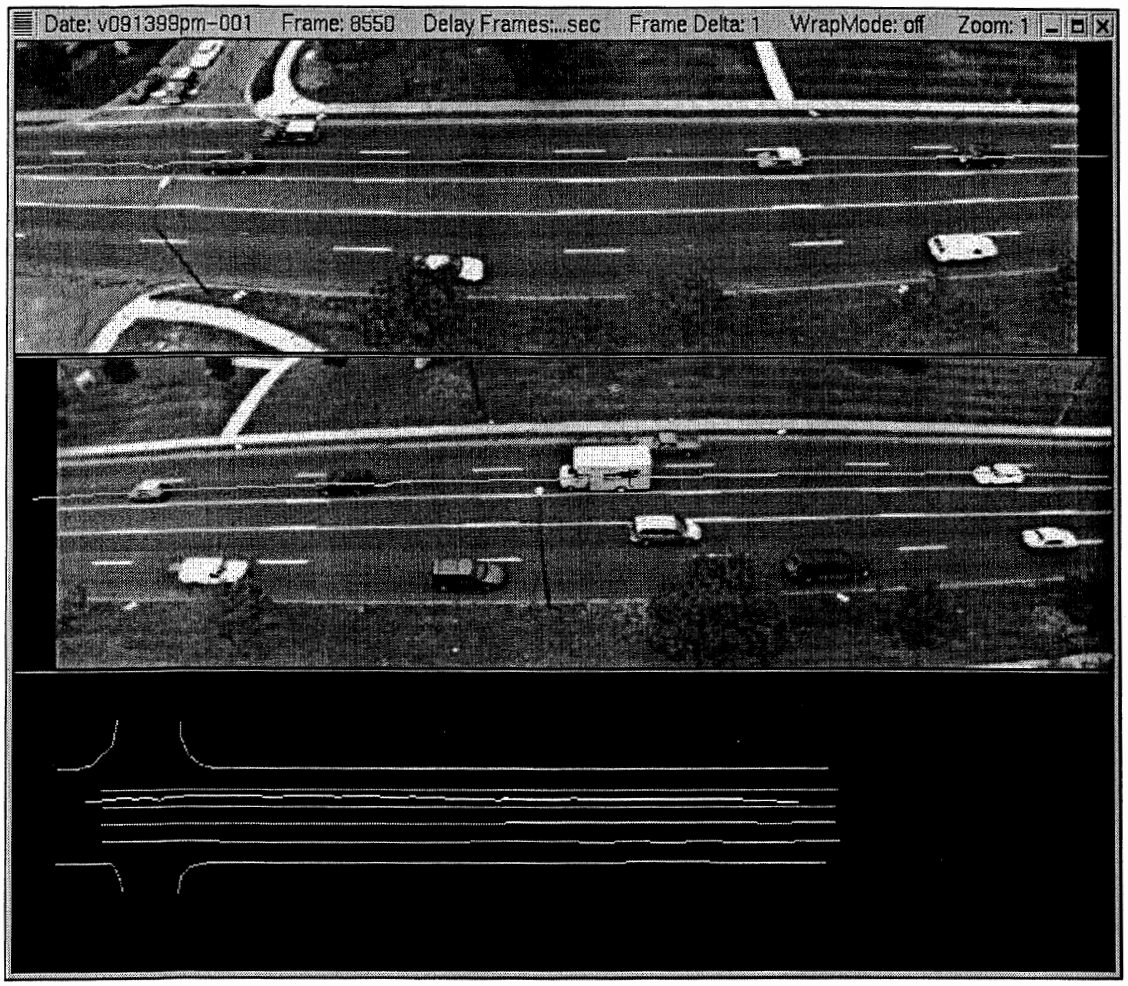

Figure 4.2.2-9. Passing on the Right Maneuver in Progress

Figure 4.2.2-10 shows the x-y trajectory of the pickup truck engaged in passing on the right. Actually, the shape of the vehicle's path reveals that the origin lane was L-1 and that the vehicle was already engaged in moving into lane L-2 by the time it entered the scene for SAVME data collection.

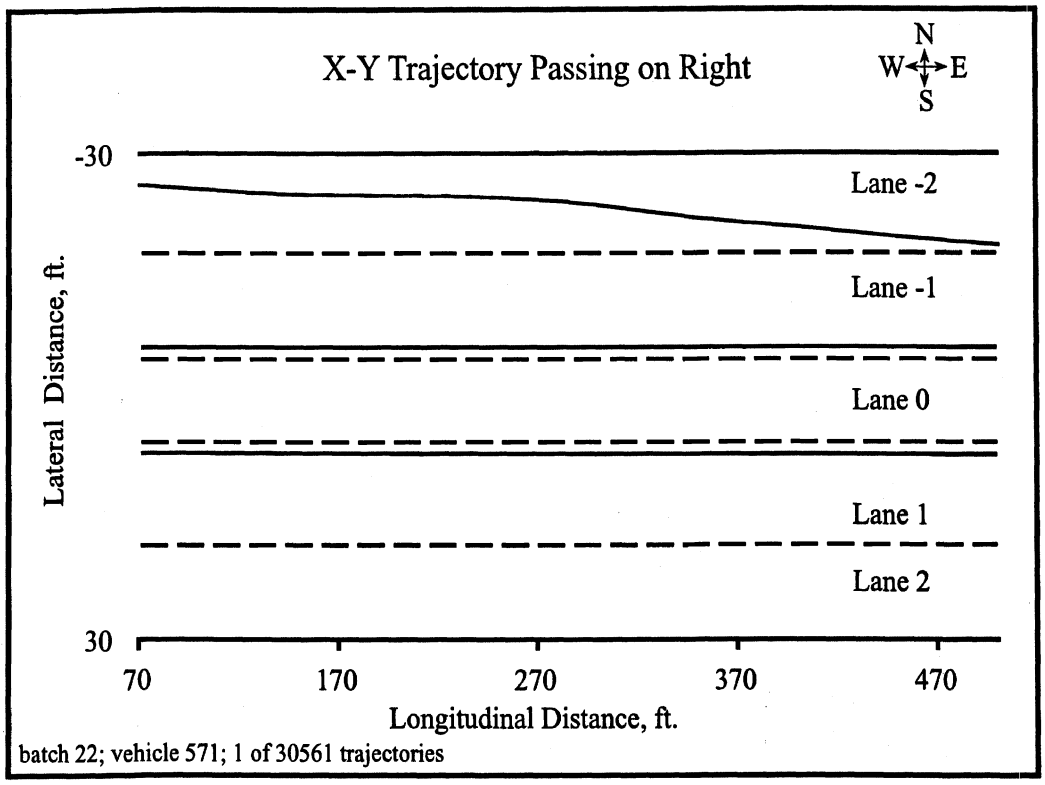

Figure 4.2.2-10. X-Y Trajectory for Passing on Right Maneuver

A query was then posed to find all cases of this type in the database. For the sake of simplicity, the query searched for vehicles that entered the scene in the interior, through lanes L1 and L-1 and yet exited the scene in the respective curb lanes L2 or L-2. The query also required that the host vehicle have located a target vehicle in its entry lane at the time of transitioning from the interior to the curb lane and that (a) the host speed be above 30 ft/sec, and (b) the headway time value at the lane change transition be within 4 seconds.

A total of 333 cases were found, in response to this query, as summarized in Figures 4.2.2-11, -12, and -13. Figure 4.2.2-11 shows the distribution of lateral velocity values (i.e., the velocity component normal to the lane centerline) at the moment of lane transition, when pulling from an interior lane into a curb lane, to pass on the right. SAVME data permit an easy means for deriving such a measure since both vehicle and roadway reference frames of measurement are known explicitly. The data show that the typical pass on the right maneuver is conducted without dramatic rates of lateral movement.

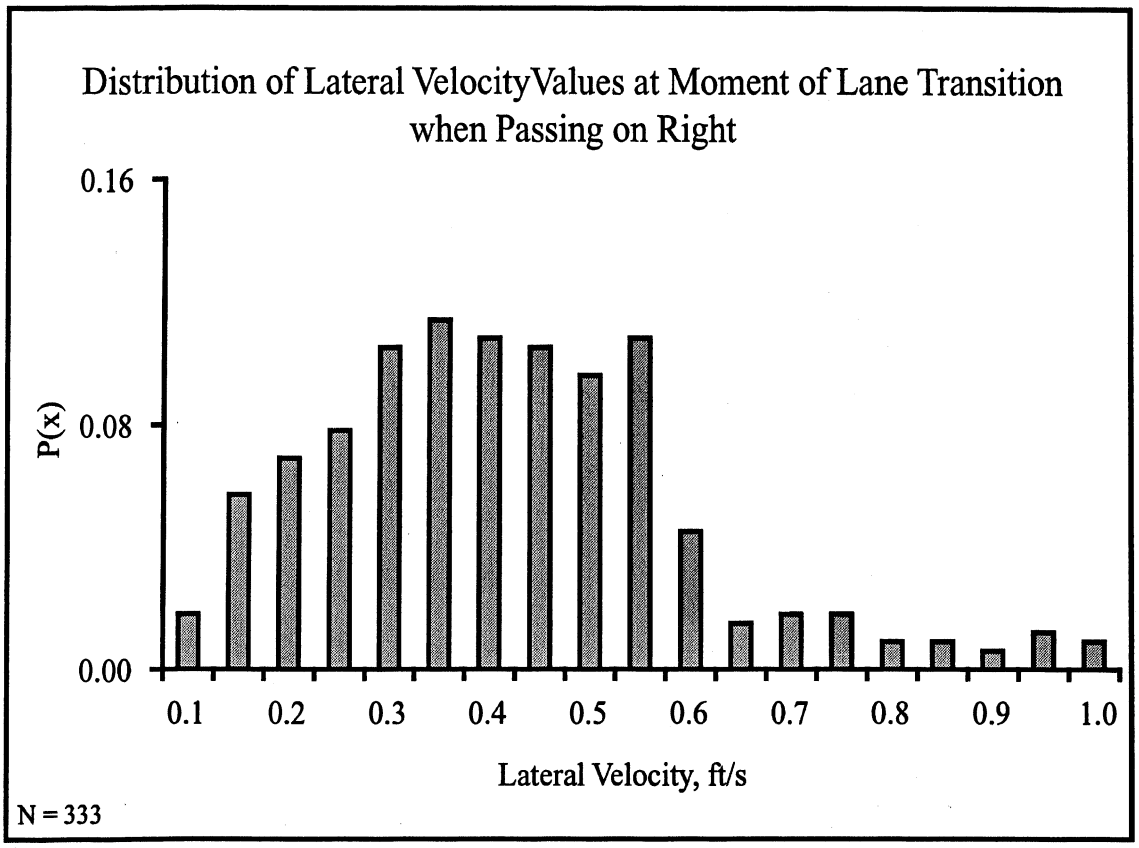

Figure 4.2.2-11. Lateral Velocity Distributions for 333 Vehicles Found By The Query For Passing On The Right

Figures 4.2.2-12 and 4.2.2-13 present distributions of the time-to-collision and headway time values existing at the moment of lane transition when pulling out to pass on the right. Note that in Figure 4.2.2-12, the number of cases yielding a real value of time-to-collision numbered only 167, indicating that the other pass-on-the-right sequences occurred without a negative value of range-rate at the time of the lane transition. The figures show that passing on the right is considerably more benign than the set of maneuvers captured under the prior query for flying pass maneuvers. This characteristic probably derives from the simple fact that while curb-lane traffic tends to encounter stopped or very slowly moving vehicles, interior lane traffic is relatively fluid or at least more continuously moving than traffic in the curb lanes. Thus, passing to the right is not generally occasioned by large values of negative range rate on the part of the approaching vehicle while in the flying pass maneuver (from right to left), substantial negative range rates are present. Again, the purpose of the present illustrations is to convey the type of content found in SAVME data, using a few forms of querying the database that were selected from among the almost limitless possibilities for query structure.

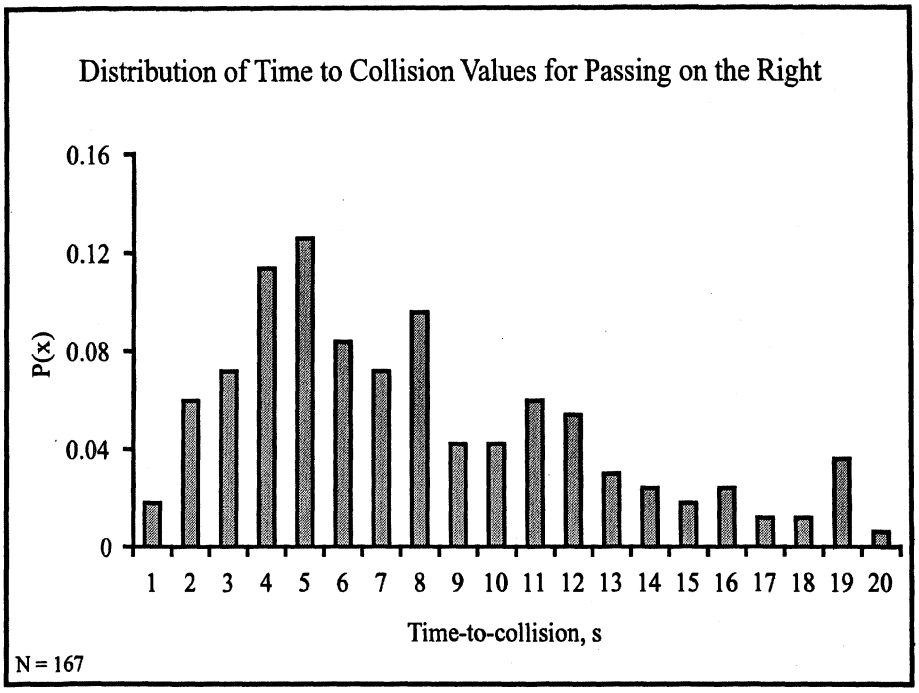

Figure 4.2.2-12. Distribution For 167 Cases Of Passing On The Right, At the Moment of Lane Transition

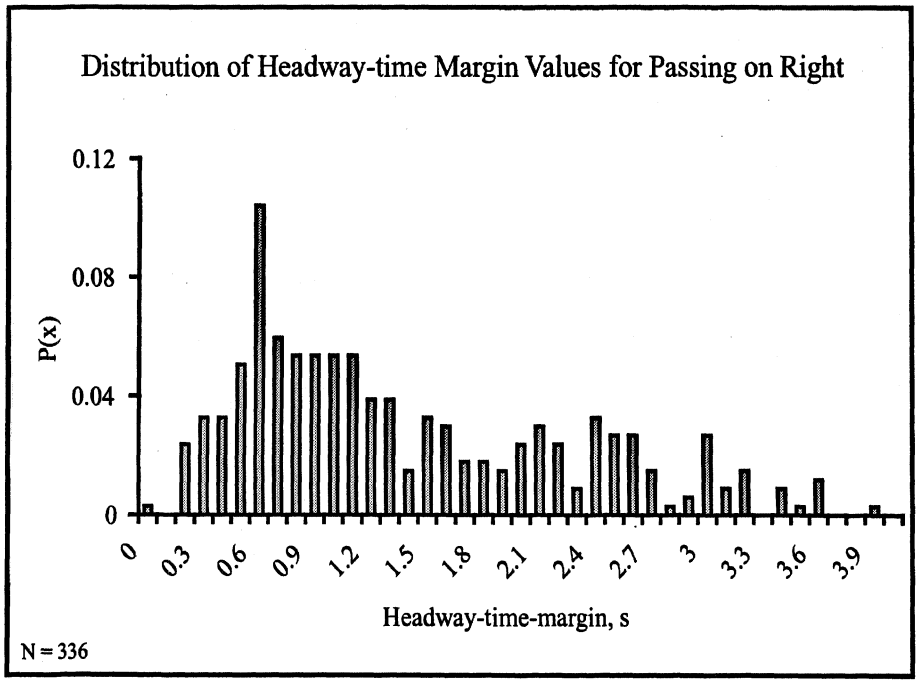

Figure 4.2.2-13. Distribution For 336 Cases of Passing On The Right, At the Moment of Lane Transition

Queue Formation

Shown in Figure 4.2.2-14 is the road scene depicting a substantial queue of vehicles that has formed in the curb lane L2. In this case, traffic has backed up from a traffic light that exists several hundred feet off to the east (right) of the data collection site. In this and the next subsection of the report, data are shown that capture the transient processes of queue formation and queue dispersal, respectively.

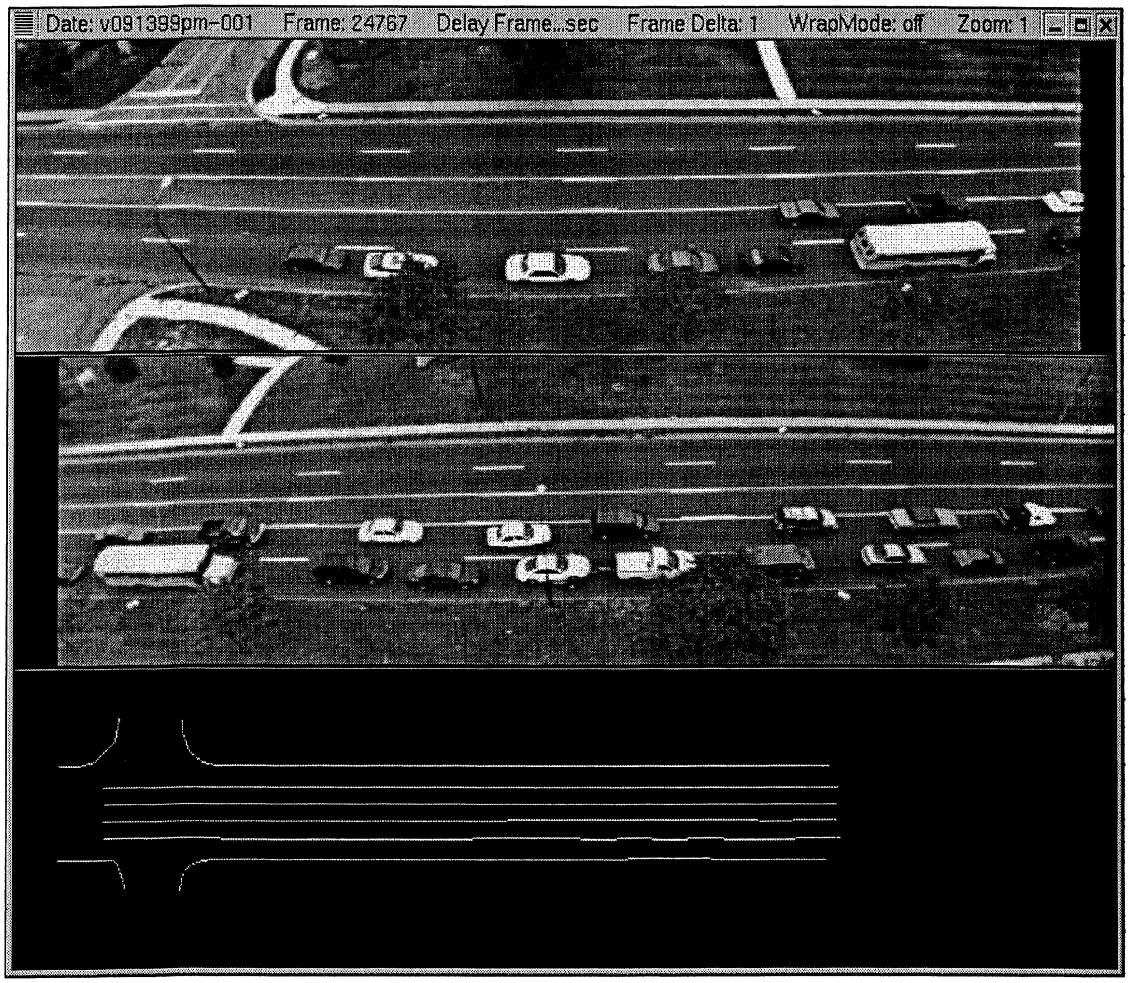

Figure 4.2.2-14. Queue In Eastbound Traffic Lanes

Figure 4.2.2-15 shows the velocity time histories of a set of eight vehicles approaching the congested portion of the road, in lane L2, and undergoing a velocity reduction down to zero and then back up and down again, as the congestion wave propagates and vehicles settle in to a stopped queue. The figure illustrates that the SAVME file contains the response properties of all vehicles which are simultaneously present at any moment in time. Note that the velocity responses of vehicles 1692, 1695, 1694, 1998, and 1701 are all registering within the scene by the time mark, t=10 seconds, but vehicles 1703-1708, and 1711 all enter the scene later than t=10 seconds. A quick look at Figure 4.2.2-15 indicates that vehicle 1711 exhibits an unusually steep velocity history, indicating that

relatively hard braking was applied upon encountering the back of the more-or-less-stopped queue. Figure 4.2.2-16 provides a closer look at this braking transient, expressing the deceleration time history of vehicle 1711, per the same time base as had been shown for the overall queue formation process. We note that this vehicle reached the rather substantial peak deceleration level of 0.37 g's. The SAVME database affords a ready recovery of any individual vehicle's time histories, as well as the relational variables and the characteristics of vehicles taken as a group.

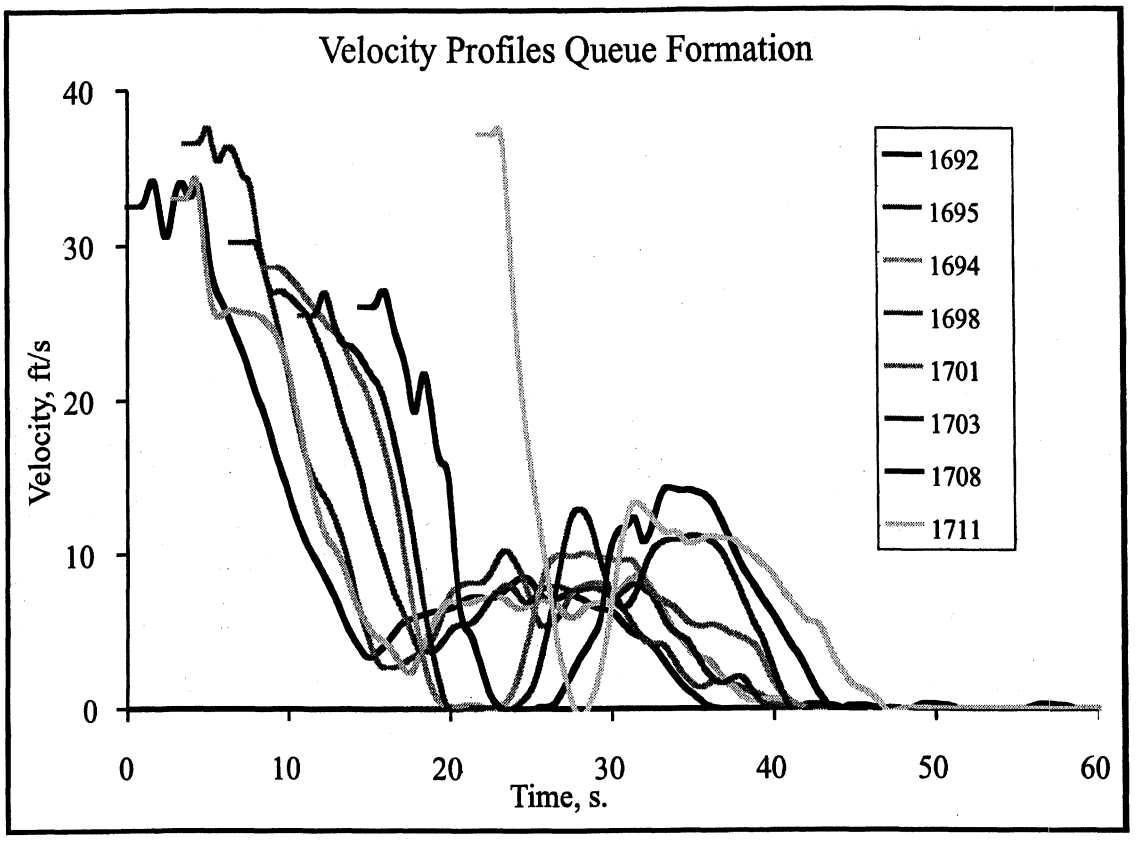

4.2.2-15. Eight Vehicles Slowing Down To Join A Queue

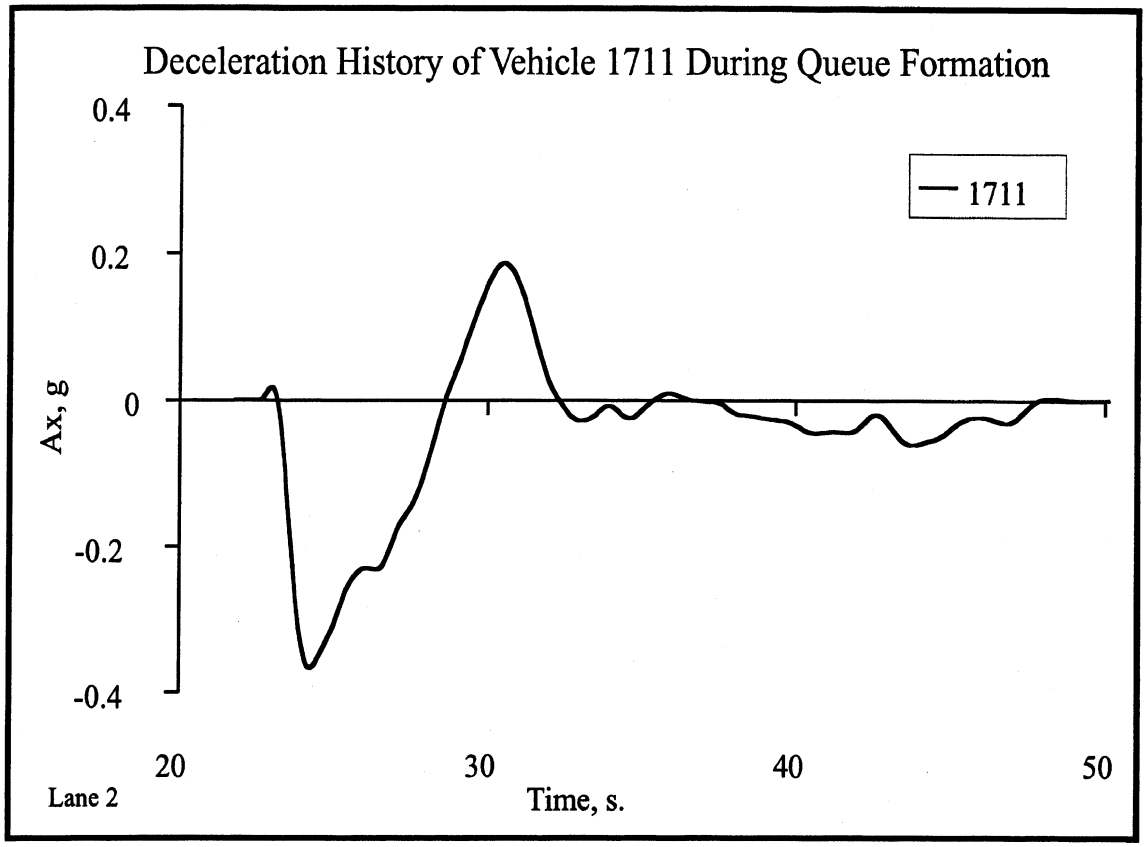

4.2.2-16. Deceleration Response Peaking Near 0.4 g's

Figures 4.2.2-17 through 4.2.2-19 illustrate a case whereby the SAVME data animator can be used effectively to help elucidate a relatively complex set of vehicle interactions. That is, in the course of the queue formation process shown above, one vehicle 1694 (shown in Figure 4.2.2-17) cut into the queue and another vehicle 1703 (shown in Figure 4.2.2-18) left the queue. Understanding that the cut-in and cut-out transients occurred along the way helps in explaining the set of intervehicular range profiles shown in Figure 4.2.2-19 for the process of queue formation. We note that the cut-in movement by vehicle 1694, at approximately t=11 seconds, caused the range value from vehicle 1698 to 1695 to vanish, becoming immediately replaced by two new range histories representing the separation between vehicles 1698 and 1694 (beginning at approximately 60 feet) and between vehicles 1694 and 1695 (beginning at approximately 7 feet). Correspondingly, when vehicle 1703 departs from the queue, what had once been two range histories separating vehicle 1708 from 1703 and 1703 from 1701, now collapses to a single, longer range dimension from 1708 to 1701.

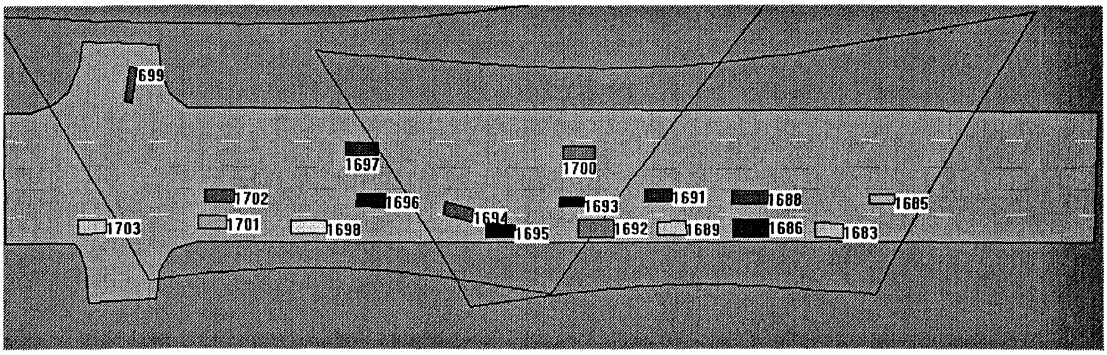

Figure 4.2.2-17 SAVME Animator Frame Showing Vehicle 1694 Cutting In To The Queue.

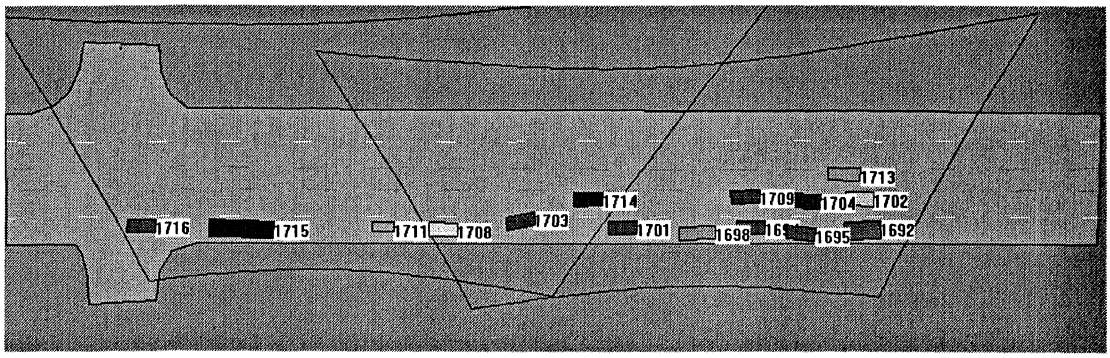

Figure 4.2.2-18. SAVME Animator Frame Showing Vehicle 1703 Cutting Out Of The Queue

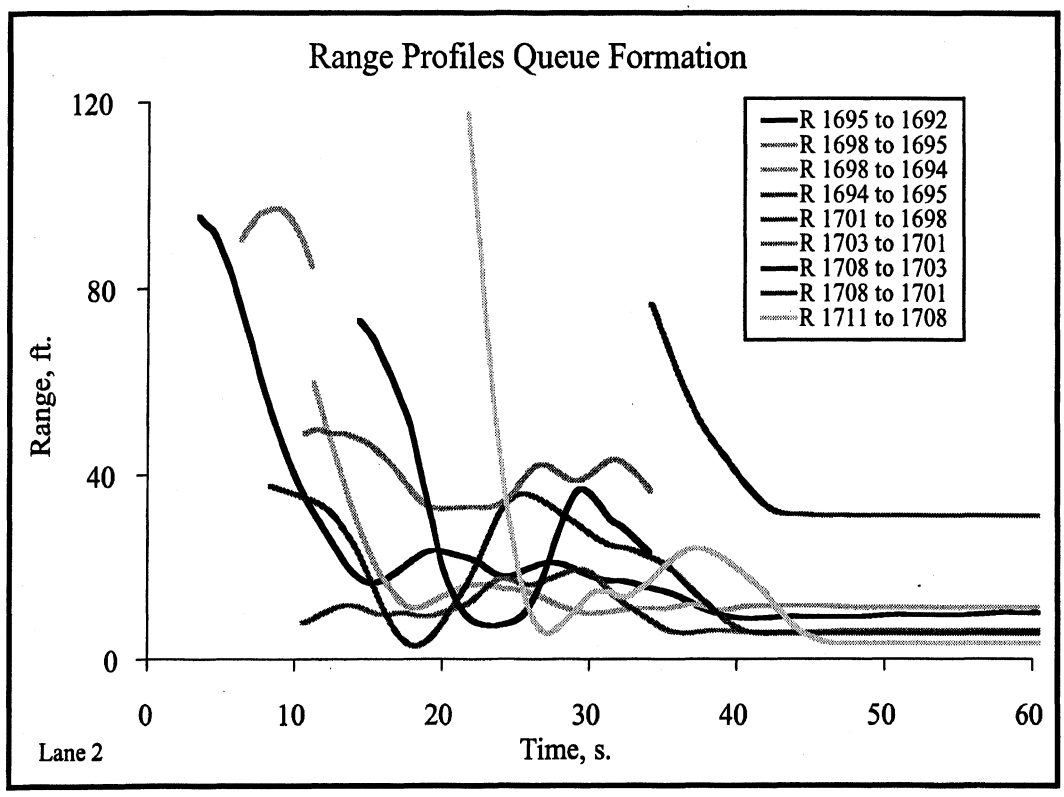

Figure 4.2.2-19. Nine Vehicles Involved in Queue Formation During which Vehicle 1694 Cuts in and Vehicle 1703 Cuts out

A query was then posed to find all cases of queue formation in the database. For the sake of simplicity, the query searched for vehicles that came to a complete stop in any of the four through-lanes of the roadway and which had a target vehicle ahead, while stopped, within a range of 30 feet or less.

A total of 464 cases were found, in response to this query, as summarized in the maximum deceleration and range-when-stopped distributions shown in Figures 4.2.2-20, -21, and -22. Decelerations are of interest, of course, in the context of the transient process of encountering stopped traffic and joining the queue. The maximum deceleration distribution looks rather like other published distributions for normal driving in the low velocity regime, as summarized here by means of the direct or cumulative-value plots of Figures 4.2.2-20 and 4.2.2-21.

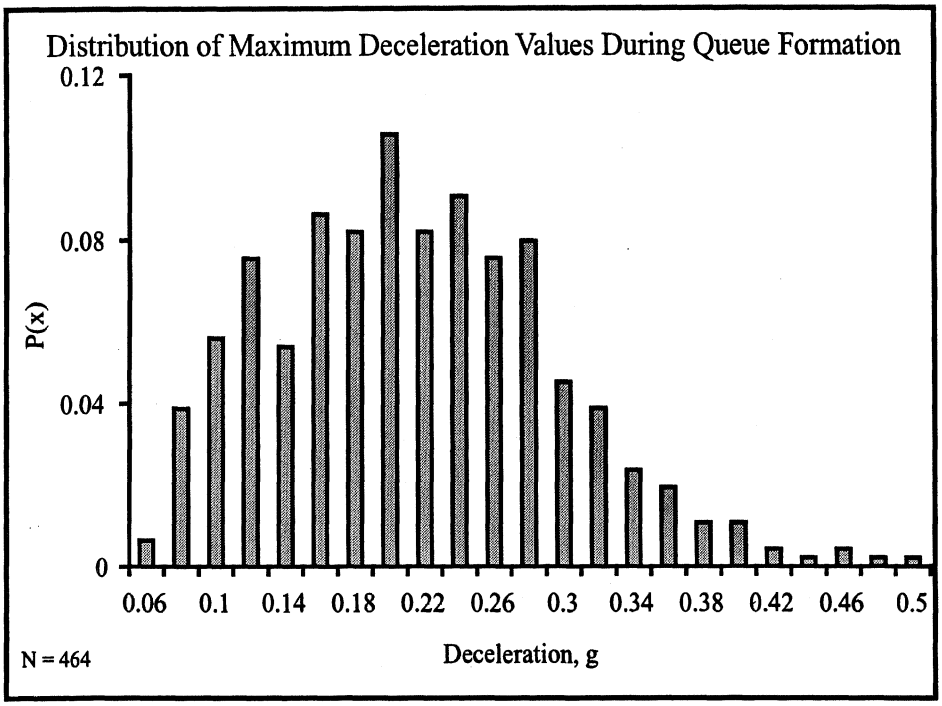

Figure 4.2.2-20. Vehicles That Came To A Halt In A Queue

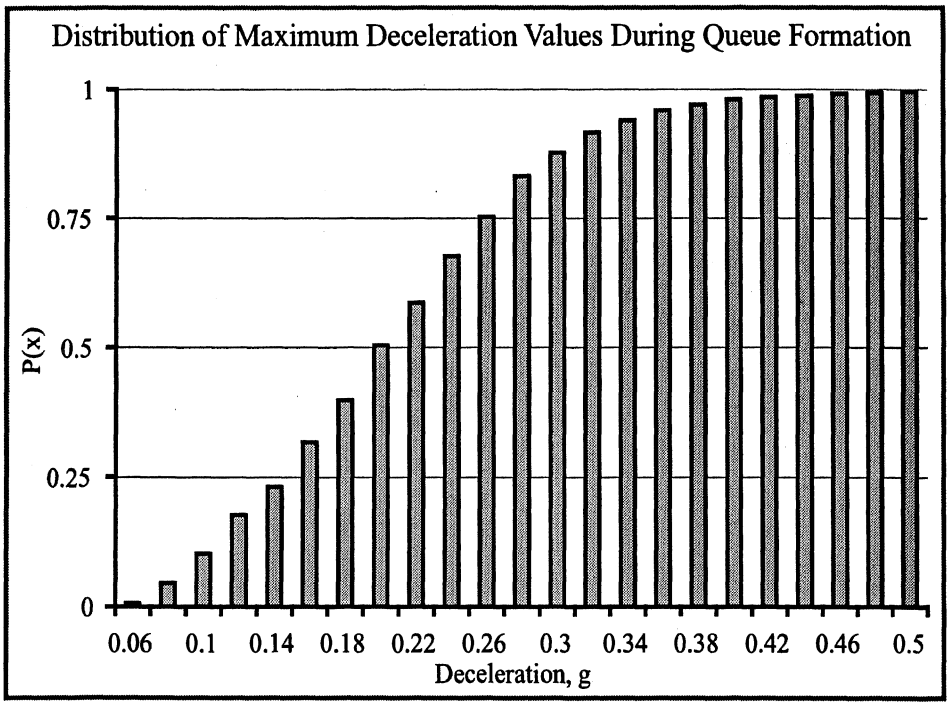

Figure 4.2.2-21. Cumulative Distribution Of Maximum Deceleration for 464 Vehicles

Once the queue has been formed to a stop, Figure 4.2.2-22 shows the cumulative distribution of inter-vehicle distances, as ranges, by which drivers choose to separate themselves from one another. Such distances are believed to be instrumental in determining the progress of stop and go traffic and to the injury dynamics occurring in chain collisions that involve stopped vehicle strings.

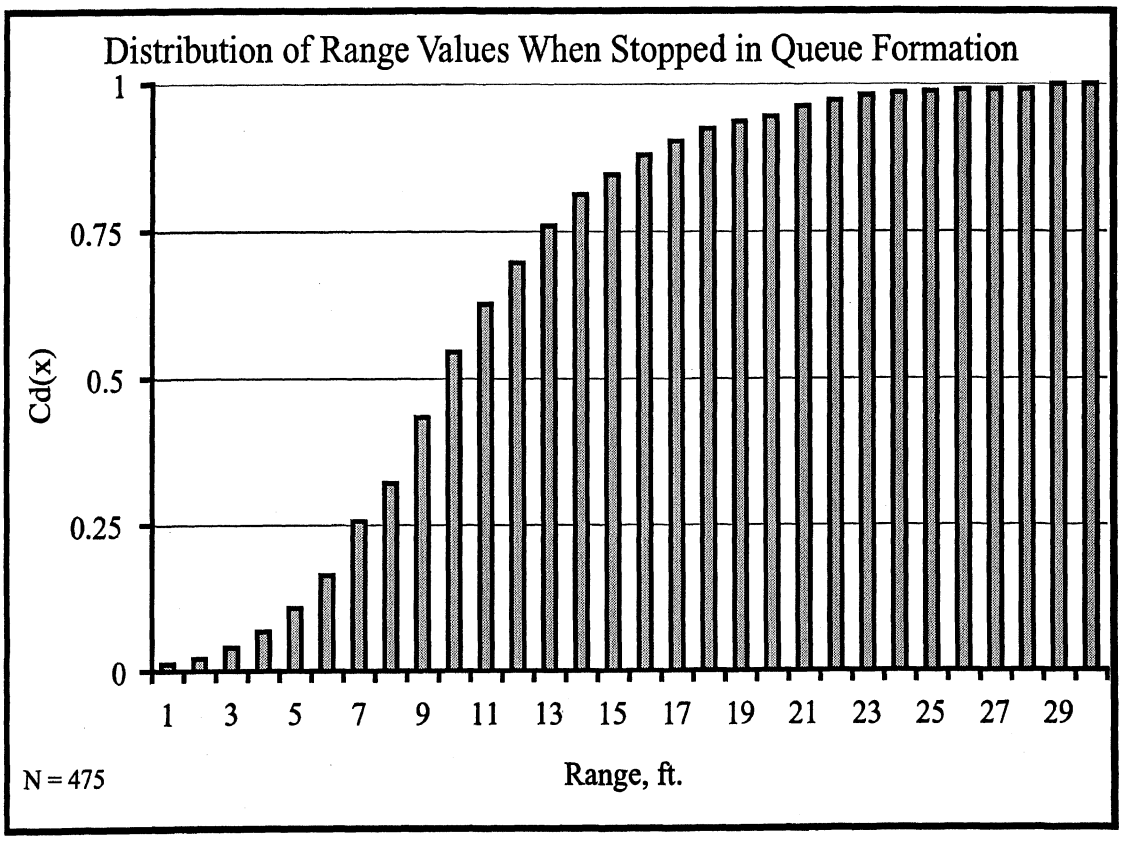

Figure 4.2.2-22. Cumulative Distribution Of Stopped-Vehicle Ranges for 475 Vehicles In Queues

Queue Dispersal

In Figure 4.2.2-23 is the SAVME animator's view of the road scene showing a queue of several vehicles in the curb lane L2 that is about to disperse. The queue contains a school bus, vehicle 1715 as well as passenger vehicle 1708, both of which will show sluggish responses in starting up, once the queue begins its dispersal. We note that vehicle 1708 has left a substantial clearance to vehicle 1701, even when at rest in Figure 4.2.2-23.

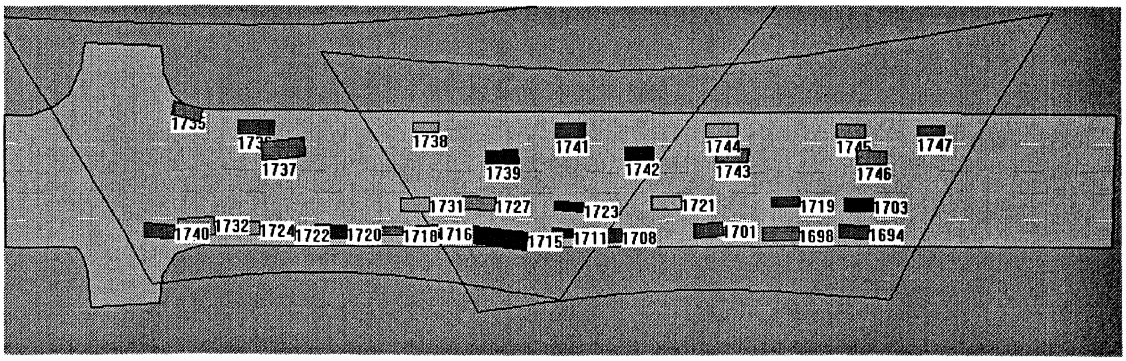

Figure 4.2.2-23. Animator Scene For Queue About To Disperse

Figure 4.2.2-24 shows the velocity time histories for a group of vehicles as they begin to move during the dispersal of the queue. The leaders show relatively brief histories as they quickly exit the scene toward the east. The others move more or less in the sequence of their placement, although some anticipatory movement is noted by vehicles toward the rear.

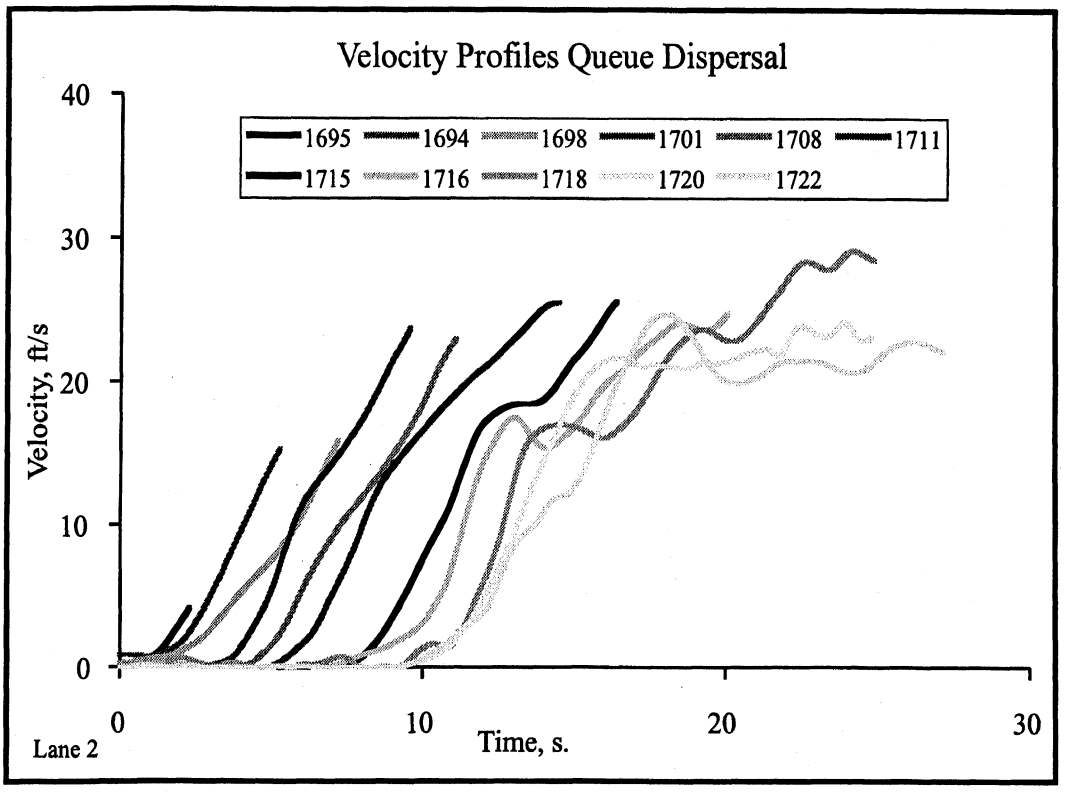

Figure 4.2.2-24. Eleven Velocity Histories As Queue Begins To Disperse

The corresponding range histories are shown in Figure 4.2.2-25. We see that vehicle 1708 has been at rest with a range of some 32 feet to the preceding vehicle and that it allows range to grow to above 70 feet before it leaves the scene at t=10 seconds, with the queue opening up. By way of contrast, vehicles 1718, 1720, and 1722 all stopped within ranges of 15 feet or less behind their leaders and managed to stay within 35 feet of them throughout the 10 or 15 seconds of their remaining appearance, before they left the scene. The school bus, vehicle 1715, allows range to grow to more than 70 feet as the queue disperses.

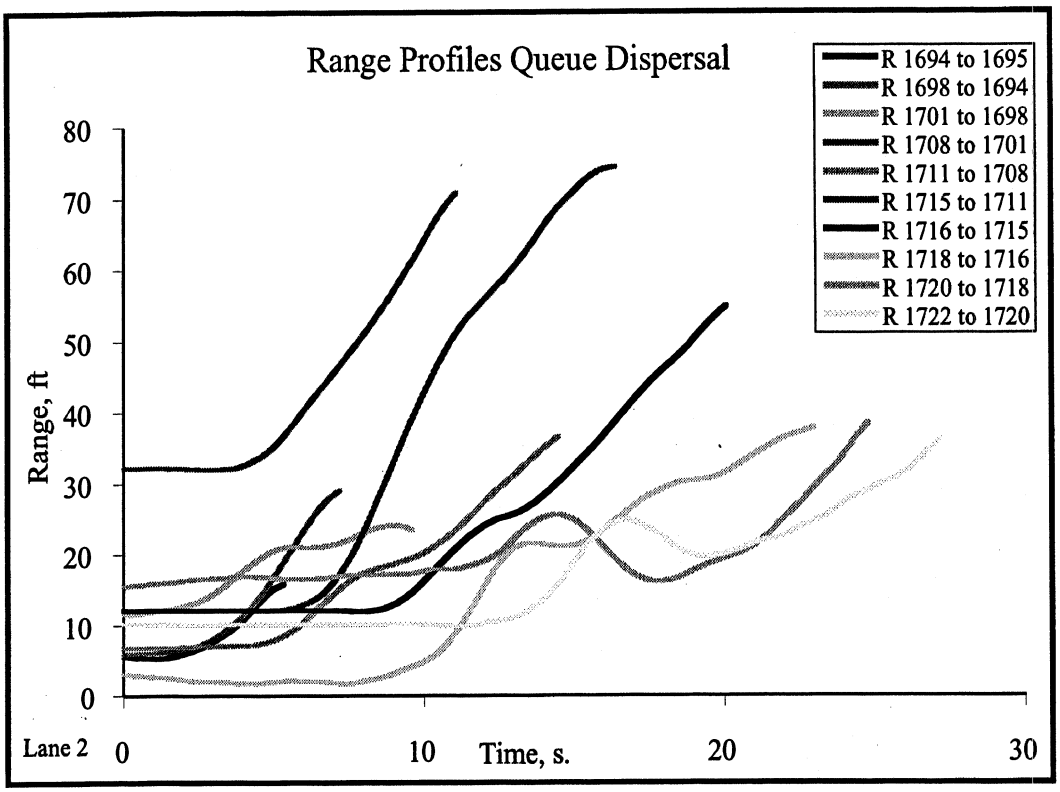

Figure 4.2.2-25. Ten Range Histories That Show Growth In Value As The Queue Disperses

While the range variable is broadly useful for analysis of traffic flow and crash avoidance phenomena, SAVME also offers the peculiar ability to locate all vehicles in the ground coordinate system, even as a time history. For example, Figure 4.2.2-26 shows the same queue dispersal sequence in terms of the x-coordinate history of the ten illustrated vehicles. One first notes that range in these data is approximated by the difference in intervening x values between successive vehicles, for any slice of time. A precise correspondence to range measurements, however, would require that we subtract the two respective half-lengths of successive vehicles, since x-coordinates are measured to the vehicular centroid while range is defined as a body-to-body clearance distance. The x histories show again that vehicle 1708 has left an unusual space between itself and the preceding vehicle, 1701, as does the school bus in its spacing behind vehicle 1711.

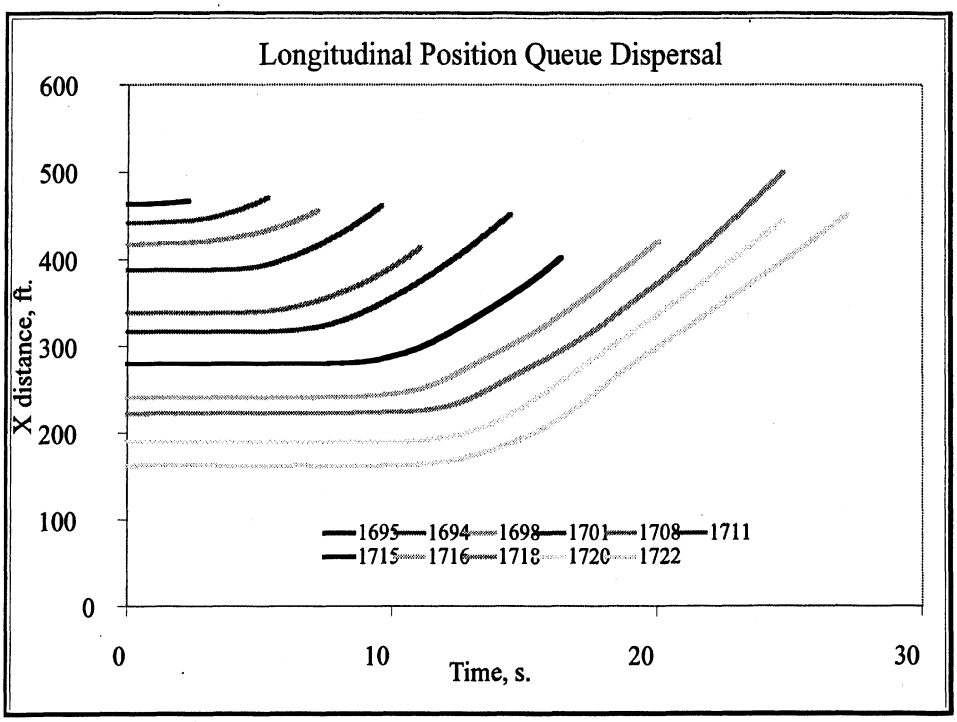

Figure 4.2.2-26. X-position Histories For Ten Vehicles During Queue Dispersal

A query was run on the database to find all cases in which a vehicle had stopped in one of the through lanes (L2, L1, L-1, or L-2) while another target vehicle was also stopped ahead within a range of 30 feet. The query also required that each such stopped vehicle, and its target, would both proceed from a stop up to at least a velocity of 6 feet per second before either of them slowed down again (in order to focus on the queue dispersal transient, as distinct from small adjustments in intra-queue spacing. Again, the authors wish to emphasize that limitless variation can exist in the details prescribed in such a query. Each example query shown here is for the sake of illustrating the database's potential rather than for authoritatively documenting any abiding principles about driving behavior). The described query yielded a total of 326 vehicles satisfying the criteria.

Two illustrative results have been derived for characterizing the responses of individual drivers during the queue dispersal transient. Figure 4.2.2-27 shows the distribution of startup delay times for 298 vehicles whose values of this metric fell within 0 to 4 seconds. Startup delay time was defined as the interval between the moment for exceedance of a 6 ft/sec speed by the preceding vehicle and the exceedance of the same speed by the (following) host vehicle. Looking back to the dispersal velocity profiles in Figure 4.2.2-24, for example, one observes that the school bus, vehicle 1715, delayed by approximately 2 seconds in reaching a velocity of 6 ft/sec, when it started to move again behind the preceding vehicle, 1711. The distribution plot in Figure 4.2.2-27 shows that the great preponderance of drivers respond with startup delay times that are less than 2 seconds.

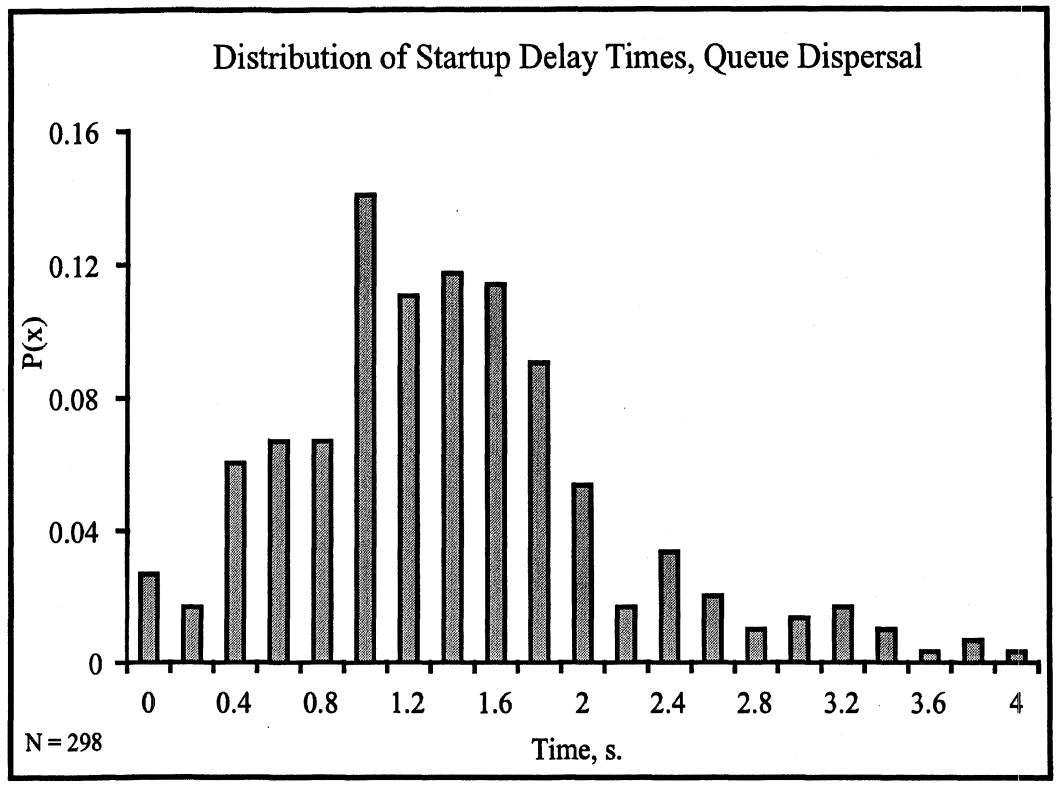

Figure 4.2.2-27 Startup Delay Times As Distributed Across 298 Vehicles.

Figure 4.2.2-28 shows the corresponding values of startup delay range, which is the range value existing at the moment the host vehicle's speed exceeds 6 ft/sec. An overlay of startup delay ranges from Figure 4.2.2-28 and the range-when-stopped values from the previous Figure 4.2.2-22 yields Figure 4.2.2-29. We see that the typical range-when-stopped value of, say, 10 feet grows to 18 feet or so due to the startup delay. Thus the typical vehicle in these data allows approximately 8 feet of growth in range before starting up from a queue.

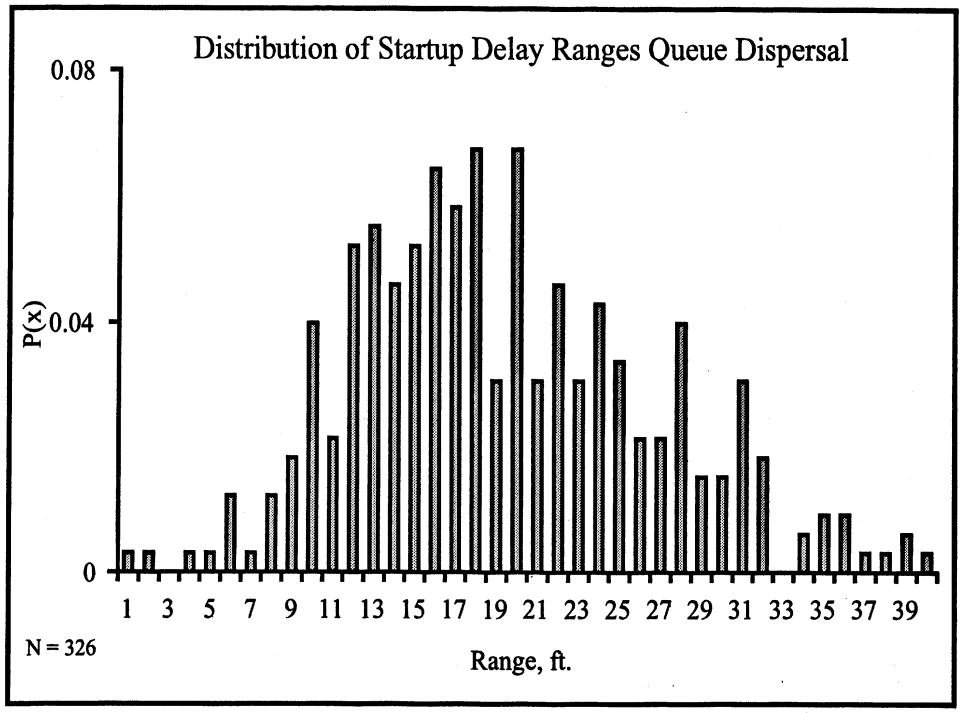

Figure 4.2.2-28. Startup-delay Range For 326 Vehicles

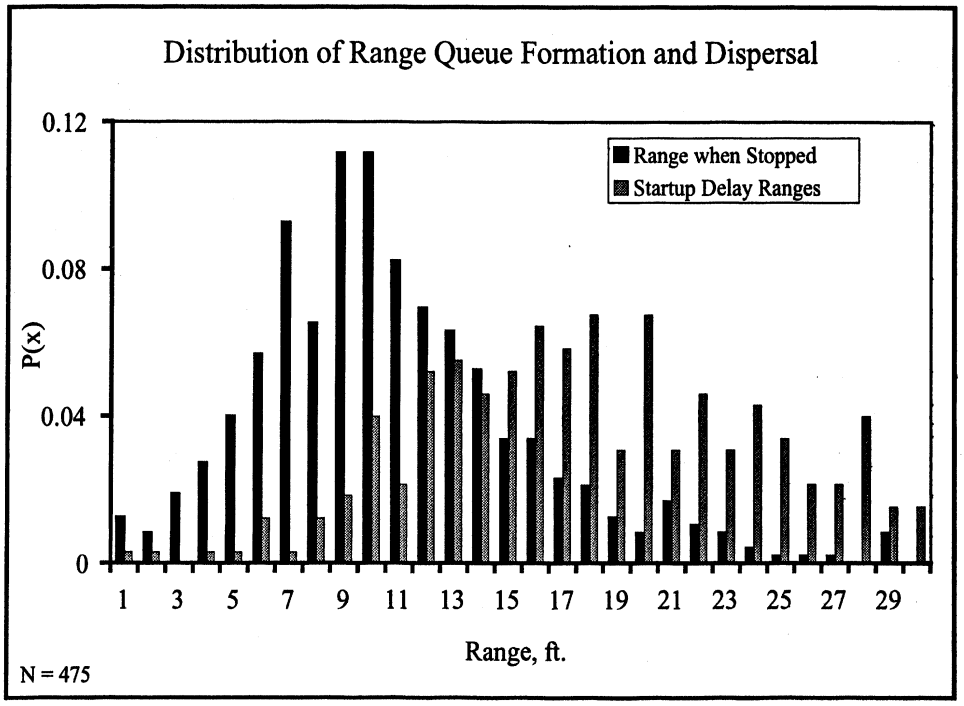

Figure 4.2.2-29. Comparison of Two Range Distributions - Vehicles When Stopped And Vehicles When Just Beginning To Start Up Again

Left Turn Across Lane of Oncoming Vehicle

Shown in Figure 4.2.2-30 is the SAVME animator's view of the road scene showing vehicle 372 at the left extremity of the scene making a left turn from the center-most lane into the intersecting roadway, L-3. Approaching westbound in the curb lane, L-2 is oncoming vehicle 365. This case presents a sample of the generic conflict posed by left turns at intersections that are not equipped with protective signaling. The left-turning driver simply judges whether the pending gap in oncoming traffic is suitable for making the turn.

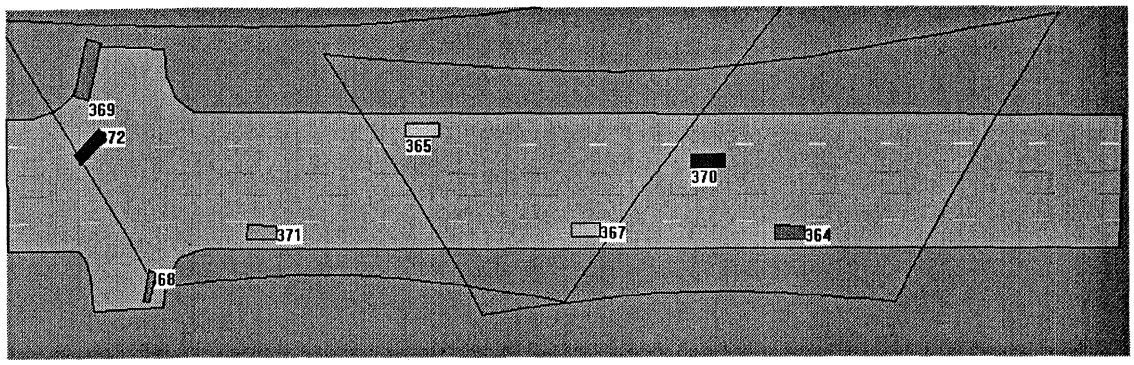

Figure 4.2.2-30. Animator Scene For Vehicle 372 Making Left Turn, With Vehicle 365 Oncoming

Figure 4.2.2-31 characterizes the gap by means of a time history that prevails from oncoming vehicle 365 to the left-turner, 372. The figure shows that vehicle 372 occupied the lane in front of the oncoming vehicle from approximately t=1 to t=1.7 seconds, reaching a minimum range value of approximately 100 feet before exiting from lane L-2. Again, the fact that SAVME data continuously locates each vehicle relative to lane boundaries enables a crisp way of expressing in-lane and out-of-lane conflict phenomena.

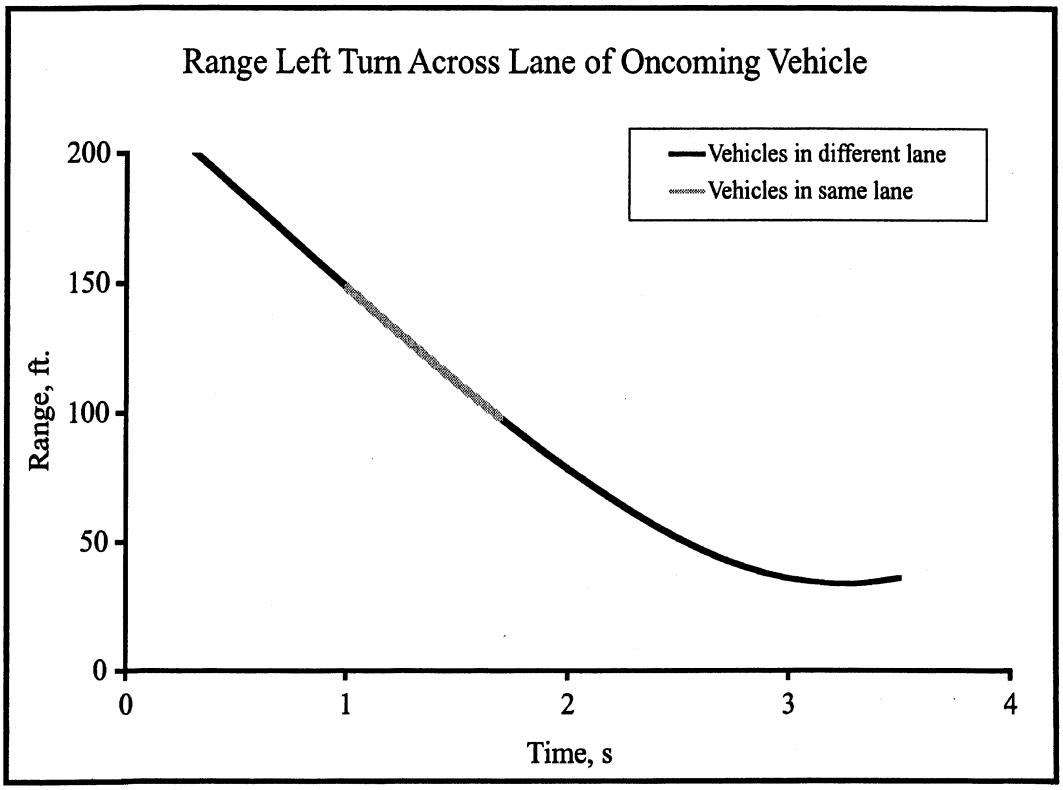

Figure 4.2.2-31 Range History Depicting The Conflict Between Vehicles 372 and 365.

Figures 4.2.2-32 and 4.2.2-33 show the range-rate and time-to-collision histories for the same maneuver, indicating that the oncoming vehicle approached at approximately 75 ft/sec and that, while vehicle 374 was in the lane, the minimum time to collision reached as little as 1.5 seconds. A scenario of this kind is recognized to be one of the fundamental challenges in the development of suitable systems for forward crash warning since drivers tend to have high confidence in their ability to predict, as in this case, that a cross-turning vehicle will clear their path before the trajectories intersect. Thus a warning presented to the driver of vehicle 365 may have been unwelcome in this scenario.

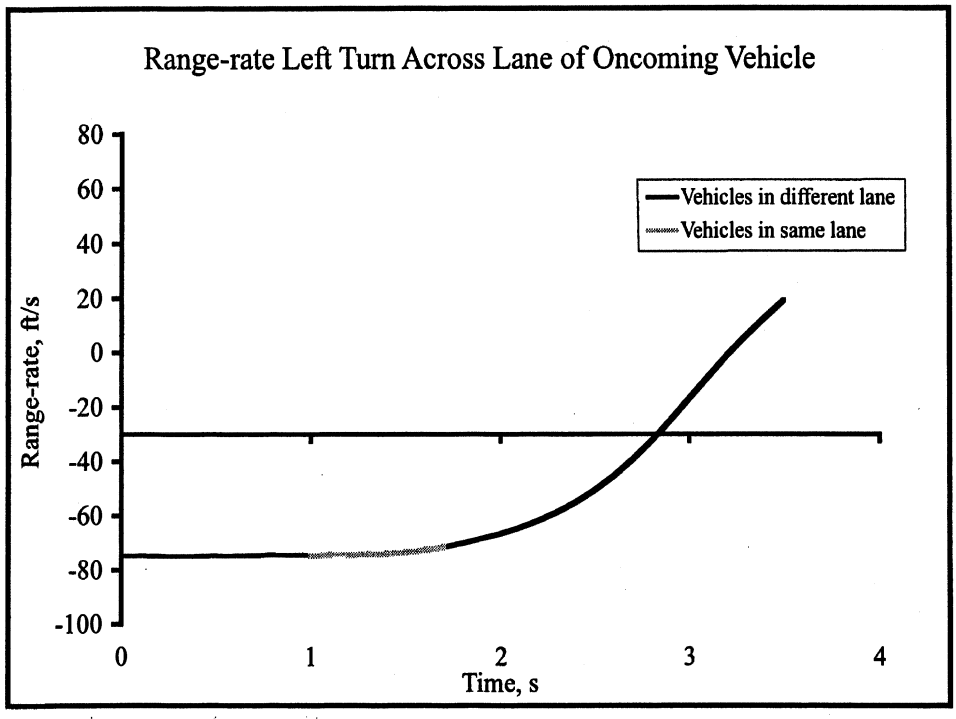

Figure 4.2.2-32. Range-rate History of The Conflict Between Vehicles 372 and 365

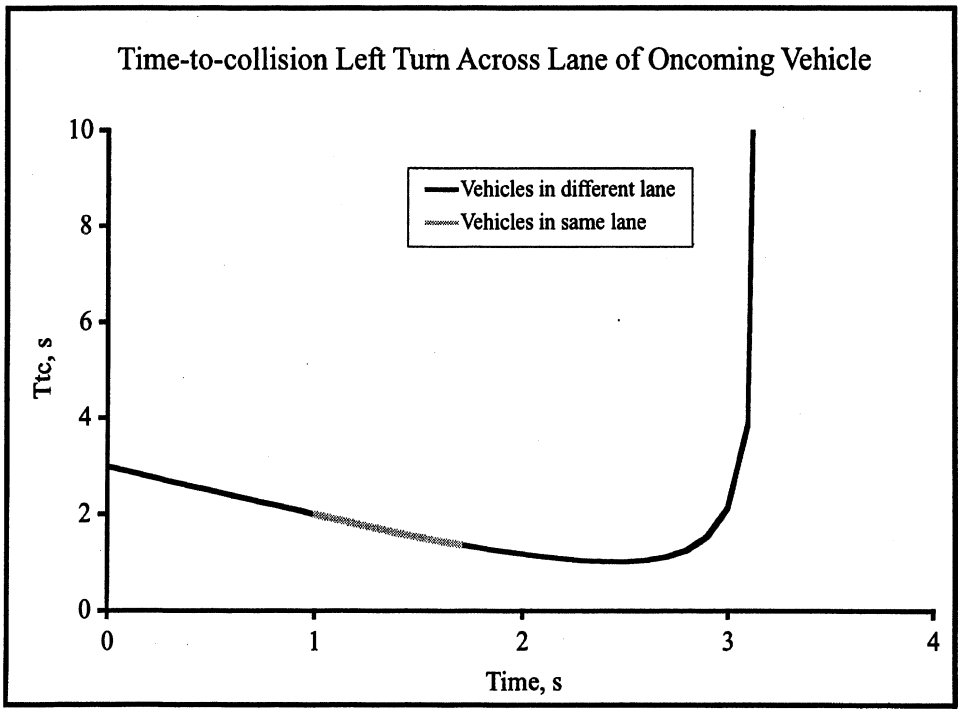

Figure 4.2.2-33. Time-to-collision History of the Conflict Between Vehicles 372 and 365

SAVME data are able to support the examination of the apparent path-prediction behaviors of drivers, as well as the explicit algorithmic computations of an onboard crash warning system, by means of SAVME's rather complete treatment of the intervehicular variable domain. Shown in Figures 4.2.2-34 and 4.2.2-35, for example, we see the range vs. azimuth angle relationships between the two vehicles identified in the left-turn conflict, above. Indeed, the SAVME database contains the complete range, range-rate, and azimuth angle relationships between every pair of vehicles that occupy the scene at any one time, both in terms of vehicle A as related to B and in terms of vehicle B as related to A (where the A-B and B-A pairs of data differ only by azimuth angles). The illustrated plots of range vs. the azimuth angle, alpha, express the viewpoint from the oncoming vehicle, 365 which "sees" the left-turner 372, initially at a range of some 220 feet and –4 degrees of azimuth, at the right extremity of the plot. Figure 4.2.2-35 shows the individual data points taken at 0.10 second intervals, during the period in which the left-turner occupied the L-2 lane of the oncoming vehicle. This point-by-point plot also reveals that one could readily compute the cross-path motion of the left-turning vehicle relative to the host, so as to predict the physical clearance of the vehicle bodies, such as a crash-warning algorithm would strive to do. Modern automotive radars commonly have the ability to resolve azimuth-to-target so as to make such predictions. The availability of SAVME data, showing the actual behaviors of real drivers, would allow the development of radar-processing algorithms in light of the conflict distributions that people encounter (and more or less tolerate) everyday.

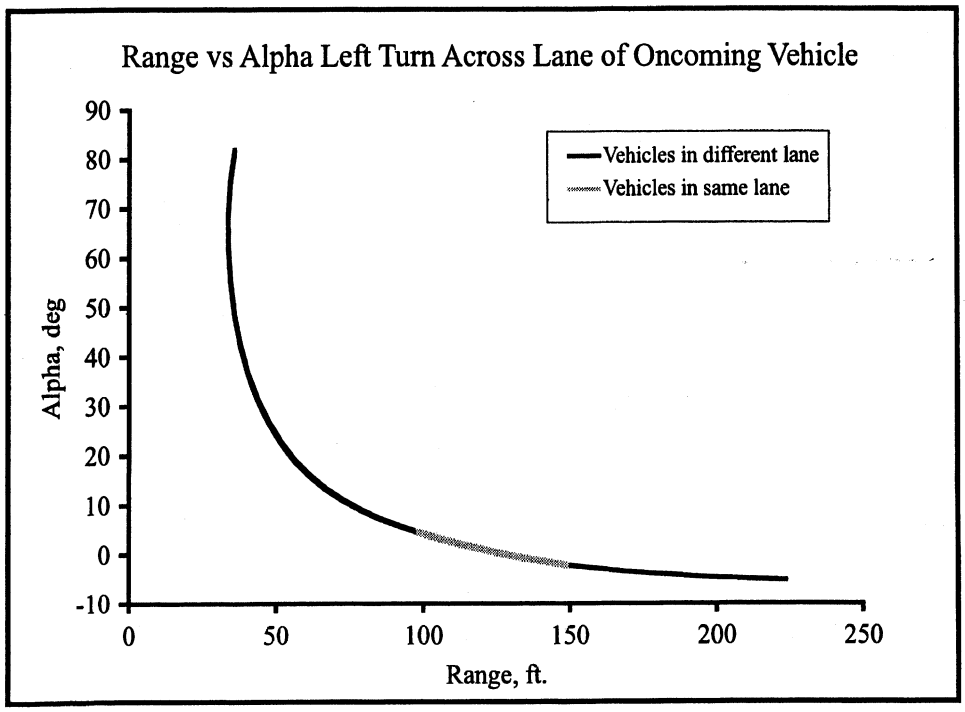

Figure 4.2.2-34. Range vs. Azimuth Angle Of The Relationship To The Target Vehicle, 372 As Seen From Host Vehicle, 365

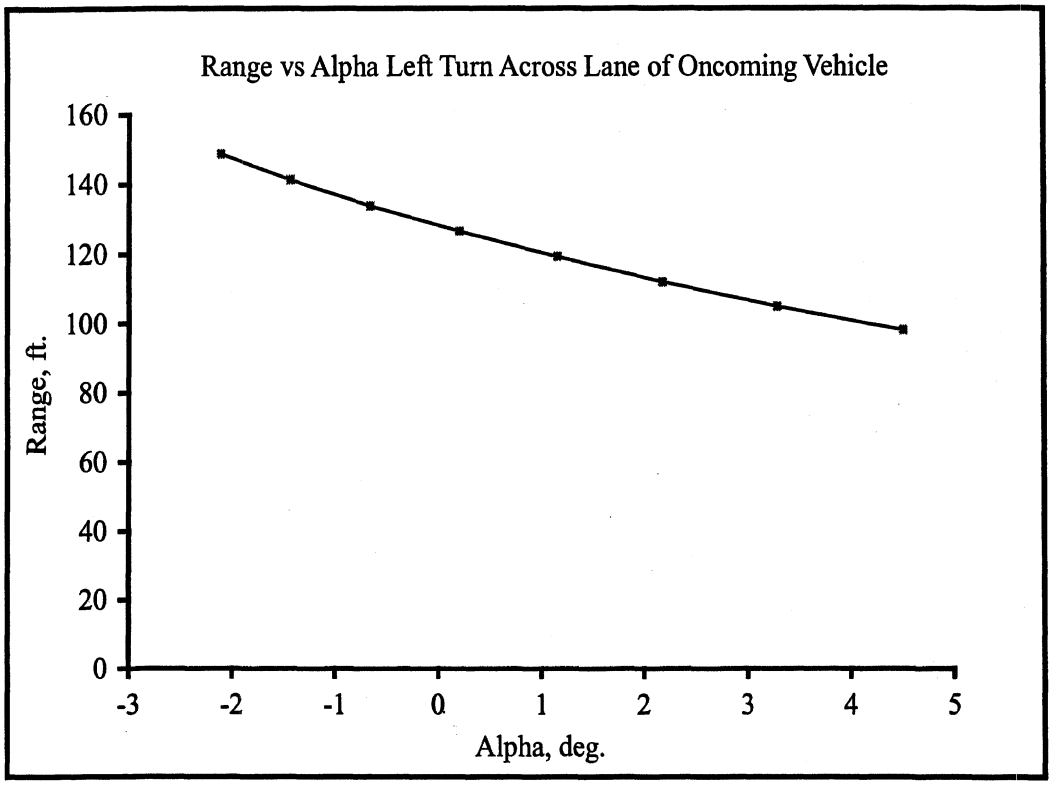

Figure 4.2.2-35. Individual Tenth-second Data Points In The Range vs. Azimuth Relationship Of Oncoming Vehicle 365 To The Left-turner, 372

A query was run on the database to find all cases in which a vehicle executed a left turn into the intersecting roadway, L-3, from the center left-turn lane, L0, and encountered an oncoming vehicle in lane L-2. The query identified 330 such cases from the database. Direct and cumulative distributions of a time-to-collision measure were obtained for all of these cases, as shown in Figures 4.2.2-36 and 4.2.2-37, respectively. In this set of cases, time-to-collision was computed right at the moment in which the left-turning vehicle crossed the northern-most lane boundary into road segment L-3. An alternative measure might have computed the time to collision from the host to left-turning-vehicle at the moment for which the body of the left-turning vehicle first fell outside of the projected path of the oncoming host vehicle body. Although such a result is straightforward to determine with SAVME data, a simpler lane transition point was used for computing the indicated results, above. The figures show that times-to-collision in unsignalized left turns at this site are at 4 seconds or less about half of the time. On the other hand, no values below 1 second were measured in this dataset.

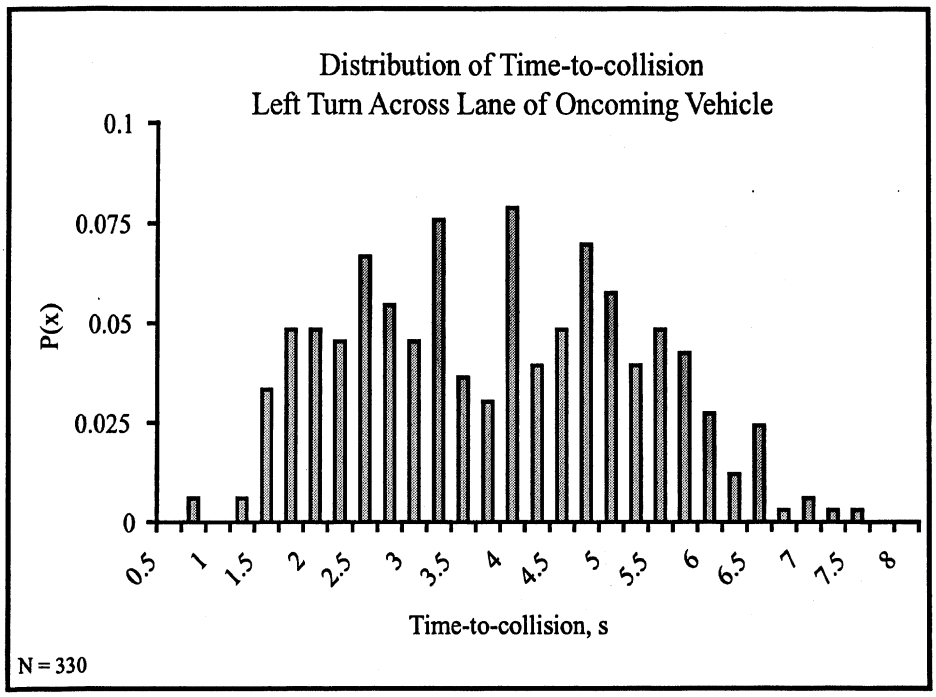

Figure 4.2.2-36. Time-to-collision For 330 Cases Of Left Turn Conflicts

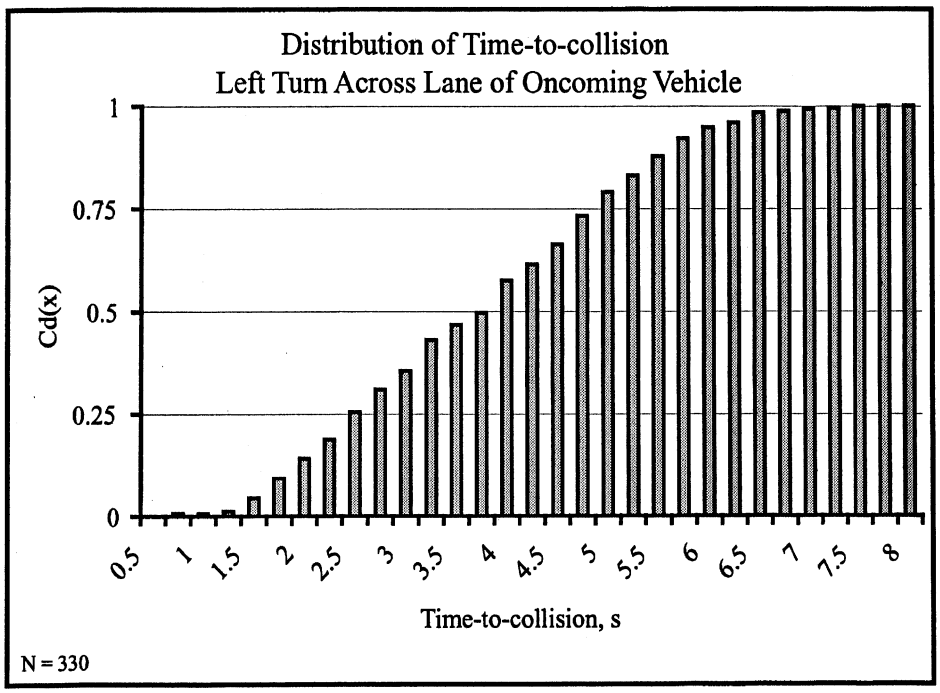

Figure 4.2.2-37. Cumulative Distribution For 330 Left Turn Conflicts

Emerging from a Stop Sign

Shown in Figure 4.2.2-38 is the SAVME animator's view of the road scene showing vehicle 390 after it has emerged from the intersecting roadway L-3, and is crossing the interior through lane L-1 as vehicle 407 is oncoming westbound in the same lane. Because the oncoming vehicle does not slow perceptibly throughout the transit of vehicle 390 across its lane, a relatively small-clearance conflict ensues, as captured in the following time histories.

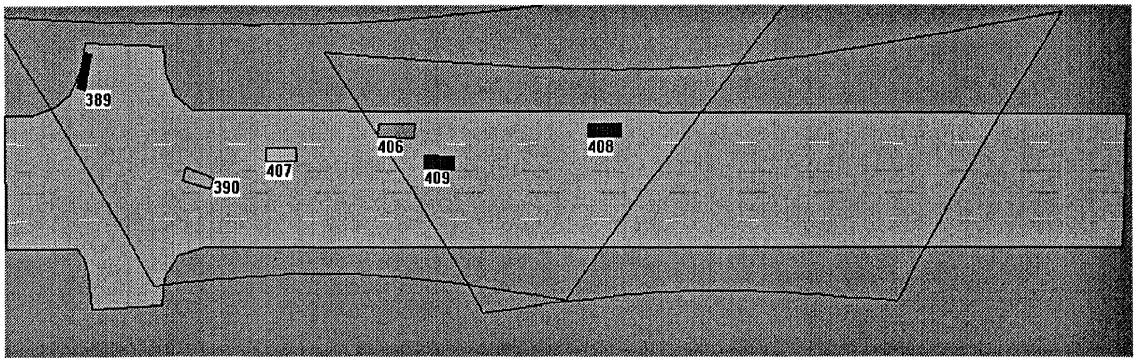

Figure 4.2.2-38. Animator View Showing Of Vehicle 390

Figure 4.2.2-39 shows the range history from its initial value of 440 feet down to a rather slim range clearance, with a highlighted segment showing range during the transit of vehicle 390 across lane L-1. While vehicle 390 was still in lane L-1, the oncoming vehicle came within approximately 40 feet of striking it at a closure speed (shown in Figure 4.2.2-40) of approximately 80 ft/sec (55 MPH) (thereby reaching a time-to-collision value near 0.5 seconds). The range-rate data show that the oncoming vehicle proceeded virtually without any speed reduction in approaching the cross-path motion of vehicle 390 (although the increase in range-rate from approximately 70 to 90 ft/sec was due to acceleration on the part of vehicle 390, as it began to assume a heading angle that was more acute to the path of oncoming vehicle 1150).

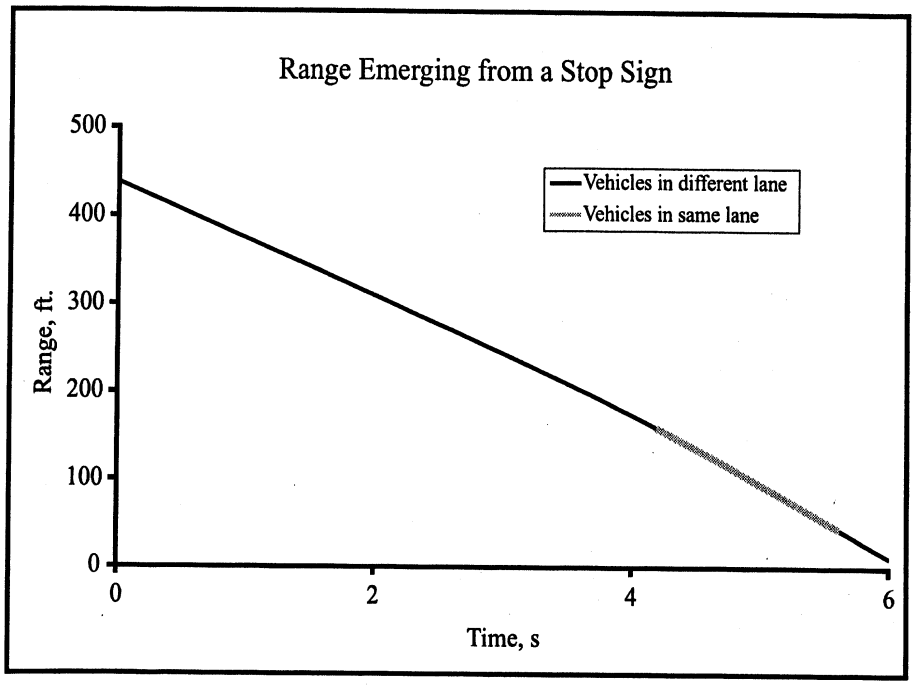

Figure 4.2.2-39. Range From Oncoming Host in Lane L -1 to Vehicle Emerging from Stop Sign

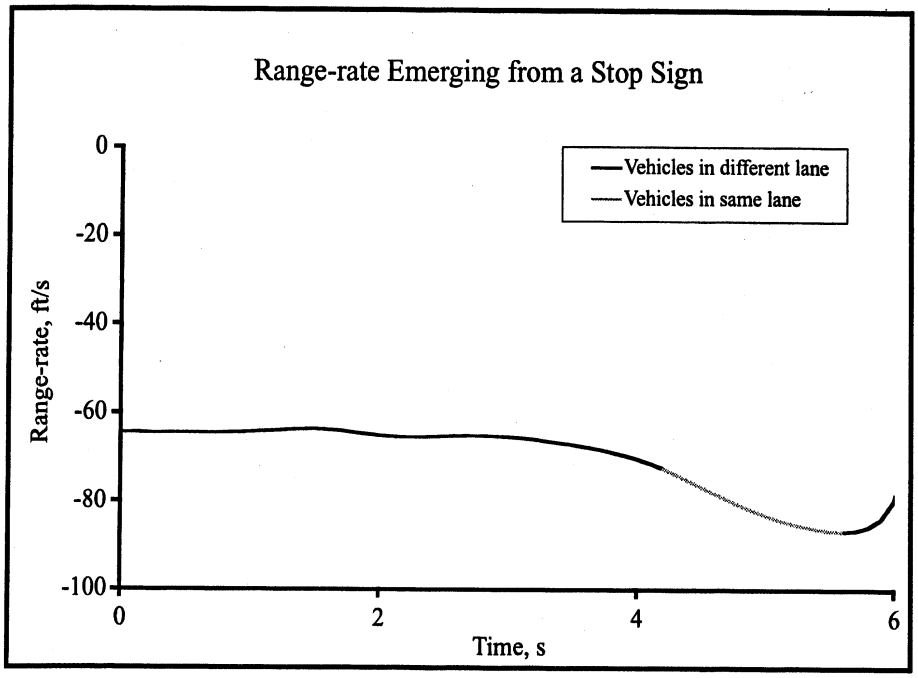

Figure 4.2.2-40. Range Rate from Oncoming Host in Lane L-1

Figure 4.2.2- 41 shows the full range vs. alpha relationship as it would be seen from the oncoming vehicle. These data show that the encounter, beginning at the upper right of the graph, was nearly straight on until range was within about 40 feet, whereafter the oncoming host vehicle passes by vehicle 390, with azimuth angle quickly transitioning through 90 degrees and beyond. Figure 4.2.2-42 shows the close-up segment of range vs. alpha, presenting each tenth-second data point for the interval during which vehicle 390 occupies lane L-1. One can imagine that the oncoming driver has estimated the left-going speed of vehicle 390 and has determined that the needed clearance will exist, however slim. A hypothetical crash warning system processing the same range vs. alpha relationship might have determined that the approach would be too close to ignore.

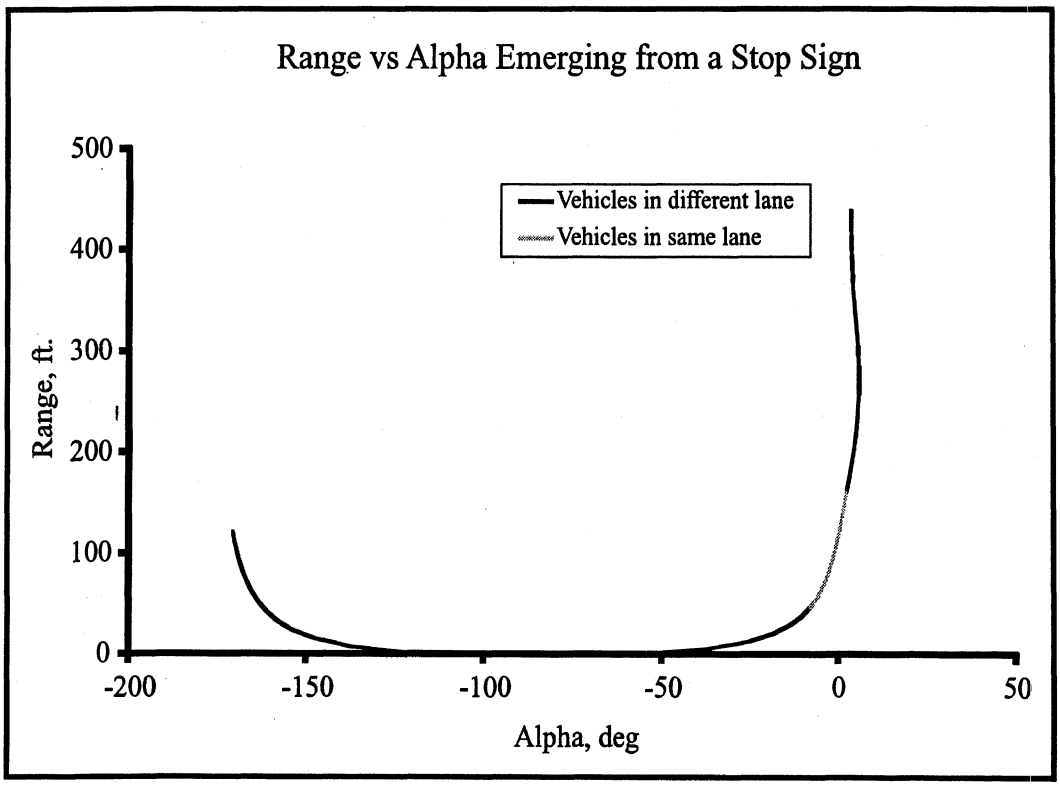

Figure 4.2.2-41. The Range vs. Azimuth Angle Relationship for a Near Encounter in Lane L-1

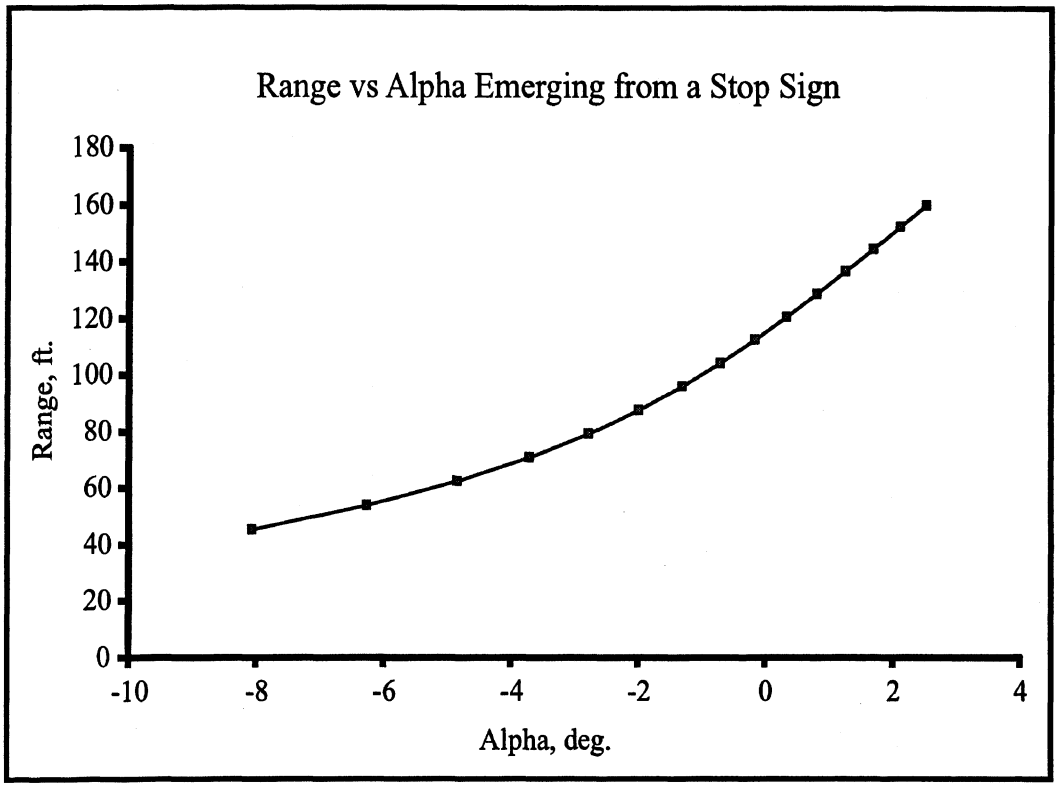

Figure 4.2.2-42. Expanded View of Range vs. Azimuth Angle

A query of the database produced 147 cases in which a vehicle made this type of maneuver, emerging from the stop sign on the intersecting roadway, L-3, and encountering an oncoming vehicle in lanes L-1 or L-2. The distribution of time-to-collision values that occurred right when the cross-path vehicle was exiting across the oncoming vehicle's lane boundary is shown in Figure 4.2.2-43. We see that typical values at this site range from 2 to 6 seconds-to-collision and that the specific case discussed earlier, with its 0.5 second value of time-to-collision, was somewhat an outlier in this modest set of results.

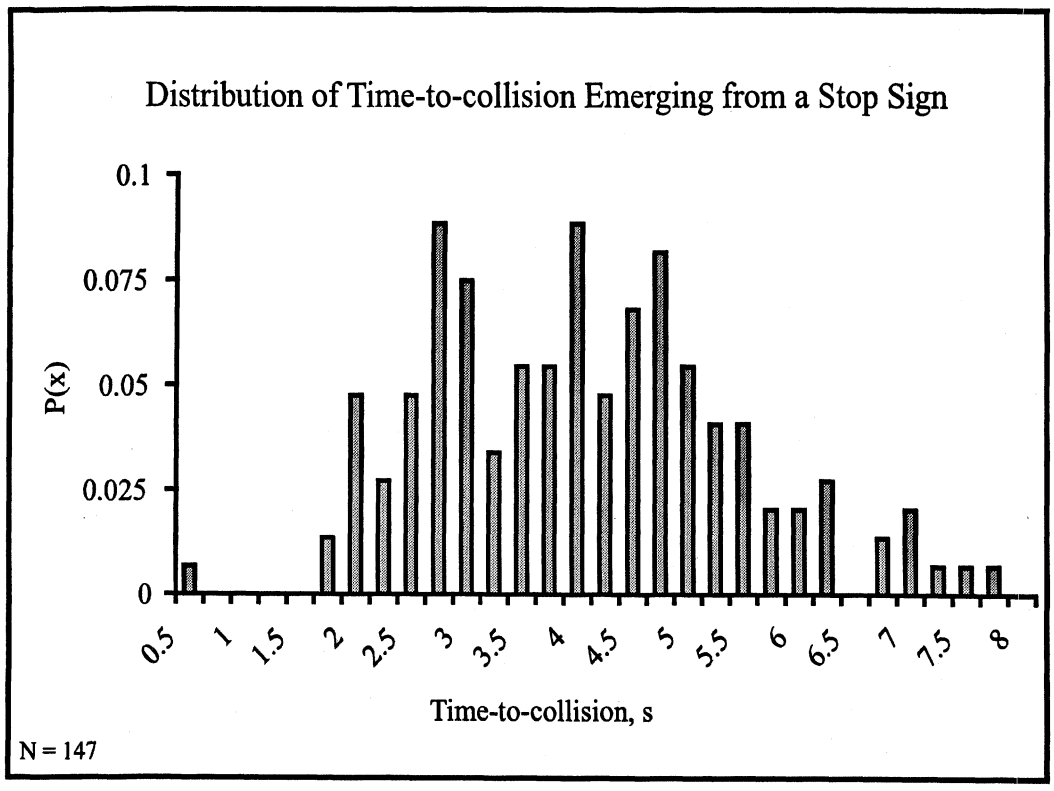

Figure 4.2.2-43. Results of a Query that Identified 147 Cases of Conflict for Vehicles Emerging from the Stop Sign at Road Segment L-3

Left Turn into a Traffic Lane

Shown in Figure 4.2.2-44 is the x-y trajectory of a vehicle that emerged from the stop sign, turning left to merge into an eastbound traffic lane, through liberal use of the center left-turn lane, L0. Upon entering the eastbound interior lane, L1, the vehicle assumes a gap in front of another eastbound vehicle in the same lane. In this case, SAVME data are being examined to characterize the situation that is developing behind a selected host vehicle, as it moves to occupy a position in a moving traffic stream. We see that the emerging vehicle traveled approximately 250 feet in the center left-turn lane before moving into the adjacent traffic lane.

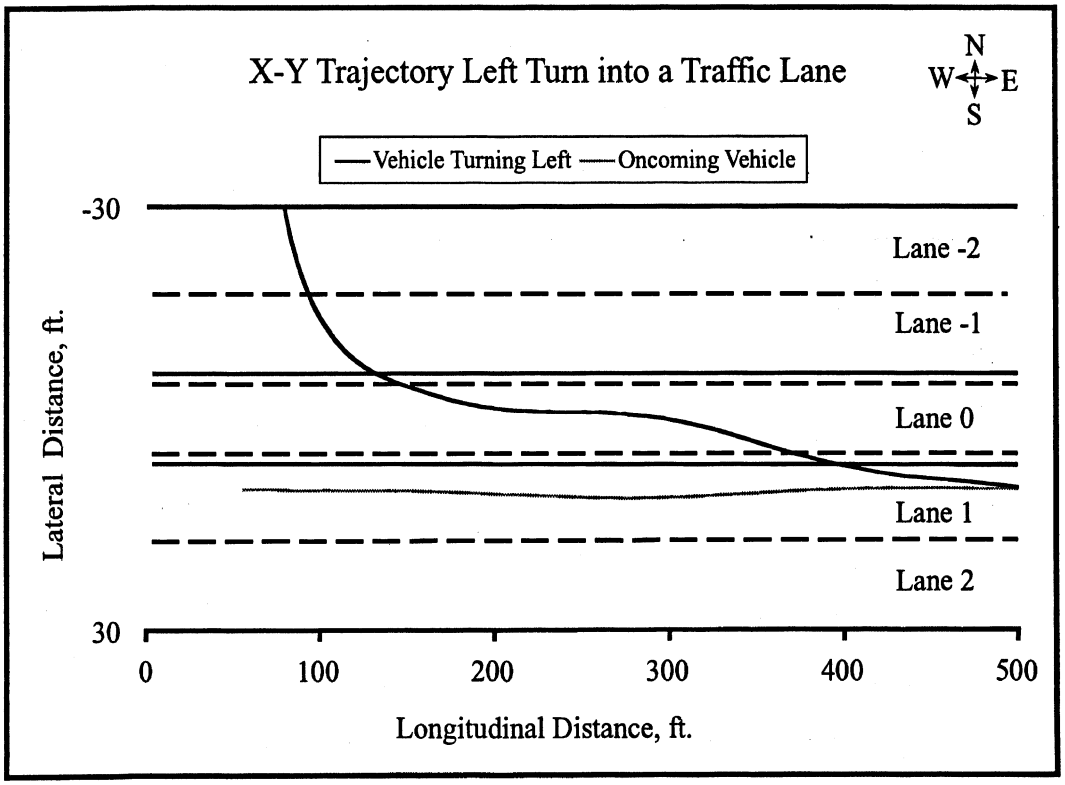

Figure 4.2.2-44. Vehicle Turns Left and Takes a Gap in Traffic to Move into Lane L1, in Front of Another Oncoming Vehicle in the Same Lane

Figure 4.2.2-45 and 4.2.2-46 clarify the transition strategy of the emerging driver since they show the range and range-rate sequences that depict a vehicle speeding up to essentially match the speed of the oncoming vehicle in lane l, with entry into the lane (at t=5 seconds) coinciding with a range rate of essentially zero and a rather tight range clearance of about 30 feet. Soon after entering lane, L1, the indicated range value continues to open up as the lead vehicle accelerates and the following vehicle coasts.

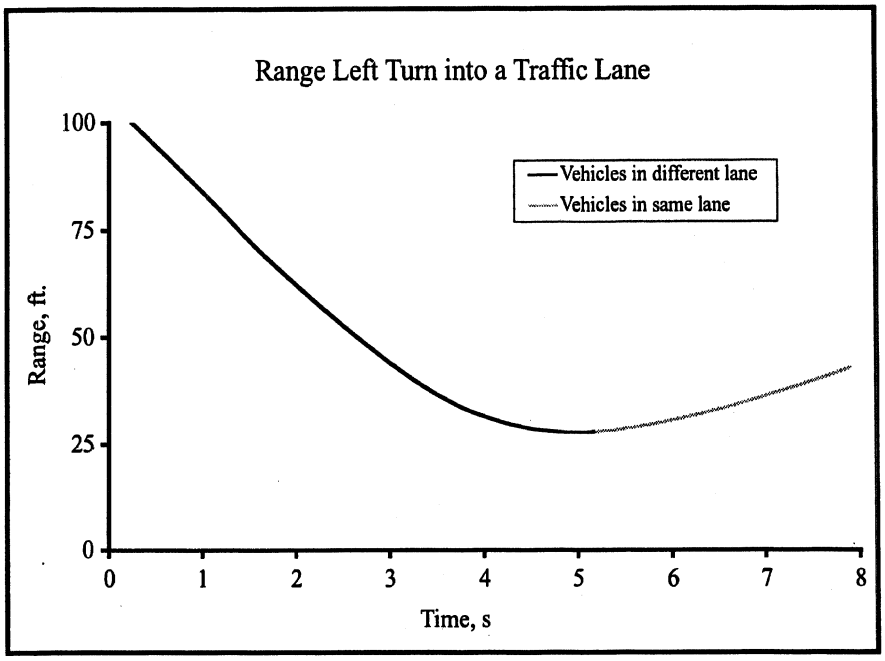

Figure 4.2.2-45. Range from Oncoming Vehicle to Left-Turner Entering Lane L1

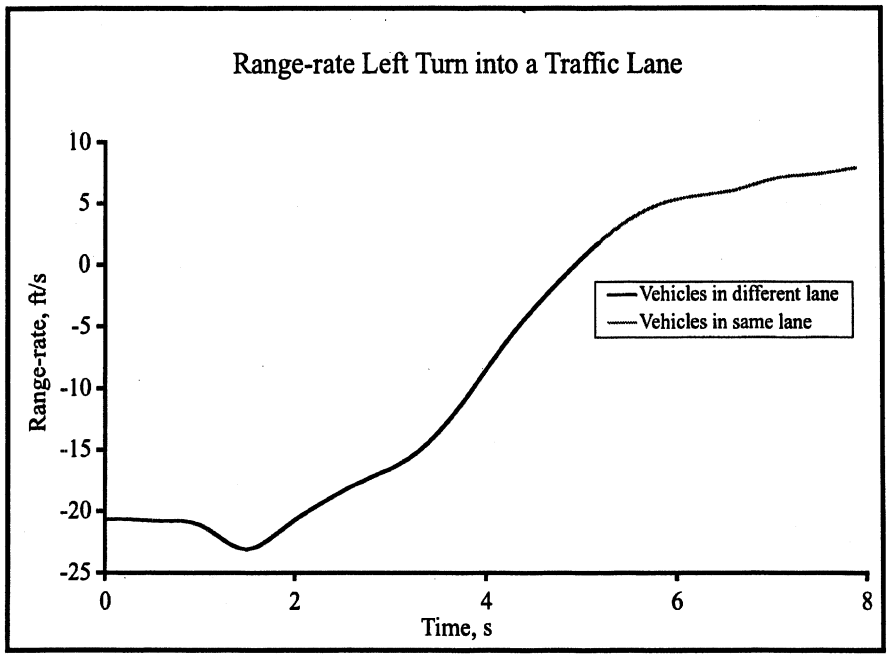

Figure 4.2.2-46. Range-Rate from Oncoming Vehicle to Left-Turner

Figure 4.2.2-47 takes the vantage point of the oncoming vehicle, showing in its Range vs. Alpha plot that the entering vehicle is first seen at a range of 100 feet and six degrees to the left. As the approach continues, azimuth angle grows to about 11 degrees as if the oncoming vehicle will pass on the right, but then the entering vehicle begins its final movement into lane, L1, causing azimuth to reduce all the way down to zero, upon assuming the gap directly in front of the oncoming vehicle, at a final range of 40 feet. Figure 4.2.2-48 shows the final progression from the vicinity of alpha = 6 degrees, when entry into lane, L1, occurs, until the merge is effectively completed by an asymptotic type of approach toward alpha=0.

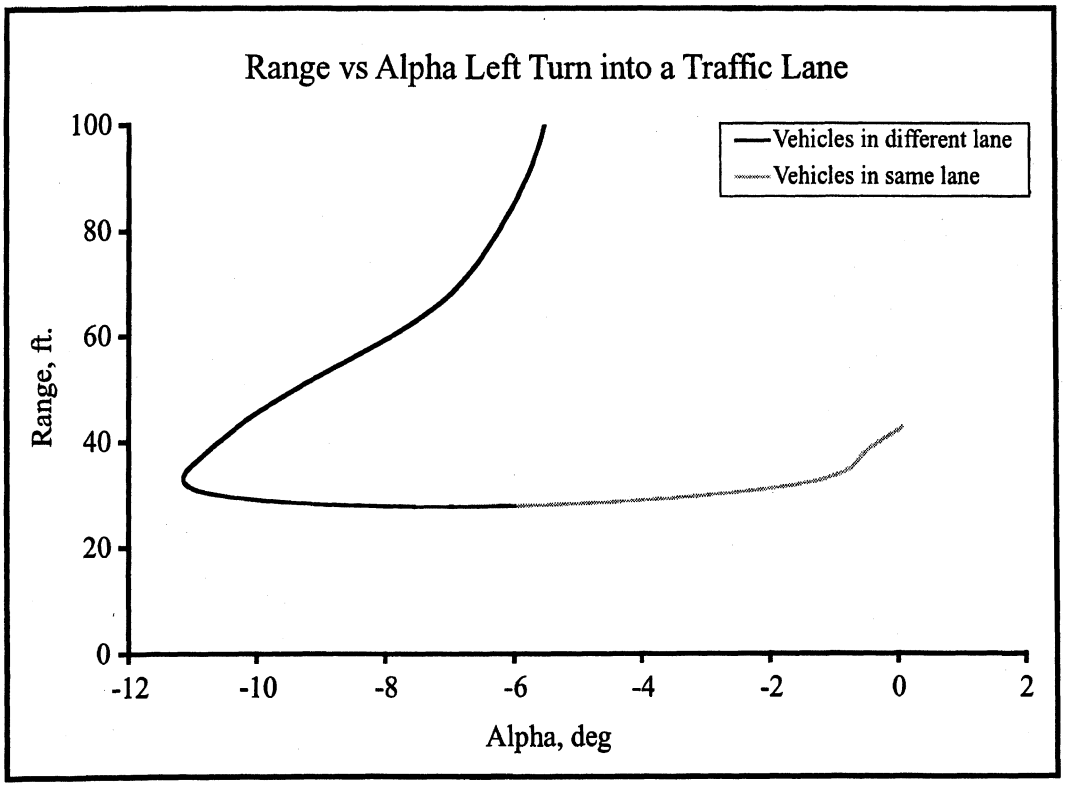

Figure 4.2.2-47. Range vs. Azimuth, Measured from Oncoming Vehicle to Left-Turner

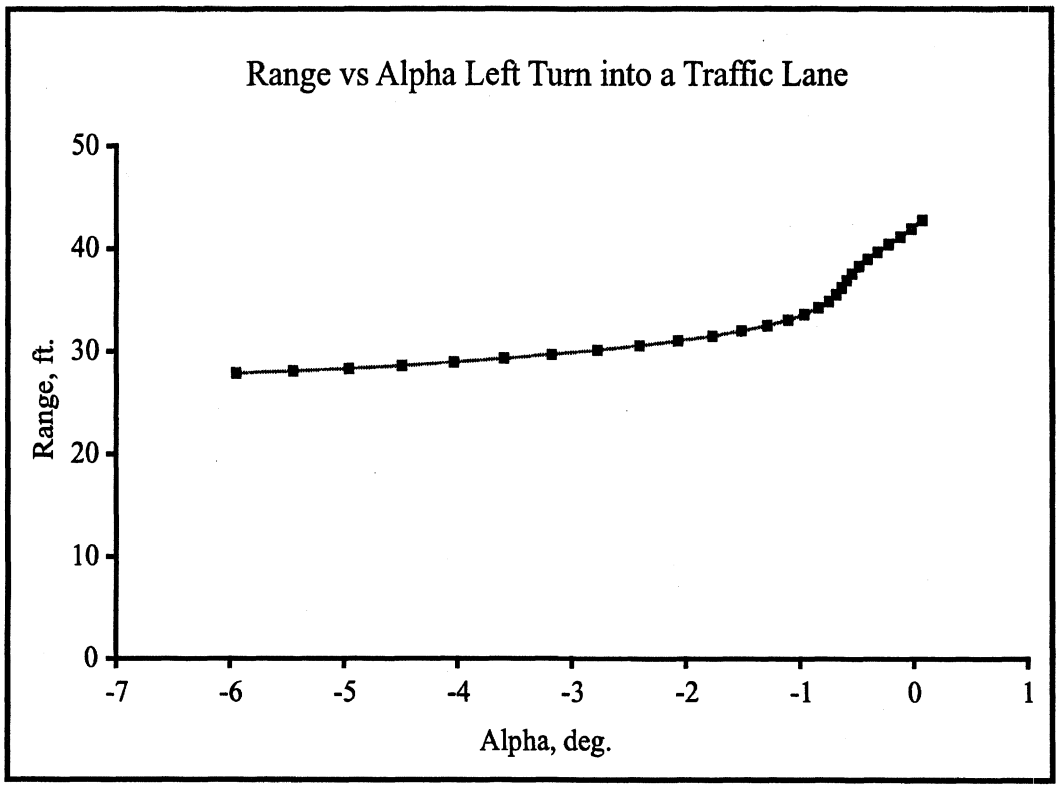

Figure 4.2.2-48. Tenth-Second Data Points Showing Range vs. Azimuth Angle

These data provide a highly definitive anatomy of the merging process. Although this process will involve different quantitative values of the respective variables from differing road conditions, nevertheless the sequence of nulling the range-rate condition and moving laterally to acquire a position within the gap is fundamental to the process.

A query of the database produced 28 cases in which a vehicle made the same maneuver, emerging to go left from the stop sign on the intersecting roadway, L-3, and taking a gap in front of an oncoming vehicle in lane, L1. The ranges, headway times, and range-rate values that prevailed between the merging vehicle and the oncoming vehicle behind it, at the moment of entry into lane, L1, are shown in Figures 4.2.2-49, -50, and -51 respectively. In each of these cases, the data are simply rank ordered from the lowest to the highest value of each respective variable, for the 28 cases found in the file.

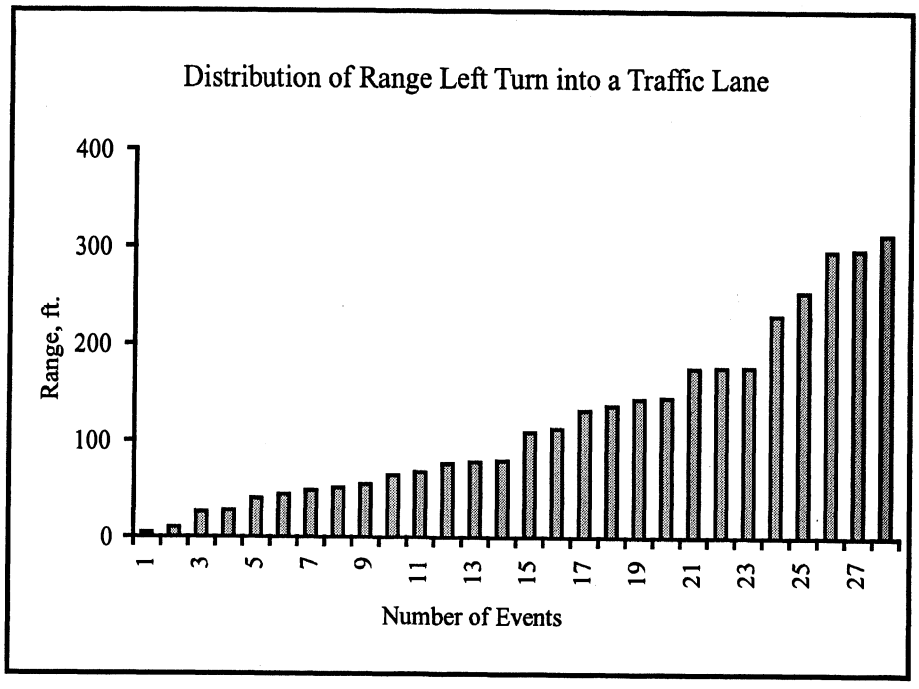

Figure 4.2.2-49. Rank Order of Values at the Moment of Transition into Lane L1

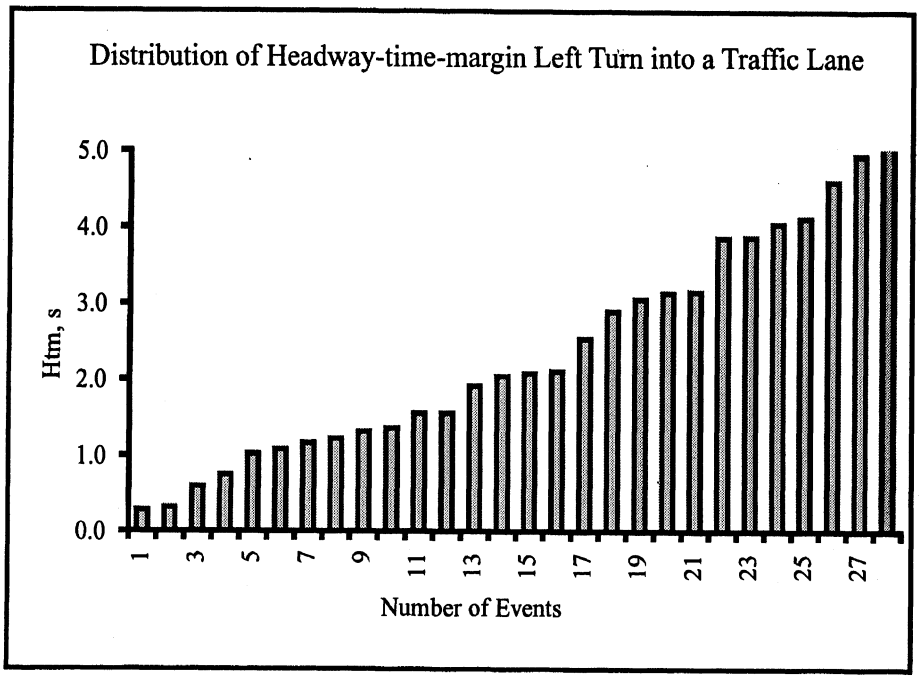

Figure 4.2.2-50. Rank Order of Headway Time Values

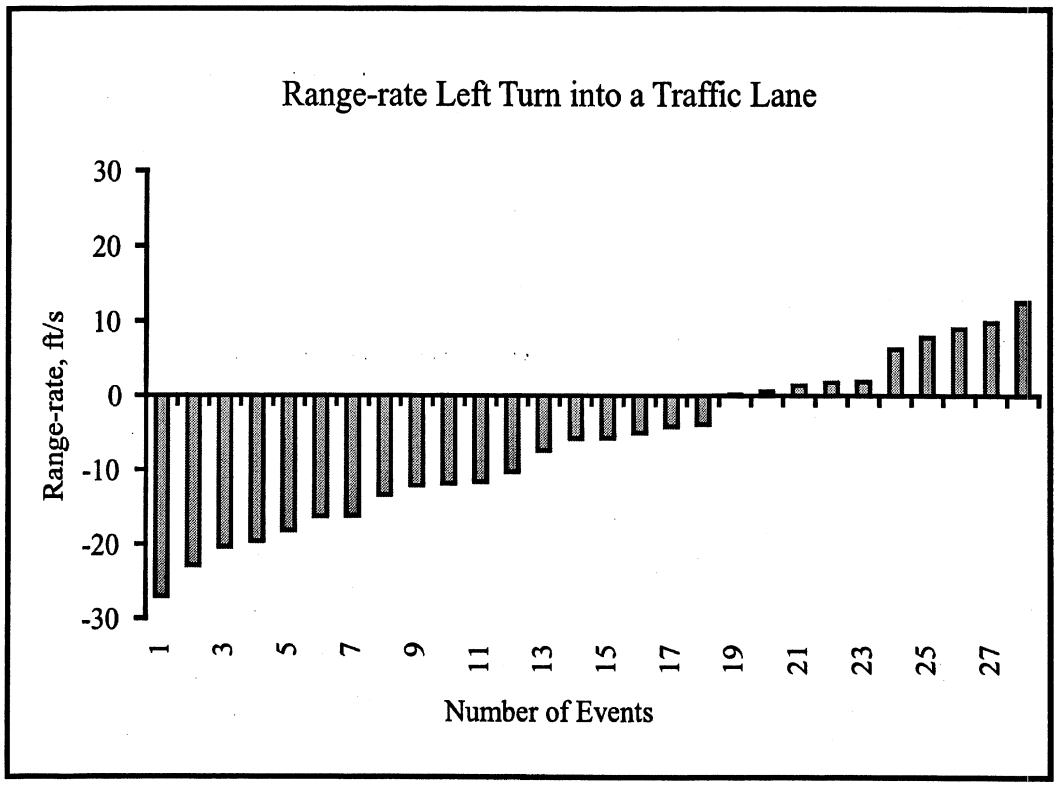

Figure 4.2.2-51 Rank Order of Range-Rate Values

Figure 4.2.2-52 provides a useful summary of the merge conflicts posed in these 28 cases, characterizing the moment of lane entry by the range and range-rate coordinates of the momentary conflict. We see that most people enter the lane in the left-side, or conflicting portion of the range, range-rate space, although none of the conflicts is particularly threatening (shortest time-to-collision = 5 seconds.) On the other hand, persons entering the lane at positive range rates occasionally insert themselves at very short range values relative to their neighbors, as appear on the right half of the diagram.

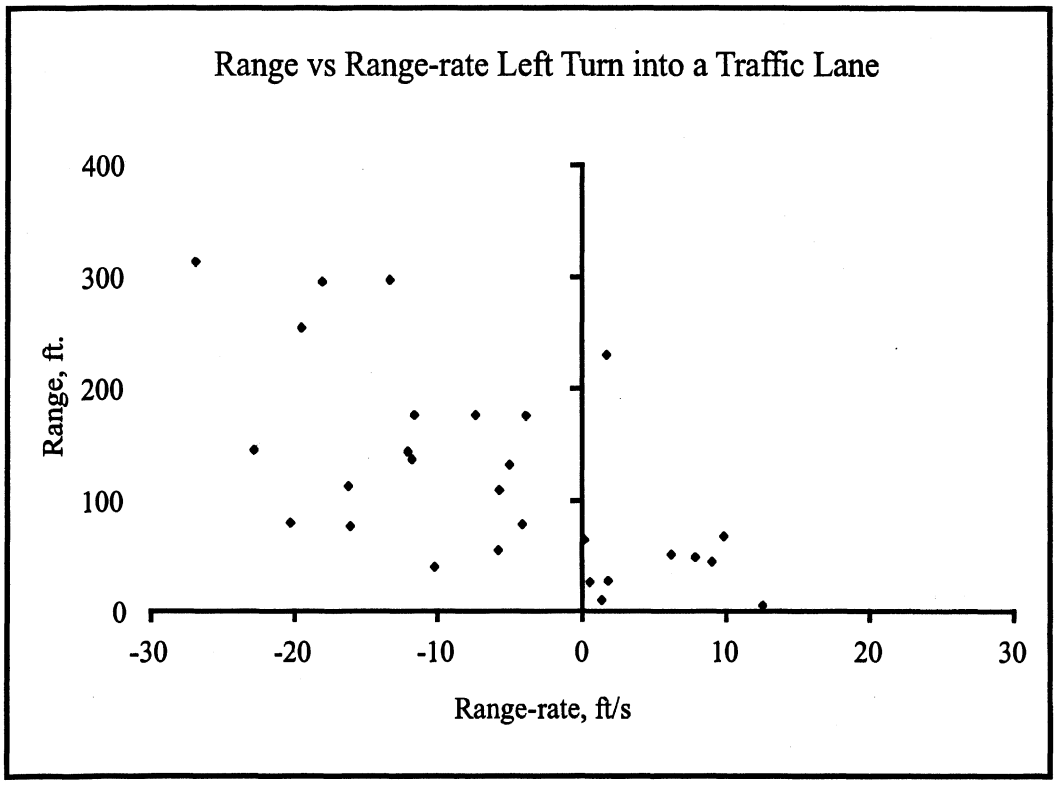

Figure 4.2.2-52. Range, Range-Rate Coordinates at the Moment of Transition into Lane L1

Finally, Figure 4.2.2-53 draws again on the ability of SAVME data to recover the absolute coordinates of any definable event, such as the moment of entry by the merging vehicles into lane L1. The figure shows that the 28 vehicles satisfying this query actually entered lane L1 over an approximate 300-foot stretch of the roadway, apparently lingering within the center left-turn lane, L0, for whatever length of travel as was needed to both accelerate up to the speed of adjacent-lane traffic and to find a suitable gap.

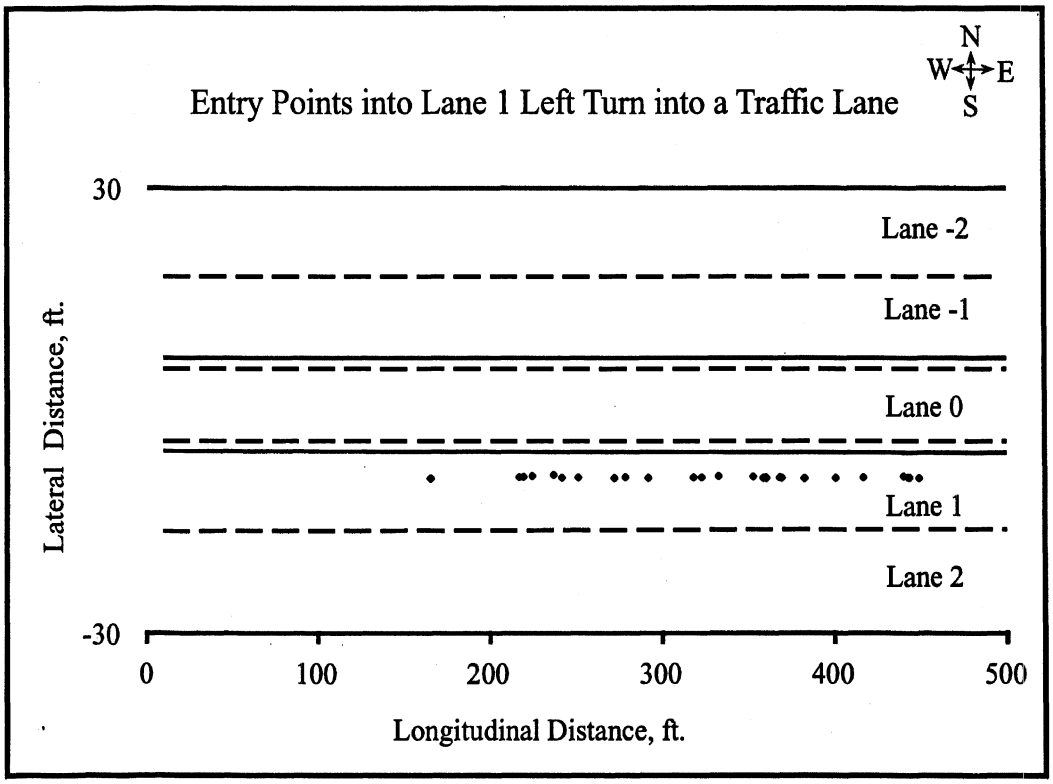

Figure 4.2.2-53. X-Position Marking the Point at which Each of the Left-Turning Vehicles Transitioned from Lane L0 to Lane L1

Figure 4.2.2-53 shows the location of the lane transition points for each of the 28 vehicles that emerged from the stop sign at lane L-3 and took a gap in traffic to enter lane L1. These results illustrate the ability in SAVME data to discover absolute position results such as may be instructive for traffic engineering purposes.

String Compression Induced by Sudden Braking at the Lead Vehicle

Shown in Figure 4.2.2-54 is an animation frame showing the position of vehicle 2348 at the head of a five-vehicle string in lane L-2. Vehicle 2348 brakes substantially in order to turn right into the intersecting roadway, L-3, and in the process induces a propagating compression of the original spacings between the successive vehicles behind it. This case is illustrated quantitatively using several time histories and is then generalized upon from a perspective that explores the significance to crash warning or avoidance systems of the ability to anticipate disturbances in a string before they are manifest to each successive driver. This perspective will then be expressed in a query of the database by which to estimate the benefit of a radar system that is capable of detecting vehicles several deep in a string.

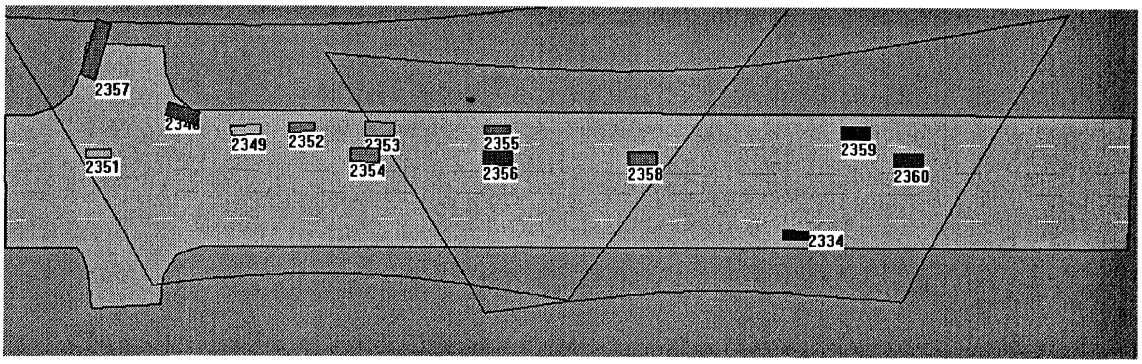

Figure 4.2.2-54. Animator Frame Showing Vehicle 2348, at the Upper Left, Braking at the Head of a Five-Vehicle String

Figure 4.2.2-55 shows the velocity histories of four following vehicles, in response to the approximate 0.2-g sustained deceleration by the leader in this string, vehicle 2348. We see that the velocities of all five vehicles were initially in the vicinity of 55 ft/sec and dropped approximately 30 ft/sec in the process of compression. Although each vehicle's speed reduction began following the response of the vehicle immediately ahead, it does appear that vehicle 2352 reacted with some anticipation of the propagating need since its showed no significant delay in decelerating behind its preceding vehicle, 2349.

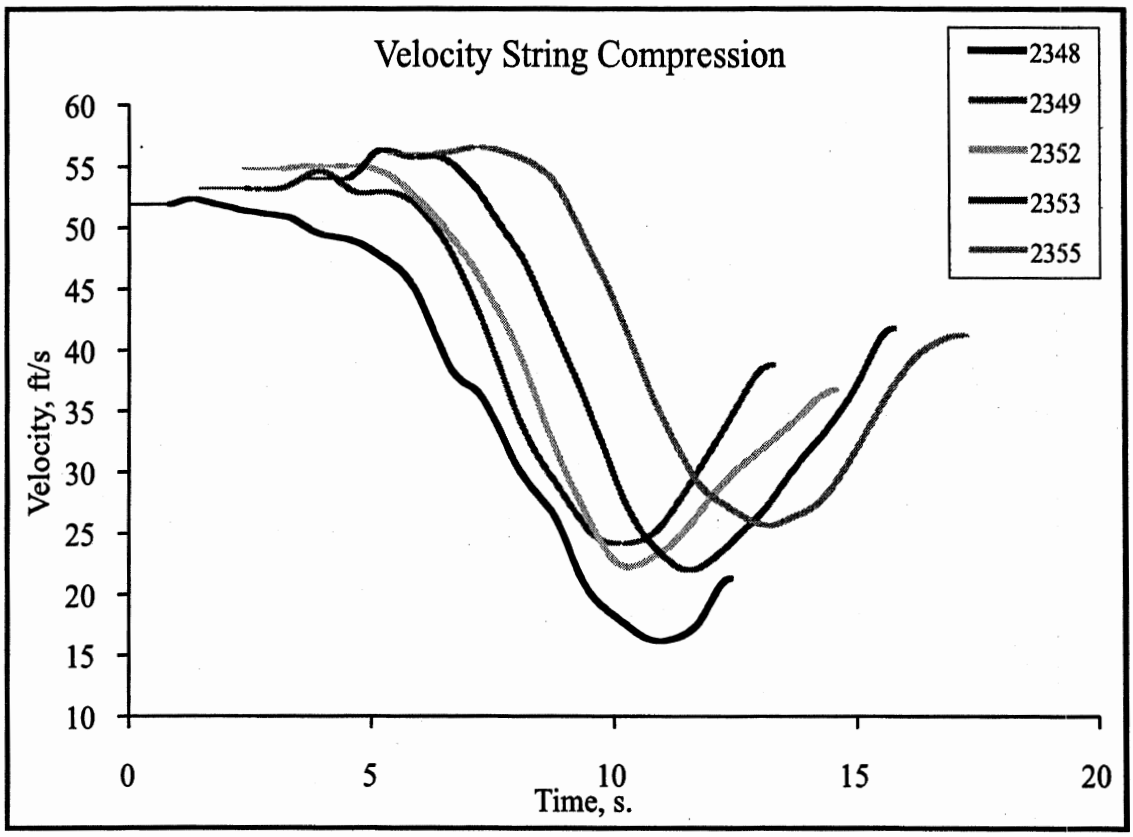

Figure 4.2.2-55. Velocity Time Histories in a Compression String

Shown in Figure 4.2.2-56, the range histories suggest that the driver of vehicle 2352 was more or less obliged to drive in a vigilant, anticipatory manner since the original range behind vehicle 2349 was less than 30 feet. The ranges of the subsequent vehicles, 2353 and 2355 show much larger initial range values and thus the ability to suffer delay in braking onset, having greater range cushions to sacrifice during the compression transient.

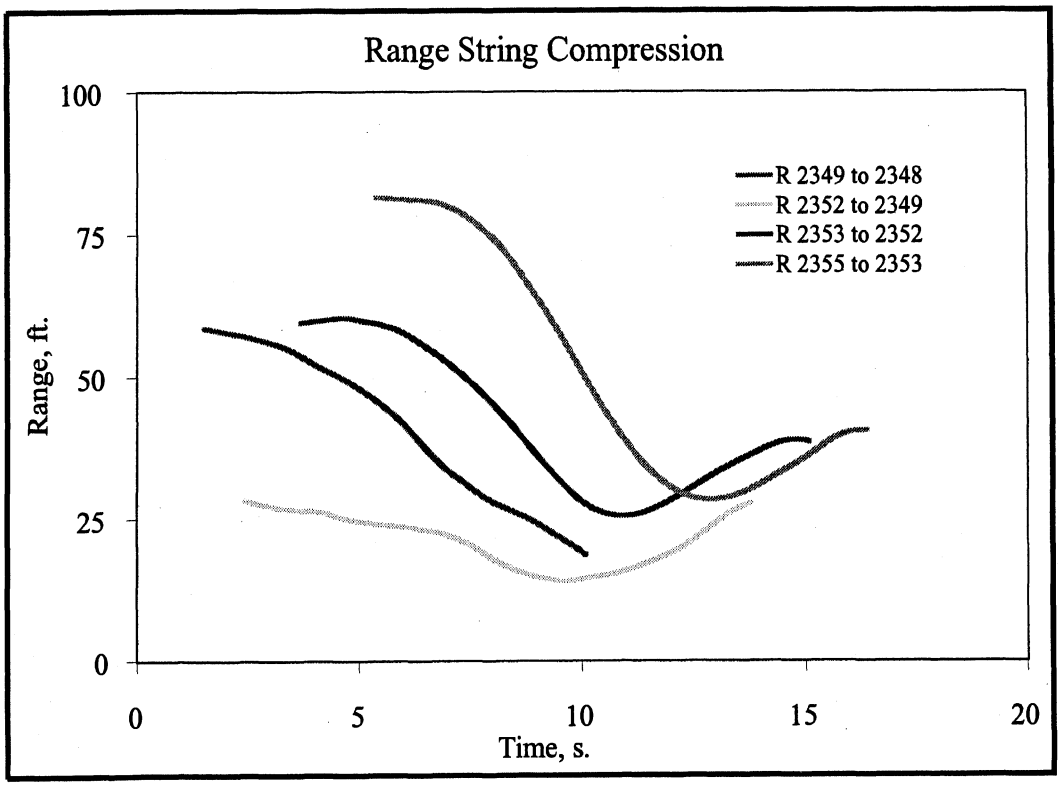

Figure 4.2.2-56. Range Histories in a Compression String

Figure 4.2.2-57 illustrates the string response by means of the combined x position histories of the five vehicles, showing that the front-to-back length of the string at say, t=6 seconds was approximately 280 feet while the string length at t=11 seconds was close to 160 feet. The figure also shows the interesting fact that each of the successive vehicles responded (by curving their x vs. time trace, revealing deceleration) at approximately the same point on the road. That is, the curvatures begin in the vicinity of x = 250 feet, although some degree of anticipation (probably by seeing brake lights up ahead) allows the aftmost vehicles to begin braking a little before the point at which the lead vehicle begins to decelerate. Also, we see the second vehicle, 2349, passing by the x position of the leader following its turn onto the intersecting roadway at t=12 seconds.

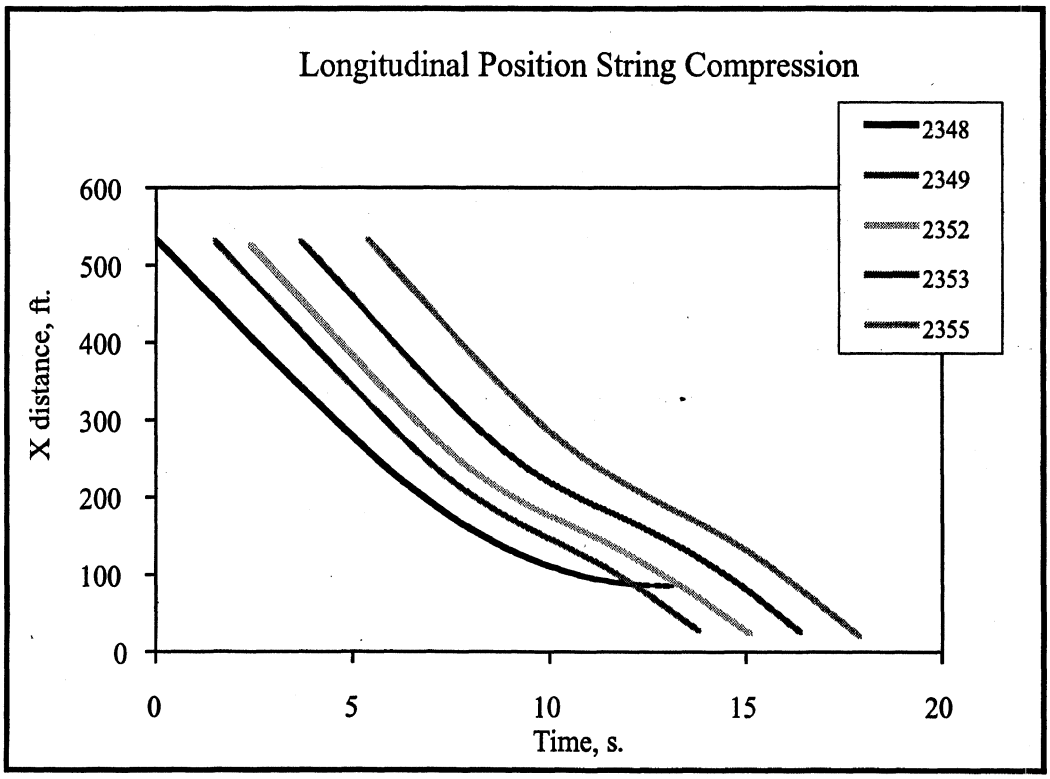

Figure 4.2.2-57. X Position History of a Compression String

Shown in Figure 4.2.2-58 are the time-to-collision histories of the four followers. We see that each of these drivers allowed their time-to-collision values to fall down into the vicinity of 3 seconds before the conflicts were resolved. The plot for vehicle 2352, following vehicle 2349, shows very long values of time-to-collision, and oscillations thereof, as the driver of 2352 anticipated braking by 2349 but then modulated its braking level rather strongly in order the manage the short range value that was pointed out earlier.

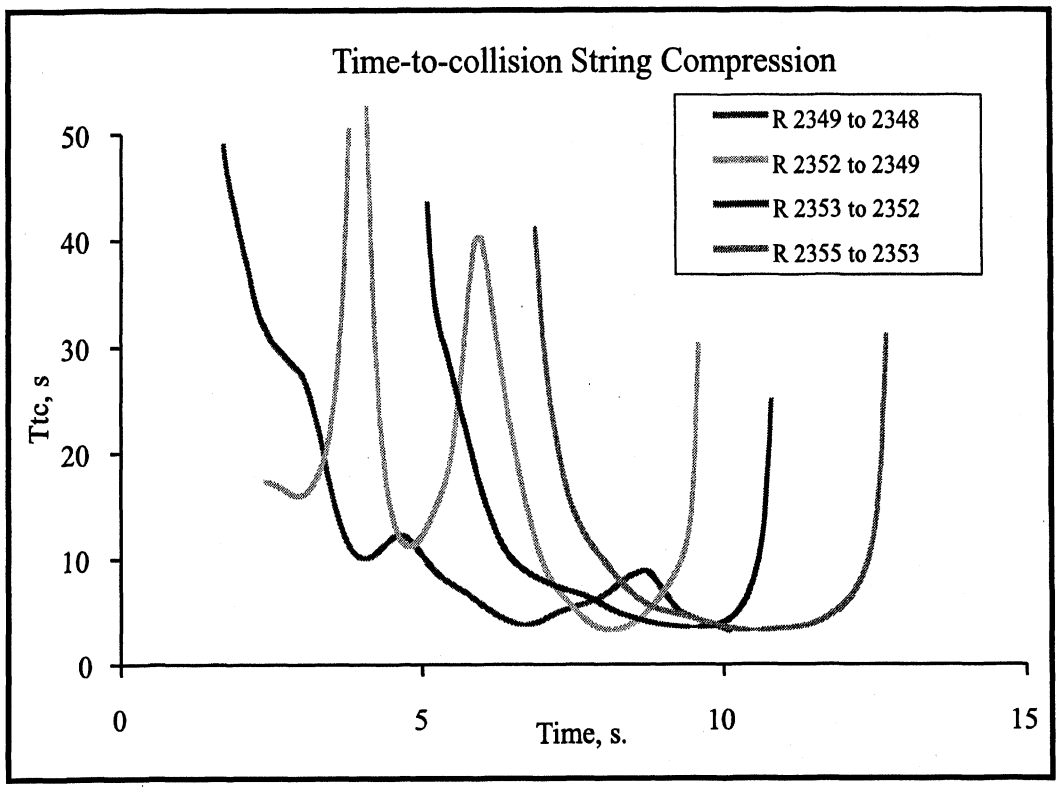

Figure 4.2.2-58. Time to Collision Histories for Compression in a String

Now as a means of examining the general question of managing the car-following task when braking conflicts can propagate along a string of vehicles, a query will be fashioned based upon the scenario posed in Figure 4.2.2-59. The figure illustrates on the right that we wish to explore the benefits of a several-deep radar capability that would be able to detect not only the vehicle ahead (e.g., vehicle 2 being detected by a radar system installed on vehicle 1) but also the vehicle ahead of that (i.e., vehicle 3 also being detected by the radar installed on vehicle 1.) This scenario is not only plausible, but most modern automotive radars do get significant signal returns that detect vehicles several deep, when they are aligned ahead in a string. The confidence level in range and range-rate measurements may decline in the detection of successive vehicles, but the raw capability is nonetheless present.

The potential significance of this scenario is depicted in the range, range-rate diagrams shown at the left side of Figure 4.2.2-59. We normally concern ourselves with the condition of, say, vehicle 1 in relation to vehicle 2, given the operating state expressed by range, $R_{1,2}$, and range rate, $Rdot_{1,2}$. If the crash warning or avoidance system installed in vehicle 1 had only these two variables to go on, it would be concerned only with the need to manage the immediate conflict posed by their combination, as characterized by the decel-to-avoid value (DA), as in:

$$(DA_{1,2}) = (Rdot_{1,2})^2 / (2\, R_{1,2} g)$$

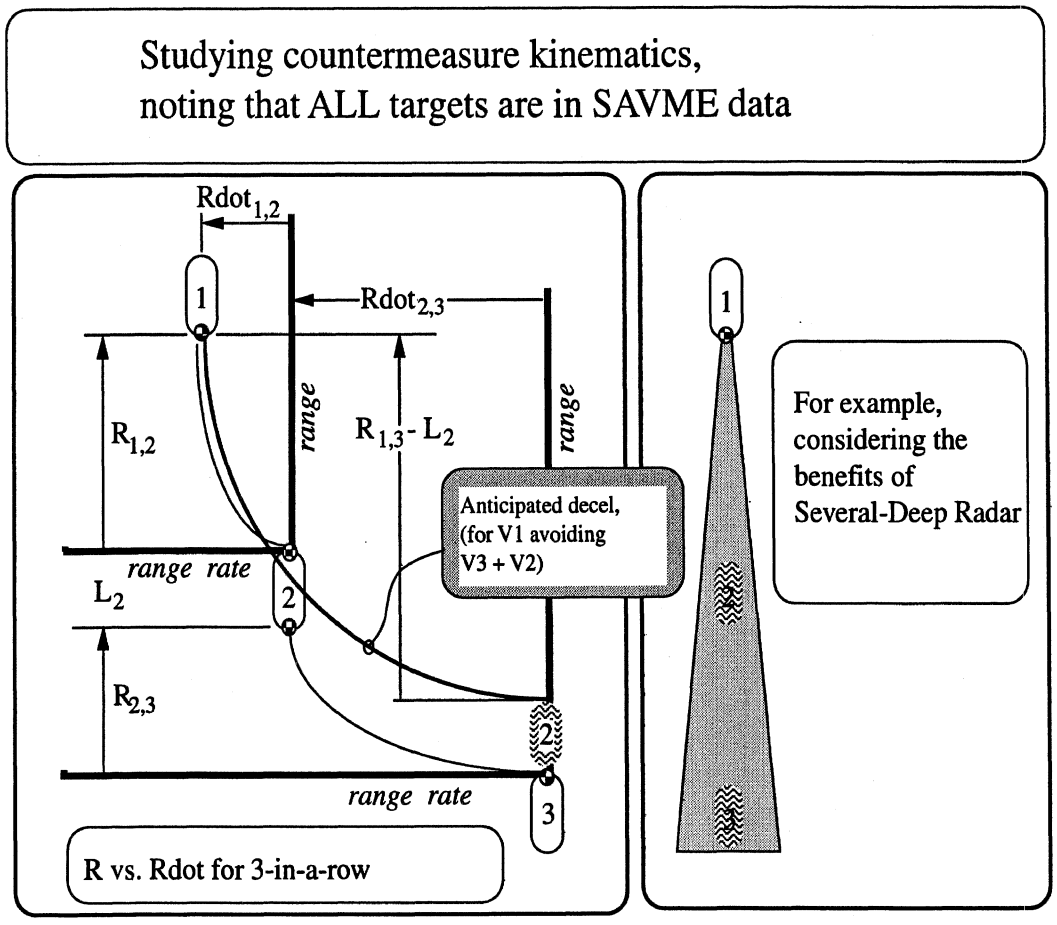

Figure 4.2.2-59. Concept for Querying the Database and Analyzing Decel-to-Avoid Values for Three Vehicles in a Row

But if another vehicle existed ahead, shown as number 3, and if a further conflict were brewing between it and its follower, number 2, as expressed by the respective range, $R_{2,3}$, and range-rate, $Rdot_{2,3}$, values, then it might very well be of concern to vehicle 1 to have anticipated such a conflict insofar as it will surely propagate rearward and will soon manifest itself as a conflict between vehicles 1 and 2. Thus, a several-deep radar offers the inherent advantage to detect and interpret conflicts that are pending ahead of the vehicle that is ahead of the host, thereby perhaps precipitating an anticipatory kind of response that would add greatly to crash avoidance, especially given the long delays that otherwise burden the human response function. In a nutshell, a several-deep radar detection capability could allow computation of $(DA_{1,3})$, derived from:

$$(DA_{1,3}) = (Rdot_{1,3})^2 / [2\,(R_{1,3}-L_2)g]$$

Whenever $(DA_{1,3})$ exceeds $(DA_{1,2})$, the implication is that vehicle 1 has a greater conflict brewing ahead of number 2 than it does with vehicle 2, itself. Of course, the full set of conflict conditions would include consideration of the instantaneous decelerations already underway by vehicles 2 and 3, but a simplification of the problem to comparative DA values as shown above will suffice for illustrating the power of SAVME data for speaking to such a scenario.

A query was run on the SAVME database, seeking the following conditions:

- For each (host) vehicle that was preceded by two or more others,
- While traveling continuously in one of the through lanes of Plymouth Road,
- With the host vehicle's speed greater than 30 ft/sec, and
- With the host tending to overtake the immediately preceding vehicle such that $Rdot_{1,2}$ was less than zero, and
- For cases in which the decel-to-avoid value, ($DA_{2,3}$) between vehicles 2 and 3 in the sequence of three vehicles was above 0.1 g for a period of 2 seconds or more (such that a disturbance was pending.)

This query thus finds those cases in which the current demand for deceleration on the part of the host vehicle (number 1) is about to be increased by the demand for deceleration that has already become present to the preceding vehicle due to its closure on the next vehicle ahead of it. If, indeed, such demands propagate to the vehicles that follow, then the typical case of a significant level of ($DA_{2,3}$) should occur in combination with lower values of ($DA_{1,2}$) for the vehicle which follows. The pending conflict for the host vehicle is instantaneously scaled by detecting and computing the overall conflict between vehicles 1 through 3 as expressed in the measure, ($DA_{1,3}$).

This query of the database produced 57 cases. In each case, values of ($DA_{1,2}$) and ($DA_{1,3}$) were computed and compared. Figure 4.2.2-60, for example, shows the distribution of each of these two DA variables, for the query cases in which a conflict already exists between the first two vehicles. We see that such conditions are typified by very low levels of ($DA_{1,2}$) between the host and its precedent, while the host's conflict relationship with the first vehicle, ($DA_{1,3}$) is distributed toward significantly higher values, including a few in the vicinity of 0.25 g's. These same results are shown as a distribution of the ratio, ($DA_{1,2}$) / ($DA_{1,3}$), in Figure 4.2.2-61. That is, the ratio expresses the relative instantaneous severity of the deceleration demand that would be interpreted by a simple radar that looks only at the vehicle immediately ahead vs. the severity of demand that would be seen at the same moment by a radar that has the several-deep detection capability.

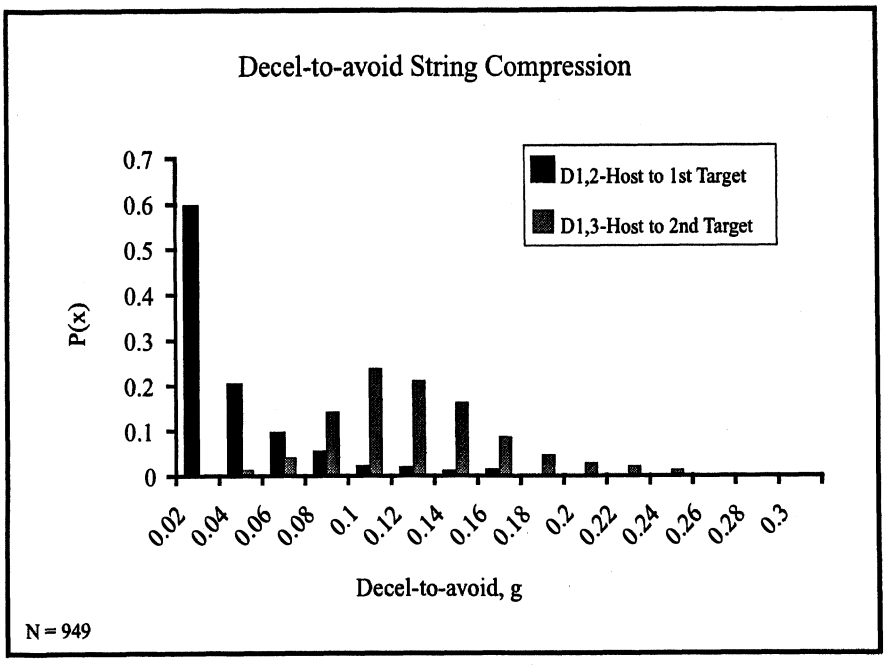

Figure 4.2.2-60. Distribution of Decel-to-Avoid Values for the Conflict within a 3-Vehicle String, Where the Lead Pair has a Decel-to-Avoid Condition of 0.1 g or Greater

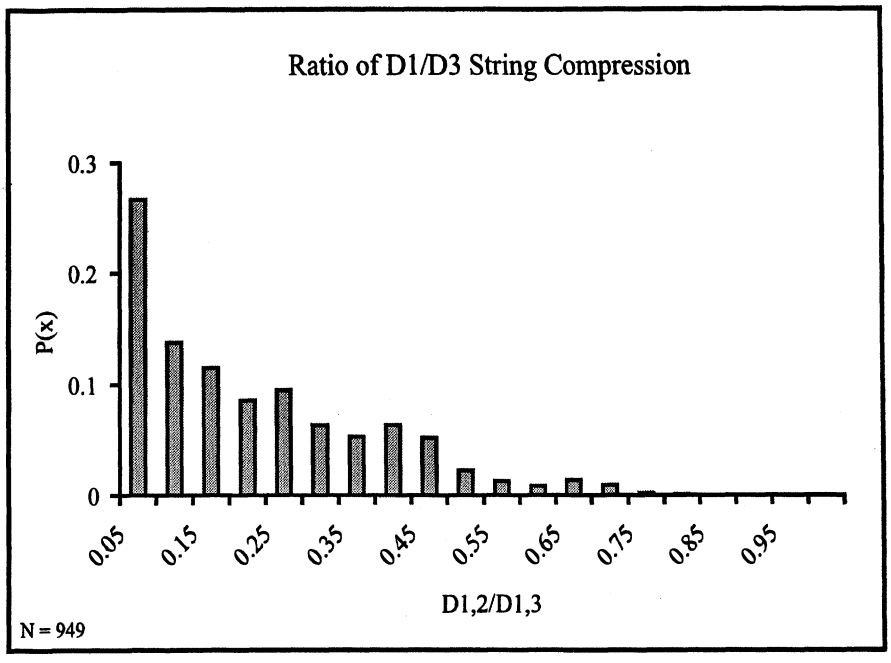

Figure 4.2.2-61. Ratios of Decel-to-Avoid Values

The data show overwhelmingly that the several-deep detection feature cannot lose, when one considers the crucial moment in which a threat has arisen ahead and has not yet been manifest as an immediate threat to the host vehicle. We note that in approximately 60% of the 57 cases, the ratio of DA values is as low as 0.25 or below, suggesting that the $DA_{1,2}$ assessment of conventional simple radars falls far below what could be anticipated in normal traffic, if several-deep capability were in place. One can observe that since the demand condition propagates as a wave along a string of vehicles, measurement of a peak value of demand at a preceding pair will virtually always be associated with a less-than-peak demand condition at the next pair aft. This is just the way traffic works, although individual drivers can anticipate these developments to some degree by watching brake lights up ahead, if they are attentive.

Blooper – Right Turn from Center Left-Turn Lane

Because the continuous nature of SAVME data collection covers the full sample of driving behaviors exhibited over a period of time, it is possible to capture not only the central tendencies in driving responses but also the odd-ball maneuvers and mistakes that each driver has probably witnessed from time to time but which tend to be overlooked when considering the typical range of conditions to be expected. Whether simply for the entertainment value of these events or for the serious purpose of analyzing crash countermeasures, recognition of these "bloopers" is part of a comprehensive understanding of traffic behavior.

Presented in Figure 4.2.2-62, for example, is an animation frame showing vehicle 2275 turning right into the intersecting roadway, L-3, beginning from a position in the center left-turn lane, L0. This west-bound driver apparently intended to turn left but then noticed that the target destination was actually on the right side of the road. The vehicle turns right, crossing in front of two oncoming vehicles in lanes L-1 and L-2 and proceeds into the L-3 roadway. Figure 4.2.2-63 plots the x-y trajectory of vehicle 2275, showing that it entered the center lane by a gradual maneuver covering 300 feet from its entry point in lane L-1.

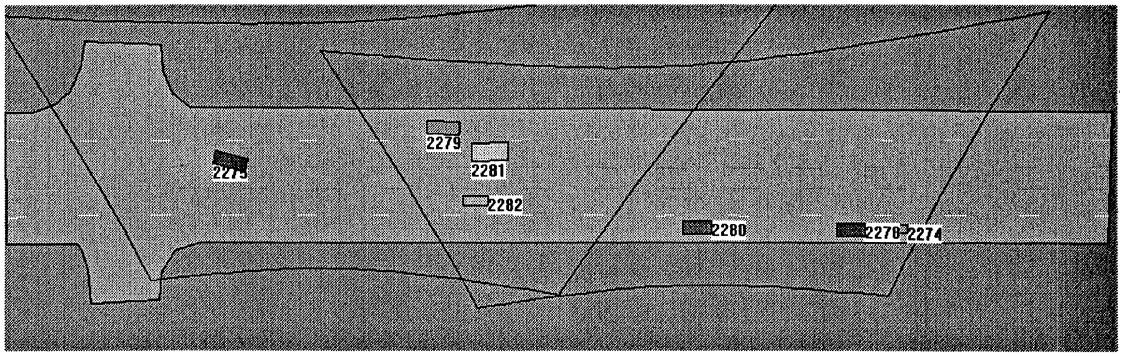

Figure 4.2.2-62. Animator Frame Showing Vehicle 2275 Turning Right from Center Left-Turn Lane

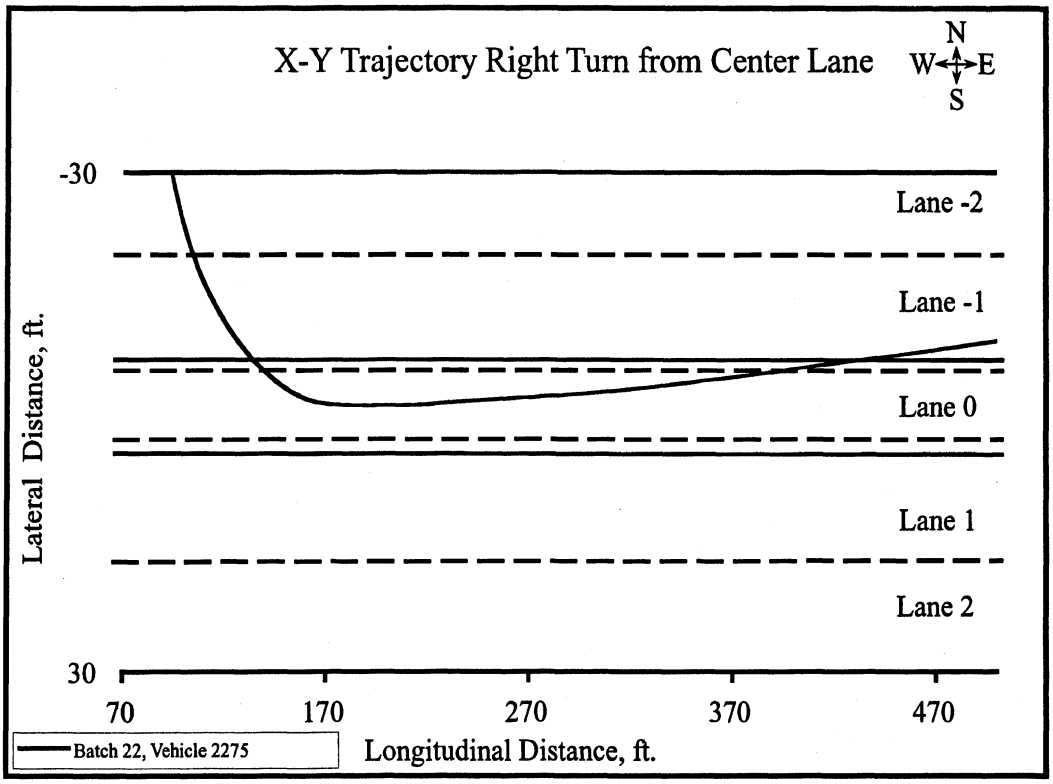

Figure 4.2.2-63 X-Y Trajectory of Vehicle 2275

Blooper – U-turn, Including Backing-Up in Traffic

Shown in Figure 4.2.2-64 is the animator frame capturing the entertaining case of vehicle 1537 which has entered the center left-turn lane, waited 10 seconds for traffic to clear, and then proceeded with a U-turn that could not be fully completed without backing up after encountering the curb in lane L-2, then proceeding westbound in that lane. The x-y trajectory for this maneuver is shown in Figure 4.2.2-65, together with the companion trajectory of vehicle 139 which was also discovered in the database by posing a SAVME query looking for any vehicles that had entered the road in eastbound or westbound through lanes, respectively, but had exited going oppositely westbound or eastbound.

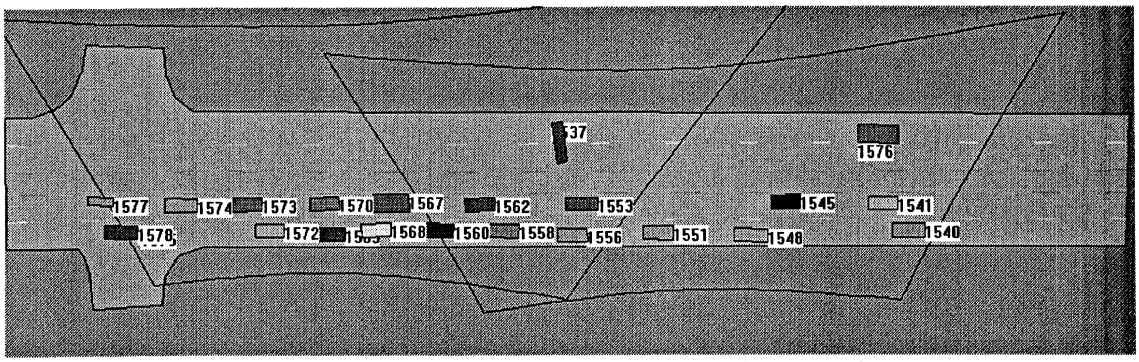

Figure 4.2.2-64. Animator Illustration of Vehicle 1537 Performing U-turn

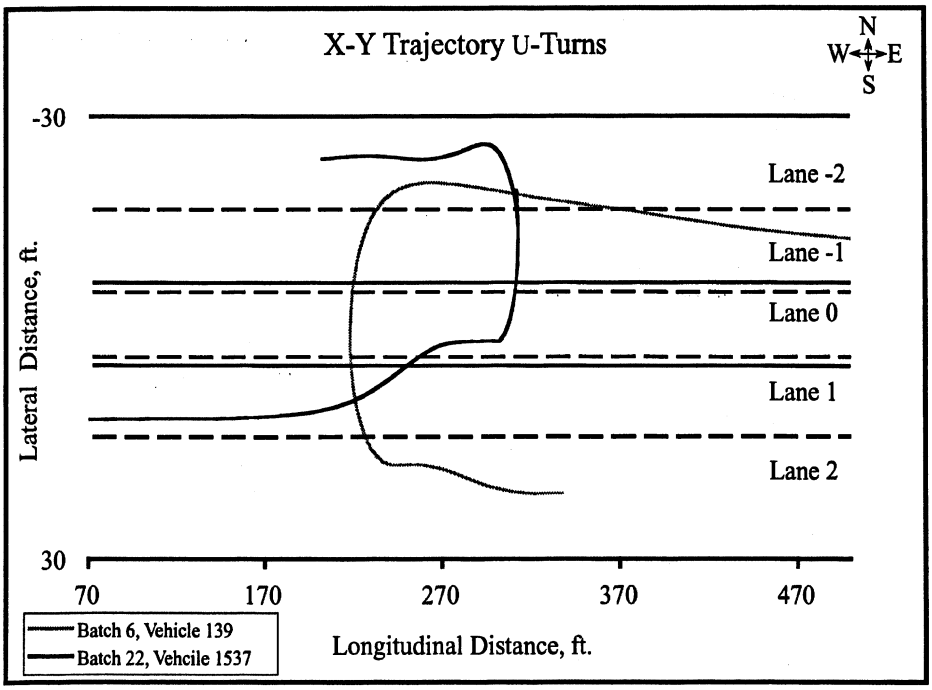

Figure 4.2.2-65. X-Y Trajectory of 2 Vehicles Performing U-turn Maneuvers

5.0 Conclusions and Recommendations

5.1 Conclusions on the Readiness of SAVME to Support a Field Program

The SAVME system (data acquisition, image processing, and trackfile processing modules) has clearly reached a state of readiness that can support specialized applications. The 18 hours of processed SAVME data produced by this project is strong evidence and demonstration of the capability of the SAVME concept.

Nevertheless, certain modest refinements in portions of the SAVME system should be considered prior to any large-scale deployments. These refinements would greatly benefit the efficiency and quality of the overall SAVME data production and would clearly benefit any such future large-scale deployments. These refinements include:

- Resolution of an intermittent camera synchronization problem discovered towards the end of this project and understood to be easily correctable with a modest technical effort.

- Improvements in the image processing module that currently produces intermittent camera-to-camera artifacts described in Section 4.1.2.Significant attenuation of these particular artifacts would greatly improve the potential of the SAVME data processing system, allowing it to produce high fidelity data sets of each vehicle's primary translational and yaw motion variables. The current database requires some smoothing of the raw data to accommodate these particular artifacts, and in doing so, thereby lessens the ability of data processing algorithms to extract more accurate estimates of certain high frequency vehicle response variables, particularly for vehicles engaged in rapid lateral maneuvering. The suggested refinement would remove this particular caveat and provide a beneficial enhancement to overall data accuracy.

These two suggested refinements can be addressed with a relatively straightforward effort and should be undertaken prior to a large-scale field program. Other suggested improvements in the overall SAVME design that can be offered (as provided in different sections of the report) are more long term in nature and would have less immediate impact on the performance of the SAVME system within a field program context.

5.2 Conclusions on the Utility of SAVME Data

The initial database of SAVME measurements reported here was found to have high utility, as exhibited by the sample results presented in section 4.2. First among the features yielding such utility are the data elements themselves, as follows:

- The eight variables yielded by Kalman filtering including some that are unavailable as direct products of image processing. The Kalman filter is seen to add particular value in the form of improved quality in all variables and especially in the production of the higher derivatives, yaw rate and longitudinal acceleration;

- The intervehicular variables establishing range, range-rate, and azimuth angle from each host to every other vehicle, thereby supporting the study of any kinematic relationship involving two or more vehicles.(We note that the SAVME intervehicular dataset is especially well suited to support the development of modern automotive radar systems since they typically yield explicit measurement of the same three variables as are included here.)

- Explicit lane locations, thereby allowing one to query the database in terms of lane-related logic and maneuvering scenarios without having to infer lane location or transitions thereof from the state variables of the vehicle, itself;

- The availability of absolute coordinates, at every time step, thereby affording the option of computing and presenting results based upon position on the ground rather than by relative measures of intervehicular relationships, only.

These aspects of SAVME data, taken together, are unique in the world, to the authors' knowledge. Further, they offer a utility for the study of driving and especially the process of crash avoidance that appears to be great, indeed. Beyond the data themselves, the architecture of the SAVME database and the tools that support its inquiry offer additional utility as follows:

- The Animator tool has value for gaining broad familiarity with the traffic and maneuvering phenomena that are characteristic of the site. Clearly, the underlying data simply represent a running history of traffic at the site, with no contrived data structure other than that afforded by the road geometry and any embedded traffic control devices such as stop signs, signals, and the like. Thus, visual perusal of traffic activity by way of an animated display of the database's contents helps the investigator formulate meaningful questions and begin posing query schemes that are likely to be fruitful.

- The VME Animator is also an indispensable aid for validating the reasonableness of any specific result obtained by means of a database query. That is, following a search of the relational variables, it is prudent to view by animation several of the sample cases satisfying the query to confirm that (a) the query was properly executed and (b) the vehicular motions found through the query are rationally in accordance with the targeted segment of all driving activity.

- Query options are, by nature, versatile in the extreme, and are aided by:
  - Explicit representation of lane locations as identified earlier;
  - Explicit indication of nominal vehicle type, inferred by the length property entered in the header for each vehicle;
  - An immediate retrieval of the population count that results from any query, thereby serving as information on the scope of the phenomena matching the query, as well as a ready check on whether the query result is in line with one's expectations for reasonableness;
  - The ability to create intermediate tables of query results, thereby rendering a facile means for further computations, (an example here, from Section 4.2.2, was the set of all cases in which three vehicles appeared in a string, above 30 ft/sec, with the first vehicle exhibiting a decel-to-avoid value above 0.1G's. Once separated as an intermediate table, subsequent queries can be addressed efficiently just to that group, including computations to model other driver assistance functionality on top of the kinematic contents of the SAVME data, themselves.)
  - The ability to export query results, data summaries, histograms, etc. into a computational and plotting utility such as Microsoft Excel, for ready presentation of results.

Finally there was some concern, initially, that the study of SAVME data would be hampered by "edge effects" associated with the fact that the imaged portion of the road is limited and that no data at all are available just beyond the envelope of video coverage. Firstly, one does note that the edges do serve to limit the utility of the database and, further, that data quality is somewhat reduced near the edges due to current anomalies in processing, especially where a vehicle first appears entering the scene. On the other hand, the authors' experience with the data shows that a great variety of meaningful results can be obtained within the edges of even the short (approximately 500-foot long) road segment studied here. Further, any given computation run on the database can readily stipulate that only cases within a specified clearance of the edges is to be considered. Thus, although edge limitations are a reality, this fact does not appear to have a major impact on the utility of a SAVME database.

5.3 Recommendations

It is recommended that SAVME data be recognized as a unique resource for studying the kinematics of the driving process and for quantifying both natural driving phenomena and what-if propositions based upon future driver assistance functions. SAVME data should be seen as a fundamental complement to data from instrumented vehicle testing and from driving simulator experiments—none of which replaces the other.

It is recommended that continual improvement in the SAVME method be undertaken to render this tool an increasingly efficient element of the NHTSA research portfolio, in keeping with the value that SAVME data appear to have for advancing the field of crash avoidance. Two key suggestions for improvement were stated in Section 5.1 of this report. These items call for an improvement that would ensure camera synchronization at all times plus an upgrade in the image processing software to ensure a smoother merging of tracks from one camera's zone of coverage to that of the next.

It is also recommended that the SAVME database be reconfigured for operation on more powerful database software such as Microsoft's SQL Server package. This improvement would ensure that the very large files that are anticipated in SAVME data can be managed and analyzed in an efficient manner.

Finally, it is recommended that NHTSA undertake an expeditious peer review of SAVME in order to, (a) validate the contractor's reported experience, (b) expand awareness of SAVME data as a knowledge resource and thereby, (c) gain support within the crash avoidance community for the appropriate level of priority in NHTSA's program of SAVME implementation.